The Dissertation Committee for Hyo Kyung Kim Certifies that this is the approved version of the following dissertation:

A Diguanylate Cyclase Acts as a Cell Division Inhibitor in a Two-Step Response to Reductive and Envelope Stresses

Committee:

Rasika M. Harshey, Supervisor

George Georgiou

Makkuni Jayaram

Theresa O'Halloran

Marvin Whiteley

A Diguanylate Cyclase Acts as a Cell Division Inhibitor in a Two-Step Response to Reductive and Envelope Stresses

by

Hyo Kyung Kim, B.S., M.S.

Dissertation

Presented to the Faculty of the Graduate School of

The University of Texas at Austin

in Partial Fulfillment

of the Requirements

for the Degree of

Doctor of Philosophy

The University of Texas at Austin

December, 2016

Dedication

To my parents

Acknowledgements

I would like to thank my advisor, Dr. Rasika M. Harshey, for her invaluable guidance and support. Her enthusiasm and passion for research is what inspires me every day. I'm grateful to all the past and present lab members of the Harshey lab, especially to Dr. Wonyoung Choi, Dr. Vincent Nieto, Dr. Jae Min Lee, Dr. Jon Partridge and Dr. Sooin Jang, who were willing to help me and teach me. To all my committee members, Dr. George Georgiou, Dr. Makkuni Jayaram, Dr. Theresa O'Halloran and Dr. Marvin Whiteley, I sincerely appreciate your time and effort. I would like to also thank all of my friends and family in Austin and back in my home country Korea for their unconditional love and well wishes. Without their support and faith in me, this would not have been possible.

A Diguanylate Cyclase Acts as a Cell Division Inhibitor in a Two-Step Response to Reductive and Envelope Stresses

Hyo Kyung Kim, Ph.D.

The University of Texas at Austin, 2016

Supervisor: Rasika M. Harshey

Bacteria use diverse nucleotide-based small molecules as second messengers to transduce various signals in their extra- and intracellular conditions, and to elicit appropriate cellular responses. The signaling molecule cyclic diguanylate (c-di-GMP) has emerged as a ubiquitous nucleotide that controls a variety of cellular processes including motility, biofilm formation, virulence and cell differentiation. The intracellular levels of c-di-GMP are determined by the balance between its synthesis by diguanylate cyclases (DGCs) and degradation by phosphodiesterases (PDEs). Single bacterial species encode multiple DGC/PDEs harboring different sensory domains, surmised to integrate various input signals to regulate a common pool of c-di-GMP, which in turn regulates wide-ranging output processes. However, some c-di-GMP pathways appear to relay information selectively by spatial sequestration of particular DGC/PDEs. Here I discovered a new signaling pathway for YfiN, one of multiple DGCs found in *E. coli* and *Salmonella*. I show that YfiN interacts directly with components of the cell division machinery to inhibit division and growth, rather than acting through its product c-di-

GMP. The DGC function of YfiN was known previously to be activated by a redox stress signal. My studies have revealed a second function, where redox-activated YfiN responds further to envelope stress by dynamically localizing to the division site and halting division. The unexpected bifunctionality of YfiN provides evidence that protein-protein interactions between c-di-GMP signaling components and their targets also confer signaling specificity, and reveals a new pathway for simultaneously inhibiting both cell division and cell growth in response to two stresses applied in a sequence.

Table of Contents

List of Tables

List of Figures

Chapter 1. Introduction

BACTERIAL SIGNALING PATHWAYS

Bacteria live in a wide range of environmental niches, where nutrient levels, temperature, acidity, moisture, osmolality, toxic agent levels and many other conditions can change rapidly and unexpectedly. To survive the fluctuating environments, bacteria have evolved sophisticated signaling networks. Using these networks, bacteria gather information from both their extracellular and intracellular conditions, and assess them to promote adaptive responses.

Two-component signal transduction system

Many of the bacterial signaling pathways operate via protein phosphorylation cascade, a mechanism referred to as the "two-component system" (TCS). The basic TCSs are comprised of sensor histidine kinases and their cognate response regulators. In individual signaling pathways, the flow of information occurs by the transfer of phosphoryl groups from a histidine kinase to its dedicated response regulator. Once a specific stimulus is detected by the sensory portion (generally extracellular) of the histidine kinase, the intracellular catalytic portion responds by catalyzing an autophosphorylation reaction on a conserved histidine residue. The phosphoryl group is then transferred to a conserved aspartate residue of its allied response regulator, causing a conformational change. The phosphorylated response regulator subsequently promotes its output response, most commonly by interacting with promoters and leading to transcriptional changes.

Two-component signaling components are among the most abundant proteins in bacteria. Analysis of numerous bacterial genome sequences revealed that bacterial species with larger genomes tend to encode more two-component genes (1). Moreover, the number of two-component genes in a bacterium is strongly related to its environmental niche. While bacteria that live in constant environments appear to encode relatively few TCSs, bacteria that inhabit highly-fluctuating environments typically encode large numbers of the signaling proteins (2). For example, *Helicobacter pylori*, an obligate bacterial parasite of the human stomach, encodes only 4 histidine kinases and 7 response regulators, and *Myxococcus xanthus*, a widely distributed bacterium that has a complex life cycle, encodes 136 histidine kinases and 127 response regulators (3, 4).

Despite the large numbers of kinases and regulators in single species, most kinases discriminate their cognate response regulator from others in the cell, ensuring signaling specificity. Previous *in vitro* studies using purified kinases and regulators demonstrated that the specificity is based on molecular recognition governed by a small number of amino-acid residues in the kinase residing near the phosphorylated histidine (5, 6). Each kinase has a unique set of amino acids that dictates specific protein-protein interaction with its regulator containing a set of complementary amino acids. The direct interaction between the two sets of residues enforces the fidelity of information flow.

Small-molecule signaling pathways

- **Intercellular signaling: Quorum sensing**

Bacteria also use freely-diffusible small molecules to convey information about fluctuating conditions. One of the well-known examples is “quorum sensing”, cell-to-cell communication using small hormone-like molecules called autoinducers. In this process,

bacterial cells monitor one another's presence in a community by sensing the extracellular concentrations of autoinducers that are produced and released by themselves. The output responses controlled by quorum sensing are usually physiological processes that are only effective when a population of bacteria acts in a coordinate manner, such as bioluminescence, biofilm formation and virulence factor expression. At a high cell density, a threshold concentration of autoinducer is achieved, which activates a signal transduction cascade on a population-wide scale. This signaling system allows bacteria to synchronize their behaviors, and thus function like a multicellular organism.

The small molecules used in quorum sensing are variable. Gram-negative and Gram-positive bacteria typically utilize *N*-acyl homoserine lactones (AHLs) and post-translationally modified oligopeptides as autoinducers, respectively (7). While most AHLs synthesized by LuxI-type proteins are freely diffusible across membranes, allowing their detection by LuxR-type proteins in the cytoplasm (8), oligopeptides do not cross membranes (9). Instead, the signaling molecules are released by dedicated oligopeptide exporters and recognized by two-component sensor kinases, which is followed by a phosphorylation cascade (9). Recent studies found additional autoinducers, including 2-heptyl-3-hydroxy-4-quinolone (PQS, *Pseudomonas* quinolone signal) that is transported within membrane vesicles (10, 11). Quorum sensing also allows communication between species using a different type of autoinducer, called AI-2 (7).

- **Intracellular signaling by nucleotide-based second messengers**

Small molecules function as messengers not only in cell-to-cell communication, but also in signal transduction within the cell. In bacteria, diverse nucleotide molecules serve as second messengers, including cAMP, (p)ppGpp and c-di-GMP. The basic

principle of nucleotide-based second messenger signaling is that a signaling molecule that is synthesized and degraded by the two opposite enzyme activities in response to environmental stimuli, binds to an effector protein/RNA to regulate its activity and trigger a functional output. In *E. coli*, cAMP is synthesized from ATP by a single adenylate cyclase (Cya) that is activated by carbon limitation, and degraded by a single phosphodiesterase (CpdA) (12). cAMP binds and allosterically activates a transcription factor, catabolite regulation protein (CRP), regulating expression levels of multiple genes (13). Another nucleotide-based messenger (p)ppGpp is synthesized from GDP (GTP) and ATP by two proteins RelA and SpoT in *E. coli* (12). The ribosome-associated RelA protein produces (p)ppGpp in response to amino acid starvation, which binds to RNA polymerase as a global transcriptional regulator that down-regulates ribosomal RNA and transfer RNA genes and up-regulates genes for amino acid synthesis and transport (14). SpoT, which synthesizes (p)ppGpp in response to more general stress signals, including carbon, fatty acid and iron starvation, is responsible for (p)ppGpp degradation as well (15). The cyclic dinucleotide molecule c-di-GMP is also a bacterial second messenger coupling environmental stimuli to intracellular responses. Unlike cAMP and (p)ppGpp, c-di-GMP is synthesized and degraded by multiple enzymes, and recognized by multiple effectors in single species, implying a unique signaling mechanism. Interestingly, c-di-GMP is often recognized by mammalian sensors as a sign of bacterial invasion, triggering an innate immune response in mammalian cells (16, 17). Further details of c-di-GMP signaling are described below.

Recently, two more cyclic dinucleotide molecules, c-di-AMP and c-di-AMP-GMP, were discovered as novel second messenger molecules in bacteria. In *Bacillus subtilis*, c-di-AMP is produced by the DNA integrity scanning protein DisA (18). When DNA damage is detected, DisA halts its diadenylate cyclase activity, and the subsequent

decrease in c-di-AMP levels blocks entry into sporulation (19). c-di-AMP also serves as a signaling molecule in other Gram-positive bacteria including *Staphylococcus aureus* and *Listeria monocytogenes*, where it plays a role in cell wall stress response and host colonization, respectively (20, 21). A third type of cyclic dinucleotide, cyclic-AMP-GMP hybrid was found in *Vibrio cholera* to be involved in virulence (22), suggesting that additional cyclic dinucleotides with diverse composition and structure await to be discovered.

BACTERIAL CYCLIC DI-GMP SIGNALING

Bis-(3′-5′)-cyclic dimeric guanosine monophosphate (c-di-GMP, Figure 1.1) has emerged as a widespread bacterial second messenger. After its first discovery in 1987 as an allosteric activator of the membrane-bound cellulose synthase in *Gluconacetobacter xylinus* (formerly *Acetobacter xylinum*) (23), c-di-GMP has been shown to be a key regulator of bacterial behavior, especially in the transition between planktonic and biofilm lifestyles. In general, low intracellular c-di-GMP levels promote a free-living/motile lifestyle, but once these levels start to rise, pathways that promote surface-attached/sessile lifestyle are switched on (Figure 1.2).

The intracellular concentration of c-di-GMP is established by the opposite activities of two protein groups, diguanylate cyclases (DGCs) and phosphodiesterases (PDEs). DGCs produce one molecule of c-di-GMP from two molecules of GTP, which is broken down into 5′-phosphoguanylyl-(3'-5')-guanosine (pGpG) by PDEs (Figure 1.3). The c-di-GMP synthetic or hydrolytic activity resides in the GGDEF domain or the EAL/HD-GYP domain, respectively, named after the conserved amino acid motif at the active site. The sequencing analysis of genomes from various bacterial species have

identified multiple proteins with GGDEF, EAL, or both domains in single species. For example, *Escherichia coli* has 29 such proteins, *Salmonella enterica* has 19 (24), *P. aeruginosa* has 38 (22), and *Vibrio* species have more than 50 (24). The majority of GGDEF/EAL domain proteins are preceded by additional N-terminal signal-input sensory domains, which control their enzymatic activities upon signal detection and impact c-di-GMP intracellular levels (25). Signals like oxygen and redox conditions are perceived by heme-containing globin and PAS domains (26, 27), blue light and temperature by the FAD-associated BLUF domain (28, 29) and signals from phosphorylation pathways by two-component receiver (REC) domains (30, 31). The sensory domains are often located in the periplasm in Gram-negative bacteria, thereby monitoring changes in the external environment.

The signals sensed by GGDEF/EAL domain proteins are relayed to downstream processes through interactions between c-di-GMP and effectors (Figure 1.3). c-di-GMP-bound effectors then interact with their protein or RNA targets to bring about the necessary change in cellular physiology. The first identified c-di-GMP-binding effectors had the PilZ domain, which has a conserved RxxxR and D/NxSxxG motif (16). YcgR and BcsA, two representative c-di-GMP effectors containing the PilZ domain, modulate bacterial behavior in response to changes in c-di-GMP levels in most enterobacteria, including *E. coli* and *Salmonella*. With an increase in intracellular c-di-GMP levels, c-di-GMP-bound YcgR interacts with components of the flagella motor complex to alter its rotational switching and speed (32-34). While motility is impaired by YcgR, biofilm formation is triggered by the cellulose synthase BcsA (23), together promoting the motile-to-sessile transition.

Recent studies have shown that, as with GGDEF/EAL domain proteins, a large number of c-di-GMP-binding effectors are encoded by single species, which extends the

range of cellular processes regulated by c-di-GMP beyond motility and biofilm formation. In *Caulobacter crescentus*, fluctuations in c-di-GMP levels determine cell polarity and its asymmetric life cycle progression by controlling multiple c-di-GMP effectors. Gene expression regulation can also be mediated by c-di-GMP that binds to various transcription factors and modulates their DNA-binding affinities. The transcription factor Clp known to regulate expression of genes encoding virulence factors in *Xanthomonas campestris* was shown to release from its target DNA in response to c-di-GMP binding (17, 35). The polynucleotide phosphorylase (PNPase), an enzyme important for mRNA turnover, is controlled upon binding to c-di-GMP in *E. coli*, resulting in c-di-GMP-responsive gene regulation (36). C-di-GMP can also modulate gene expression through c-di-GMP-sensing RNAs called riboswitches. The untranslated regions of mRNAs undergo structural alterations by binding c-di-GMP, which affect their transcription and translation (7, 9). Although single bacterial species have multiple c-di-GMP-binding effectors, their affinities for c-di-GMP are not the same, which allows differential regulation of c-di-GMP-mediated downstream processes. For example, the PilZ domain effector YcgR has a 43-fold higher affinity for c-di-GMP compared to another PilZ domain effector BcsA in *Salmonella* (37). This difference provides sequential activation of YcgR and BcsA in the motile-to-sessile transition: when the cell has a moderate level of c-di-GMP, only YcgR is activated causing motility inhibition; a further increase in the c-di-GMP concentration is required to activate the cellulose synthase BcsA.

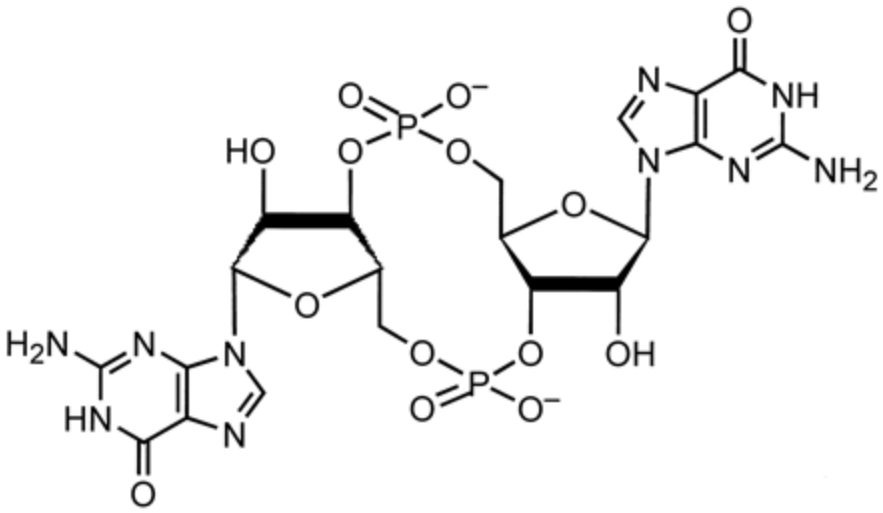

Figure 1.1 Structure of bis-(3′-5′)-cyclic dimeric guanosine monophosphate (c-di-GMP)

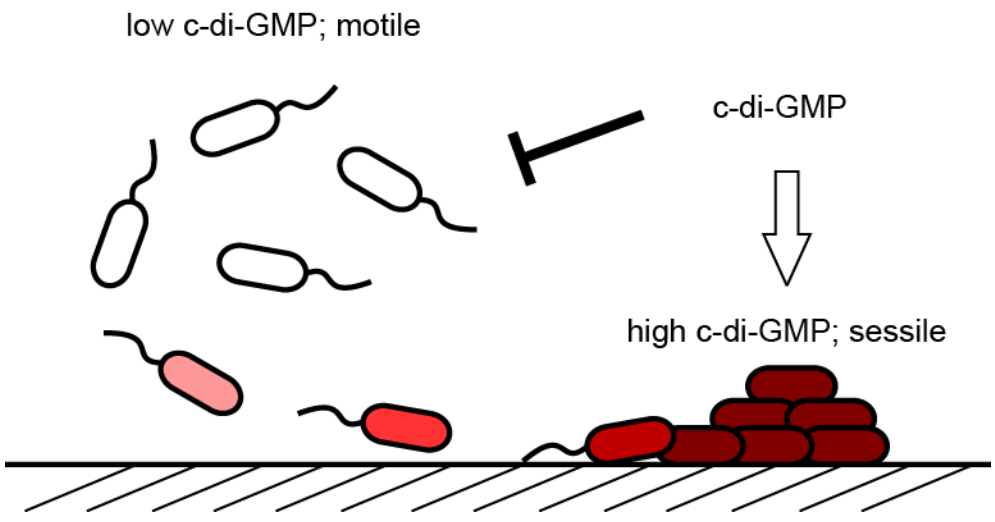

Figure 1.2 Effect of c-di-GMP on bacterial lifestyle. The accumulation of c-di-GMP impairs motility and promotes biofilm formation.

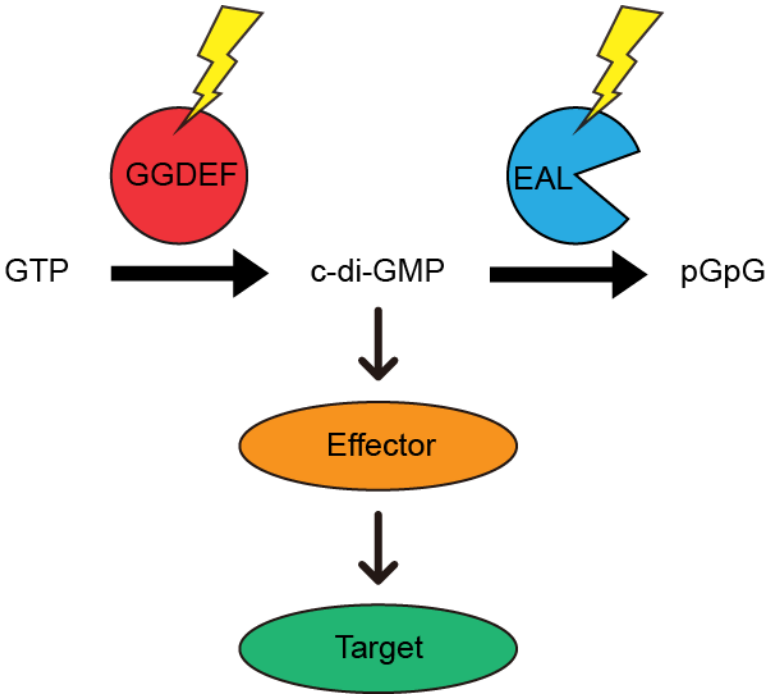

Figure 1.3 The basic components of c-di-GMP signaling. The intracellular levels of c-di-GMP is regulated by two groups of enzymes, diguanylate cyclases (DGCs) and phosphodiesterases (PDEs). DGCs containing a GGDEF domain synthesize c-di-GMP, which is degraded by PDEs containing an EAL domain. The fluctuations in c-di-GMP levels are recognized by c-di-GMP-binding effectors that promote physiological responses by interacting with targets.

SPECIFICITY OF C-DI-GMP SIGNALING

The multiplicity of GGDEF/EAL domain proteins and c-di-GMP-binding effectors allows bacterial cells to integrate a wide range of stimuli and make a change in their behavior accordingly. However, this also raises the question of how bacteria manage the multiple c-di-GMP signaling pathways: do they converge on a common pool of c-di-GMP? In this scenario, a single concentration of c-di-GMP throughout the cell is determined by multiple DGCs and PDEs, which in turn controls multiple downstream processes (Figure 1.4A). The only parameter that provides output specificity would be the difference in c-di-GMP affinities of effectors.

Alternately, it has been suggested that the c-di-GMP signaling network functions with high signaling specificity by not allowing convergence. Input signals detected by each of DGCs and PDEs would be processed in parallel and would modulate only their target downstream processes, avoiding unwanted crosstalk (Figure 1.4B). Consistent with this idea, a number of studies have claimed that individual DGCs or PDEs are specifically associated with downstream responses. In *P. aeruginosa*, single mutants of two DGCs RoeA and SadC showed the same levels of intracellular c-di-GMP, yet displayed distinct phenotypes - impaired extracellular polysaccharide production and enhanced swarming motility, respectively (10). The lack of correlation between the total c-di-GMP concentration and c-di-GMP-mediated downstream responses was also observed with overexpression of different DGCs. When a specific c-di-GMP responsive phenotype was monitored under a broad range of c-di-GMP concentrations generated by each of multiple DGCs, the phenotypic output was determined by which DGC was used, not by the total concentration of c-di-GMP (11). The functional association between DGC/PDEs and downstream targets cannot be explained by the common c-di-GMP pool

model, in which the same phenotypic output would be observed as long as the total c-di-GMP concentrations are at the same.

How then is signaling specificity achieved in bacteria? As a possible mechanism, it has been proposed that "local pools" of c-di-GMP are generated by spatial sequestration of c-di-GMP signaling components (15, 25). DGC/PDEs, differentially localizing nearby their downstream effectors and targets, might introduce several subcellular pools of c-di-GMP within the cell (Figure 1.4C). There is increasing evidence for such a scenario. The two membrane-associated DGCs RoeA and SadC, which contribute to biofilm formation by modulating two different downstream targets in *P. aeruginosa* as described above, showed distinct patterns of localization (10).

The specific localization of DGC/PDEs has been best illustrated in *C. crescentus*, a bacterium in which c-di-GMP signaling plays a major role in cell differentiation. This uniflagellated bacterium undergoes asymmetric cell division generating two different daughter cells, a flagellated/motile swarmer cell and a surface attached/non-motile stalked cell. While the stalked cell continuously divides producing another swarmer cell, the motile cell halts cell division until it finds a surface to attach. Once the cell lands on a surface, the flagellum is ejected and a new stalk develops at the same pole, while a new flagellum is synthesized at the opposite pole. The swarmer-to-stalked cell transition is driven by fluctuations in c-di-GMP concentration. The DGC PleD, one of the key contributors to the c-di-GMP upshift observed in stalked cells (38), is evenly distributed within the swarmer cell, but localizes to the emerging stalked pole only when it is activated by phosphorylation during the swarmer-to-stalked cell transition (31). The spatial sequestration of active PleD at the stalked pole, which leaves the opposite pole PleD-free, is speculated to provide a local accumulation of c-di-GMP. The local activity of PleD is also proposed to cause the asymmetric distribution of c-di-GMP observed in

two daughter cells after cell division (39). PleD is not the only DGC/PDE exhibiting distinct subcellular localization in *C. crescentus*. The dynamic polar localizations of the DGC DgcB and its antagonist PDE PdeA were also shown to be important for coordinating cell differentiation (40). Although there are a number of examples for DGC/PDEs spatially restricted in the cell, it remains unclear how the local pools of c-di-GMP, if any, would insulate themselves from each other.

The notion of a freely diffusible small molecule that differentially regulates numerous cellular processes through compartmentalization is not new in eukaryotes. 3', 5'-cyclic adenosine monophosphate (cAMP) is the classic example of such a second messenger acting locally. Similar to bacterial c-di-GMP signaling, cAMP is produced by membrane-associated adenylate cyclases (ACs) in response to activation of surface signal receptors, and subsequently binds to effectors to transduce signals to downstream targets (41, 42). Despite the high diffusion coefficient of cAMP (measured around 500 $\mu m^2\ s^{-1}$ in the cytoplasm (43, 44)), individual cAMP signaling pathways selectively activate their downstream targets. In an effort to explain the signaling specificity, researchers developed optical biosensors for cAMP based on fluorescence resonance energy transfer (FRET), which allowed a direct observation of microdomains with differential concentrations of cAMP in living cells (45). This study emphasized the role of cAMP-phosphodiesterases (cAMP-PDEs), enzymes that degrade cAMP, in maintaining spatial gradients of cAMP based on the observation that the cAMP microdomains disappeared upon addition of cAMP-PDE inhibitors (45). Given the diversity of cAMP-PDEs with more than 50 isoenzymes (46) and the fast kinetics of cAMP degradation by cAMP-PDEs, it is suggested that differentially localized cAMP-PDEs act as sinks and/or enzymatic barriers that restrict free diffusion of cAMP, thereby generating spatially confined high cAMP concentrations in the cell (41, 42). Other factors including

electrostatic channeling between ACs and effectors, physical barriers, buffering by cAMP-binding proteins and high viscosity of the cytoplasm, have also been proposed as explanations for cAMP spatial gradients.

An attempt to visualize compartmentalization of a small signaling molecule using FRET-based biosensors was also made for c-di-GMP signaling in bacterial cells. In *C. crescentus*, the asymmetric cell division was observed to produce two daughter cells with different concentrations of c-di-GMP, the swarmer cell with low c-di-GMP levels and the stalked cell with high c-di-GMP levels (39). However, although the FRET system readily observed heterogeneity in cellular c-di-GMP levels within populations (47, 48), it could not detect spatial gradients of c-di-GMP within single cells. Moreover, the upshift of c-di-GMP during the swarmer-to-stalked cell transition in *C. crescentus*, which was observed using mass spectrometry (38), was not captured in the FRET system (39). It is worth noting that the range of cAMP microdomains observed by FRET in mammalian cells were larger than 1 μm, which is larger than the small size of bacterial cells (diameter of *E. coli* is less than 1 μm). Monitoring the dynamics of c-di-GMP in bacterial cells is still a challenge, requiring techniques with high spatial and temporal resolution.

Although there is no experimental evidence for compartmentalized pools of c-di-GMP in bacterial cells, physical interactions between c-di-GMP signaling components have been reported in an increasing number of cases, suggesting that c-di-GMP signaling might occur in macromolecular complexes. For example, in *E. coli*, oxygen levels are sensed by the DGC DosC and the PDE DosP through their heme-containing sensory domains (26). The two c-di-GMP-metabolizing proteins were found to form a complex with the RNA modifying enzyme PNPase, which is a c-di-GMP-binding effector, suggesting that the fluctuation of c-di-GMP generated by DosC and DosP might directly communicate to the effector due to their physical proximity (36). Direct interaction

between DGC/PDEs with their cognate effector is also exemplified by the DGC from *Pseudomonas fluorescens* GcbC, which binds to the c-di-GMP-responsive biofilm regulator LapD. When the interaction was altered by mutations, GcbC was no longer able to trigger biofilm formation (49), implying that the physical interaction is essential for signaling fidelity. In *E. coli*, a pair of c-di-GMP-metabolizing enzymes YdaM (DGC) and YciR (PDE) specifically regulates expression of the biofilm regulator CsgD via multiple direct interactions with the transcription factor MlrA (50). Interestingly, the PDE YciR and the DGC YdaM were shown to regulate the activity of MlrA by direct interaction rather than by c-di-GMP fluctuations, leading to a proposal that signaling specificity might be achieved by protein-protein interactions between c-di-GMP signaling components and downstream targets without the necessity of spatial gradients of c-di-GMP.

Using *Salmonella* and *E. coli* as model organisms, here I have studied the distinct localization and function of c-di-GMP metabolizing enzymes. To see which GGDEF/EAL domain proteins are involved with c-di-GMP signaling network under laboratory conditions, I evaluated motility phenotypes of mutants in each of the 19 GGDEF/EAL domain proteins in *Salmonella* (Chapter 3). Of the 19 proteins, 5 GGDEF/EAL domain proteins were identified to contribute to intracellular c-di-GMP levels. Their localization was examined to determine if it correlates to their phenotypic output. Unexpectedly, one of the DGCs, YfiN was found to localize to the division site and inhibit division, unveiling a new function of c-di-GMP signaling in cell division regulation (Chapter 4). This function was studied in more detail to understand the environmental stresses that trigger YfiN localization, the nature of the downstream target, and the specific regions of YfiN that sense signals and mediate regulation of cell division.

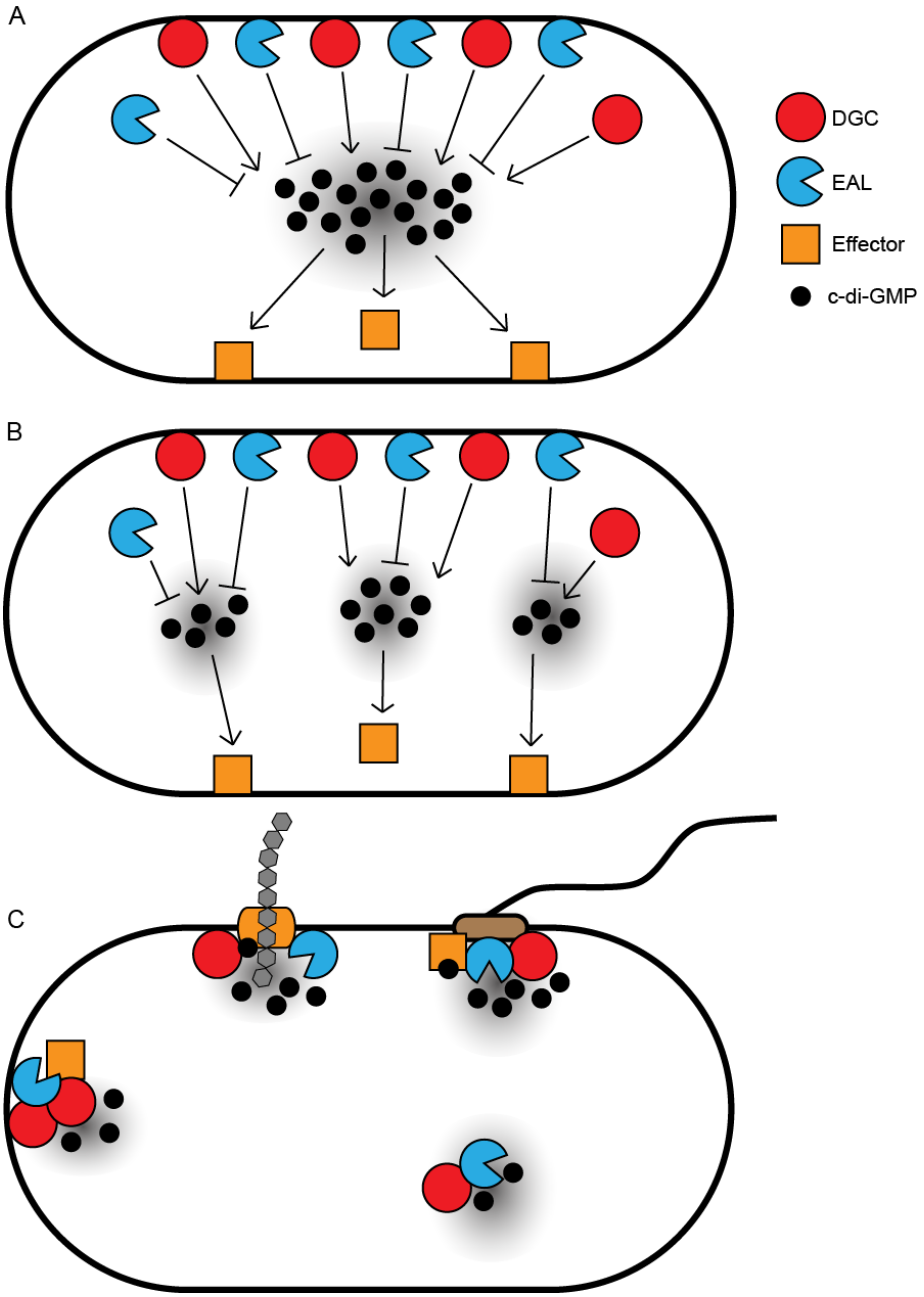

Figure 1.4 Models for c-di-GMP signaling specificity. The multiplicity of DGC/PDEs in single bacterial species can be explained by two models. (A) c-di-GMP signaling functions with low specificity by having all DGC/PDEs contribute to a common pool of c-di-GMP. (B) c-di-GMP signaling functions with high specificity by differentially regulating subsets of DGC/PDEs. (C) The locally-sequestered subsets of c-di-GMP signaling components provide distinct pools of c-di-GMP, ensuring high specificity.

Chapter 2. Materials and Methods

STRAINS AND GROWTH CONDITIONS

All strains used in this study are listed in Table 2.1. Wild type parent strains for *S. enterica, E. coli* and *P. aeruginosa* were 14028, MG1655 and PAO1, respectively. Mutants of *Salmonella* and *E. coli* were constructed by inserting a kanamycin resistance cassette into the designated gene as previously described (51). Excision of the inserted cassettes was achieved by expression of the FLP recombinase encoded on pCP20 (51). The resulting strains were confirmed by DNA sequencing. Mutant combinations were prepared by P22 transduction.

All strains were grown in LB broth (10 g/L tryptone, 5 g/L yeast extract, 5 g/L NaCl). When appropriate, antibiotics were used; ampicillin (100 μg/ml), chloramphenicol (20 μg/ml), kanamycin (50 μg/ml) and gentamicin (30 μg/ml). For inducible plasmids, IPTG and L-arabinose were added as indicated.

Table 2.1 Strains used in this study

Strain	Genotypes	Source (ref.)
S. enterica		
14028	wild type ATCC strain	Laboratory collection
HK132	Δ*yfiN*; 14028 with deletion of *yfiN*	This study

Table 2.1 continued

QW262	Δ*yhjH*	(52)
HK133	Δ*STM1987*	This study
HK134	Δ*yeaJ*	This study
HK135	Δ*STM4551*	This study
HK136	Δ*adrA*	This study
HK137	Δ*yjcC*	This study
HK138	Δ*ylaB*	This study
HK139	Δ*STM1827*	This study
HK140	Δ*STM0343*	This study
HK141	Δ*STM2215*	This study
HK142	Δ*STM3388*	This study
HK143	Δ*yciR*	This study
HK144	Δ*yegE*	This study
HK145	Δ*yhdA*	This study
HK147	Δ*ydiV*	This study
HK148	Δ*STM2503*	This study
HK149	Δ*yhjK*	This study
HK150	Δ*yfeA*	This study

Table 2.1 continued

HK164	Δ*yhjH* Δ*yfiN*; 14028 with double deletions of *yhjH* and *yfiN*	This study
HK165	Δ*yhjH* Δ*STM1987*	This study
HK166	Δ*yhjH* Δ*yeaJ*	This study
HK167	Δ*yhjH* Δ*STM4551*	This study
HK168	Δ*yhjH* Δ*adrA*	This study
HK169	Δ*yhjH* Δ*yjcC*	This study
HK170	Δ*yhjH* Δ*ylaB*	This study
HK171	Δ*yhjH* Δ*STM1827*	This study
HK172	Δ*yhjH* Δ*STM0343*	This study
HK173	Δ*yhjH* Δ*STM2215*	This study
HK174	Δ*yhjH* Δ*STM3388*	This study
HK175	Δ*yhjH* Δ*yciR*	This study
HK176	Δ*yhjH* Δ*yegE*	This study
HK177	Δ*yhjH* Δ*yhdA*	This study
HK178	Δ*yhjH* Δ*ydiV*	This study
HK179	Δ*yhjH* Δ*STM2503*	This study
HK180	Δ*yhjH* Δ*yhjK*	This study
HK181	Δ*yhjH* Δ*yfeA*	This study

Table 2.1 continued

HK185	HK164 + pBAD30	This study
HK261	HK132 + pBAD30-$^{S}YfiN_{GFP}$	This study
HK247	QW262 + pBAD30-$^{S}YhjH_{GFP}$	This study
HK263	HK135 + pBAD30-$^{S}STM4551_{GFP}$	This study
HK265	HK137 + pBAD30-$^{S}YjcC_{GFP}$	This study
HK267	HK150 + pBAD30-$^{S}YfeA_{GFP}$	This study
HK259	*flhDC::kan*	This study
HK260	HK259 + pBAD30-$^{S}YhjH_{GFP}$	This study
HK435	HK132 + pBAD30-$^{S}YfiN$	This study
HK269	HK132 + pBAD30-DgcA	This study
HK375	HK132 + pBAD33-$^{S}YfiN_{YFP}$ + pBAD30-$^{S}FtsA_{CFP}$	This study
HK373	HK261+ pBAD33	This study
HK372	HK261 + pBAD33-$^{S}SulA$	This study
HK683	HK132 + pBAD33-$^{S}YfiN_{YFP}$ + pBAD30-$_{CFP}{}^{S}FtsN$	This study
HK369	HK132 + pBAD33-$^{S}YfiN_{YFP}$	This study
HK698	14028 + pBAD33-$^{S}SulA$	This study
HK631	14028 + pBAD30- $^{S}YfiN_{GFP}$	This study
HK632	14028 + pBAD30- $^{E}YfiN_{GFP}$	This study

Table 2.1 continued

HK633	14028 + pBAD30-^{P}YfiN$_{GFP}$	This study
HK668	HK132 + pBAD30-^{E}YfiN[^{S}TM^{S}PAS]$_{GFP}$	This study
HK653	HK132 + pBAD30-^{E}YfiN[^{S}PAS]$_{GFP}$	This study
HK670	HK132 + pBAD30-^{E}YfiN[^{S}TM]$_{GFP}$	This study
HK666	HK132 + pBAD30-^{E}YfiN[^{P}PAS]$_{GFP}$	This study
HK680	HK132 + pBAD30-^{S}YfiN[^{E}TM]$_{GFP}$	This study
HK732	HK132 + pBAD30-^{S}YfiN[^{P}HAMP]$_{GFP}$	This study
HK734	HK132 + pBAD30-^{S}YfiN[^{P}GGDEF]$_{GFP}$	This study
HK735	HK132 + pBAD30-^{P}YfiN[^{S}HAMP]$_{GFP}$	This study
HK740	HK132 + pBAD30-^{P}YfiN[^{S}GGDEF]$_{GFP}$	This study
HK741	HK132 + pBAD30-^{P}YfiN[^{S}HAMP^{S}GGDEF]$_{GFP}$	This study
E. coli		
MG1655	K12 wild type strain: F^{-}, λ^{-}, *rph*-1	Laboratory Collection
HK359	Δ*yfiN*; MG1655 with deletion of *yfiN*	This study
HK360	Δ*yfiB*; MG1655 with deletion of *yfiB*	This study
HK361	Δ*yfiR*; MG1655 with deletion of *yfiR*	This study
WM1125	MG1655 *lacU169 ftsZ84*	(53)
WM1115	MG1655 *lacU169 ftsA12*	(54)

Table 2.1 continued

PS223	W3110 *zipA1*	(55)
JW3832	BW25113 *dsbA::kan*	(56)
BTH101	F$^-$,*cya*-99, *ara*D139, *gal*E15, *gal*K16, *rps*L1, *hsd*R2, *mcr*A1, *mcr*B1	(57)
XL1-blue	*RecA1, endA1, gyrA96, thi-1, hsdR17, supE44, relA1, lac,* [F′, *proAB, lac1qZΔM15, Tn10 (tet′)*]	Stratagene
HK365	HK359 + pBAD30-^{E}YfiN$_{GFP}$	This study
HK366	HK360 + pBAD30-^{E}YfiN$_{GFP}$	This study
HK549	HK359 + pBAD33-^{E}YfiN$_{GFP}$	This study
HK489	MG1655 *yfiN::* ^{E}*yfiN-gfp*	This study
HK531	MG1655 *yfiR::kan*(←)	This study
HK532	MG1655 *yfiR::kan*(←) *yfiN*::P$_{BAD}$-^{E}*yfiN-gfp*	This study
HK604	MG1655 + pBAD30-DgcA	This study
HK381	WM1125 + pBAD30-^{E}YfiN$_{GFP}$	This study
HK380	WM1115 + pBAD30-^{E}YfiN$_{GFP}$	This study
HK590	PS223 + pBAD30-^{E}YfiN$_{GFP}$	This study
HK470	BTH101 + pUT18 + pKNT25	This study
HK469	BTH101 + pUT18-zip + pKNT25-zip	This study
HK597	BTH101 + pUT18-^{E}YfiN + pKNT25-^{E}YfiN	This study
HK598	BTH101 + pUT18-^{E}YfiN + pKNT25-^{E}FtsZ	This study

Table 2.1 continued

HK599	BTH101 + pUT18-^{E}YfiN + pKNT25-^{E}FtsA	This study
HK600	BTH101 + pUT18-^{E}YfiN + pKNT25-^{E}ZipA	This study
HK725	BTH101 + pUT18C-^{E}MreB + pKNT25- ^{E}FtsZ	This study
HK726	BTH101 + pUT18C-^{E}MreB + pKNT25- ^{E}YfiN	This study
HK571	HK359 + pBAD33-^{E}YfiN(GGAAF)$_{GFP}$ + pTrc99A	This study
HK572	HK359 + pBAD33-^{E}YfiN(GGAAF)$_{GFP}$ + pTrc99A-DgcA	This study
HK580	BTH101 + pBAD33 + pUT18-^{E}YfiN(GGAAF) + pKNT25-^{E}FtsZ	This study
HK582	BTH101 + pBAD33 + pUT18-^{E}YfiN(GGAAF) + pKNT25	This study
HK576	BTH101 + pBAD33-DgcA + pUT18-^{E}YfiN(GGAAF) + pKNT25-^{E}FtsZ	This study
HK578	BTH101 + pBAD33-DgcA + pUT18-^{E}YfiN(GGAAF) + pKNT25	This study
HK608	BTH101 + pBAD33 + pUT18-^{E}YfiN(GGAAF) + pKNT25-^{E}ZipA	This study
HK609	BTH101 + pBAD33 + pUT18-^{E}YfiN(GGAAF) + pKNT25	This study
HK606	BTH101 + pBAD33-DgcA + pUT18-^{E}YfiN(GGAAF) + pKNT25-^{E}ZipA	This study
HK607	BTH101 + pBAD33-DgcA + pUT18-^{E}YfiN(GGAAF) + pKNT25	This study
HK551	HK359 + pBAD33-^{E}YfiN$_{GFP}$ + pTrc99A	This study
HK552	HK359 + pBAD33-^{E}YfiN$_{GFP}$ + pTrc99A-^{E}YfiR	This study
HK367	HK361 + pBAD30-^{E}YfiN$_{GFP}$	This study
HK626	JW3832 + pBAD33-^{E}YfiN$_{GFP}$ + pTrc99A-^{E}YfiR	This study

Table 2.1 continued

HK634	MG1655 + pBAD30-^{S}YfiN$_{GFP}$	This study
HK635	MG1655 + pBAD30-^{E}YfiN$_{GFP}$	This study
HK636	MG1655 + pBAD30-^{P}YfiN$_{GFP}$	This study
HK669	HK359 + pBAD30-^{E}YfiN[^{S}TM^{S}PAS]$_{GFP}$	This study
HK655	HK359 + pBAD30-^{E}YfiN[^{S}PAS]$_{GFP}$	This study
HK671	HK359 + pBAD30-^{E}YfiN[^{S}TM]$_{GFP}$	This study
HK667	HK359 + pBAD30-^{E}YfiN[^{P}PAS]$_{GFP}$	This study
HK681	HK359 + pBAD30-^{S}YfiN[^{E}TM]$_{GFP}$	This study
P. aeruginosa		
PAO1	PAO1 wild type	gift from M. Whiteley
HK376	PAO1 + pJN105-^{P}YfiN$_{GFP}$	This study

PLASMIDS

Plasmids used in this study are listed in Table 2.2. For cloning, gene sequences were amplified using PCR from the genomic DNA of wild type strains and introduced into pBAD30, pBAD33, pTrc99A and pJN105. For DgcA expression vectors, pAB551, a gift from U. Jenal (58), was used as a template. Fusion proteins and an active site mutant

of YfiN were constructed using overlap extension PCR. All the resulting constructs were confirmed by DNA sequencing.

Table 2.2 Plasmids used in this study

Plasmid	Genotype	Source (ref.)
pKD4	Kanamycin resistance gene template	(51)
pKD46	λ Red Recombinase	(51)
pCP20	FLP recombinase	(51)
pBAD30	Cloning vector; P_{BAD} and Amp^R	(59)
pBAD33	Cloning vector; P_{BAD} and Cm^R	(59)
pTrc99A	Cloning vector; P_{Trc} and Amp^R	(60)
pJN105	Cloning vector; P_{BAD} and Gm^R	(61)
pAB551	P_{BAD}::*dgcA* from *C. crescentus*	(58)
pBAD30-^{S}YfiN	P_{BAD}:: ^{S}*yfiN*	This study
pBAD30-^{S}YfiN(GGAAF)	P_{BAD}::^{S}*yfiN*(D327A E328A)	This study
pBAD30-^{S}YfiN$_{GFP}$	P_{BAD}:: ^{S}*yfiN-gfp*	This study
pBAD30-^{S}YhjH$_{GFP}$	P_{BAD}:: ^{S}*yhjH-gfp*	This study
pBAD30-^{S}STM4551$_{GFP}$	P_{BAD}:: ^{S}*stm4551-gfp*	This study

Table 2.2 continued

pBAD30-^{S}YjcC$_{GFP}$	P$_{BAD}$:: ^{S}*yjcC-gfp*	This study
pBAD30-^{S}YfeA$_{GFP}$	P$_{BAD}$:: ^{S}*yfeA-gfp*	This study
pBAD33-^{S}YfiN(GGAAF)$_{GFP}$	P$_{BAD}$:: ^{S}*yfiN*(D327A E328A)-*gfp*	This study
pBAD33-^{S}YfiN$_{YFP}$	P$_{BAD}$:: ^{S}*yfiN-yfp*	This study
pBAD30-^{S}FtsA$_{CFP}$	P$_{BAD}$:: ^{S}*ftsA-cfp*	This study
pBAD33-^{S}SulA	P$_{BAD}$:: ^{S}*sulA*	This study
pBAD30-$^{S}_{CFP}$FtsN	P$_{BAD}$::*cfp*-^{S}*ftsN*	This study
pBAD30-^{E}YfiN$_{GFP}$	P$_{BAD}$:: ^{E}*yfiN-gfp*	This study
pUT18	P$_{lac}$::-*T18*; Amp^{R}	(57)
pUT18C	P$_{lac}$::*T18*-; Amp^{R}	(57)
pKNT25	P$_{lac}$::-*T25*; Kan^{R}	(57)
pUT18-zip	P$_{lac}$:: leucine zipper region from yeast GCN4-*T18*	(57)
pKNT25-zip	P$_{lac}$:: leucine zipper region from yeast GCN4-*T25*	(57)
pUT18-^{E}YfiN	P$_{lac}$:: ^{E}*yfiN-T18*	This study
pUT18-^{E}FtsZ	P$_{lac}$:: ^{E}*ftsZ-T18*	This study
pUT18-^{E}FtsA	P$_{lac}$:: ^{E}*ftsA-T18*	This study
pUT18-^{E}ZipA	P$_{lac}$:: ^{E}*zipA-T18*	This study

Table 2.2 continued

pKNT25-^{E}YfiN	P_{lac}:: ^{E}*yfiN-T25*	This study
pUT18C-^{E}MreB	P_{lac}::*T18-*^{E}*mreB*	This study
pBAD33-^{E}YfiN(GGAAF)$_{GFP}$	P_{BAD}::^{E}*yfiN* (D329A E330A)-*gfp*	This study
pTrc99A-DgcA	P_{trc}::*dgcA* (amplified from pAB551)	This study
pUT18-^{E}YfiN(GGAAF)	P_{lac}:: ^{E}*yfiN* (D329A E330A)-*T18*	This study
pBAD30-DgcA	P_{BAD}::*dgcA*	This study
pBAD33-DgcA	P_{BAD}::*dgcA*	This study
pBAD33-^{E}YfiN$_{GFP}$	P_{BAD}:: ^{E}*yfiN-gfp*	This study
pTrc99A-^{E}YfiR	P_{trc}:: ^{E}*yfiR*	This study
pJN105-^{P}YfiN$_{GFP}$	P_{BAD}:: ^{P}*yfiN-gfp*	This study
pBAD30-^{P}YfiN$_{GFP}$	P_{BAD}:: ^{P}*yfiN-gfp*	This study
pBAD30-^{E}YfiN[^{S}TM^{S}PAS]$_{GFP}$	P_{BAD}::^{E}*yfiN-gfp* (aa21-177 replaced with ^{S}TM and ^{S}PAS)	This study
pBAD30-^{E}YfiN[^{S}PAS]$_{GFP}$	P_{BAD}::^{E}*yfiN-gfp* (aa44-154 replaced with ^{S}PAS)	This study
pBAD30-^{E}YfiN[^{S}TM]$_{GFP}$	P_{BAD}::^{E}*yfiN-gfp* (aa21-43 and aa155-177 replaced with ^{S}TM)	This study
pBAD30-^{E}YfiN[^{P}PAS]$_{GFP}$	P_{BAD}::^{E}*yfiN-gfp* (aa44-154 replaced with ^{P}PAS)	This study
pBAD30-^{S}YfiN[^{E}TM]$_{GFP}$	P_{BAD}::^{S}*yfiN-gfp* (aa20-42 and aa154-176 replaced with ^{E}TM)	This study
pBAD30-^{S}YfiN[^{P}HAMP]$_{GFP}$	P_{BAD}::^{S}*yfiN-gfp* (aa178-232 replaced with ^{P}HAMP)	This study

Table 2.2 continued

pBAD30-^{S}YfiN[^{P}GGDEF]$_{GFP}$	P_{BAD}::^{S}*yfiN-gfp* (aa233-end replaced with ^{P}GGDEF)	This study
pBAD30-^{P}YfiN[^{S}HAMP]$_{GFP}$	P_{BAD}::^{P}*yfiN-gfp* (aa182-236 replaced with ^{S}HAMP)	This study
pBAD30-^{P}YfiN[^{S}GGDEF]$_{GFP}$	P_{BAD}::^{P}*yfiN-gfp* (aa237-end replaced with ^{S}HAMP)	This study
pBAD30-^{P}YfiN[^{S}HAMP^{S}GGDEF]$_{GFP}$	P_{BAD}::^{P}*yfiN-gfp* (aa182-end replaced with ^{S}HAMP)	This study

SWIMMING MOTILITY ASSAY

LB swim plates were made using 0.3% Bacto agar. Plates were inoculated with 5 µl of overnight cultures in the center and incubated at 37°C for 8 (*Salmonella*) or 12 hrs (*E. coli*).

FLUORESCENCE MICROSCOPY

Overnight cultures of cells with plasmids encoding fluorescent fusion proteins were diluted 1:100 in fresh LB medium with antibiotics and grown at 30°C with 0.005% arabinose for 4 hrs (unless otherwise stated). For imaging cells under no stress, a cell suspension (80 µl) was applied to a polylysine-coated slide, incubated for 15 min and washed with LB medium (80 µl) before imaging. For imaging cells under stress (mostly *E. coli*), after 15 min of incubation, cells were washed and treated with LB containing the indicated stress-causing agents (80 µl) and incubated for 30 min before imaging. All slides for microscopy were prepared at room temperature. Stress-induced relocation was not dependent on immobilization by polylysine since it was also observed when stressors were directly added to broth cultures. For the *E. coli* temperature sensitive mutants, after

30 min of stress exposure at room temperature, cells were incubated for another 30 min at the indicated temperature (30°C or 42°C) before microscopy. Images were acquired using an Olympus BX53 microscope, appropriate filters and cellSens standard software (version 1.6) from Olympus, and minimally processed using Adobe Photoshop 11.0.

HADA LABELING

LB Nascent peptidoglycan synthesis was probed by the fluorescent D-amino acid HADA (purchased from M. Van Nieuwenhze at Indiana University) as described previously (62). *Salmonella* 14028 Δ*yfiN* carrying a pBAD33 encoding ^{S}yfiN-yfp was grown at 30°C for 4 hrs with 0.2% glucose or 0.005% arabinose, and HADA was added to a final concentration of 500 μM. After 1 min of incubation at 30°C, cells were fixed in ice-cold 70% ethanol and incubated on ice for 15 min. The fixed cells were washed and resuspended in PBS, and then imaged on 1% agarose pads (62).

BACTERIAL TWO-HYBRID ASSAY

To construct plasmids used for BACTH analysis (57), gene sequences (*yfiN*, *ftsZ*, *ftsA*, *zipA* and *mreB*) were amplified using PCR from the genomic DNA of wild type *E. coli* MG1655. Amplified DNA fragments were introduced between the HindIII and XbaI sites (*yfiN*, *ftsZ* and *zipA*) or between the XbaI and SacI sites (*ftsA*) of pUT18 and pKNT25 vectors, or between the XbaI and BamHI sites (*mreB*) of pUT18C. The *E. coli* K-12 strain XL1-Blue (Stratagene) was used in all of the cloning steps, and DNA sequences of the constructs were verified by sequencing.

For interaction analysis, plasmid combinations of pUT18(C)- and pKNT25- were co-transformed into the *E. coli* strain BTH101. 5 μl of overnight cultures of transformants

were spotted onto LB agar plates supplemented with ampicillin, kanamycin, IPTG (0.5 mM) and 40 μg/ml of 5-bromo-4-chloro-3-indolyl-β-D-galactopyranoside (X-gal). For analysis of c-di-GMP-stimulated interaction, chloramphenicol and arabinose (0.2%) were additionally added to the LB agar plates. Images of the plates were taken after 36 hrs of incubation at 30°C.

QUANTIFICATION OF C-DI-GMP

c-di-GMP concentrations were measured following a previously reported method (63). *E. coli* MG1655 wild type and MG1655 carrying pBAD30-^{E}YfiN$_{GFP}$ cells were grown at 30°C for 4 hrs in 5 ml LB supplemented with 0.005% arabinose (the optical density at 600 nm reached around 1.2). Intracellular nucleotides were extracted with a mixture of acetonitrile/methanol/water (40/40/20, v/v/v) as described earlier (63). Samples were analyzed by liquid chromatography-tandem mass spectrometry (HPLC/MS/MS) at the Metabolomics Core Facility at the University of Texas Health Science Center at San Antonio, using Thermo Fisher Q Exactive mass spectrometer with online separation by a Thermo Fisher/Dionex Ultimate 3000 HPLC. As described (63), 0.1% (v/v) acetic acid in water with 10 mM ammonium acetate was used as LC Solvent A, and Solvent B was methanol. For a standard curve, c-di-GMP and xanthosine 3′, 5′-cyclic monophosphate (cXMP) purchased from Axxora, LLC (San Diego, CA) were used. As internal standard, 1 μM of cXMP was added to the extract.

Chapter 3. Systematic analysis of diguanylate cyclases and phosphodiesterases in *Salmonella*

ABSTRACT

The transition of bacterial behavior between motile and sessile growth is regulated by the signaling molecule cyclic diguanylate (c-di-GMP). In most bacteria, high levels of c-di-GMP impair flagellum/pilus-driven motility and enhance exopolysaccharide production, thereby promoting biofilm formation. Bacterial cells control c-di-GMP metabolism by regulating enzymatic activities of diguanylate cyclases (DGCs) and phosphodiesterases (PDEs). Single bacterial species encodes multiple putative DGC/PDEs, as exemplified by *Salmonella* having 19 such proteins. However, of the multiple DGC/PDEs, only the strong PDE YhjH has been characterized in detail. In addition, previous studies have suggested that individual c-di-GMP-metabolizing enzymes relay signals to downstream processes with high specificity by localizing nearby their targets, but a systematic analysis of subcellular localization of DGC/PDEs has not been performed. By monitoring motility phenotypes of mutants lacking each DGC and PDE, I identified five of these proteins to be active in *Salmonella* under laboratory conditions; these were YhjH, YfiN, STM4551, YjcC and YfeA. Of these five proteins, GFP fusions of YhjH and YfiN showed unique localization patterns, which may be related to their particular cellular roles.

INTRODUCTION

Cyclic-di-GMP, previously reported as an allosteric activator for membrane-bound cellulose synthase, is now known as a second messenger that regulates a bacterial phenotypic switch between motile and sessile growth. Generally, high levels of c-di-GMP lead to surface attachment and biofilm formation by inhibiting motility and stimulating extracellular polysaccharide production.

Intracellular c-di-GMP levels are adjusted by c-di-GMP synthesis and hydrolysis performed respectively by DGCs and PDEs. Bioinformatic studies revealed that single bacterial species encode multiple potential DGCs (identified by GGDEF domains) and PDEs (EAL domains) (25). In *Salmonella*, there are 19 proteins harboring either GGDEF or EAL, or both domains (Table 3.1). Most of the GGDEF/EAL domains are linked to different N-terminal sensory input domains, often flanked by transmembrane helices, thereby allowing regulation of the c-di-GMP metabolizing activities in response to diverse internal/external signals (25, 64). Proteins that have both GGDEF and EAL domains are often bifunctional, selectively regulating the two opposite activities in response to input signals. ScrC in *Vibrio parahaemolyticus*, a protein containing both GGDEF and EAL domains, shows DGC activity when it is alone (65). However, it shows PDE activity when its partner proteins ScrA and ScrB interact in response to extracellular stimuli (65). Some of the GGDEF/EAL domain proteins carry non-conserved/degenerate active site motifs, which have lost their enzymatic activities. However, many of these proteins still function as c-di-GMP signaling components by retaining their ability to bind to c-di-GMP or by interacting with other components. The degenerate GGDEF protein PopA in *C. crescentus* regulates cell differentiation by sensing c-di-GMP through the autoinhibitory (I) site (66). The degenerate EAL domain protein YdiV in *E. coli* neither

degrades nor binds to c-di-GMP, but still involved in the motile-to-sessile transition by binding the master regulator FlhDC and inhibiting flagellum biogenesis (35).

The fluctuating levels of c-di-GMP convey the response to their target cellular processes by regulating the activities of c-di-GMP-binding effectors. The first example of such effectors are PilZ domain proteins. A PilZ domain protein YcgR, controls flagellar motility by sensing the intracellular levels of c-di-GMP in enterobacteria including *E. coli* and *Salmonella*. Once c-di-GMP levels increase either by inactivation of PDEs or activation of DGCs, the c-di-GMP-bound YcgR interacts with the components of the flagellum complex to reduce the flagella rotation speed and/or induce CCW motor bias (32-34). The cellulose synthase BcsA is another PilZ domain protein. Upon c-di-GMP binding, BcsA is activated to synthesize cellulose, the main exopolysaccharide of the biofilm matrix. Although YcgR and BcsA are the only PilZ domain proteins in most enterobacteria, recent studies have revealed alternative mechanisms of c-di-GMP binding, including enzymatically inactive GGDEF/EAL domain proteins and c-di-GMP-binding RNA aptamers (riboswitches) (25).

While several decades of previous research focused on identification of individual domain/proteins that have the abilities to synthesize, degrade or bind to c-di-GMP, how bacteria orchestrate the individual c-di-GMP signaling components to obtain a desired phenotypic output, is still elusive. As described in Chapter 1, it has been proposed that spatial localization of many c-di-GMP signaling components can generate exquisite specificity. This study was initiated to assess whether individual c-di-GMP metabolizing proteins in *Salmonella* display distinct subcellular localization. The first aim was to select active GGDEF/EAL domain proteins that modulate c-di-GMP levels under laboratory conditions. Although *Salmonella* genome encodes 19 proteins that potentially are able to synthesize or degrade c-di-GMP, functions of the proteins other than the strong PDE

YhjH have not been characterized. YhjH is a stand-alone EAL domain protein that keeps the global levels of c-di-GMP low in motile cells, thus mutants lacking YhjH accumulate high levels of c-di-GMP, which inhibit motility and promote biofilm formation (32, 33). The effects of the other 18 proteins on c-di-GMP levels were monitored using a motility assay. Of the 19 proteins, only five, YhjH, YfiN, STM4551, YjcC and YfeA were observed to modulate motility. The localization of these five proteins was examined using green fluorescent protein (GFP) fusions. Of these, only YhjH and YfiN showed distinct localization patterns, one polar and the other at the mid-cell.

Table 3.1 GGDEF/EAL domain proteins in *Salmonella*.

	Domain organization
GGDEF domain proteins	
STM2672 (YfiN)	
STM1987	
STM1283 (YeaJ)	
STM4551	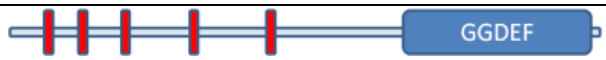
STM0385 (YaiC/AdrA)	
EAL domain proteins	
STM4264 (YjcC)	
STM0468 (YlaB)	
STM1827	
STM0343	
STM2215 (Rtn)	
STM3611 (YhjH)	
Hybrid (GDDEF/EAL) proteins	
STM3388	
STM1703 (YciR)	
Degenerate GGDEF/EAL proteins	
STM2123 (YegE) [GGDEF/WLV]	
STM3375 (YhdA) [HRSDF/ELM]	
STM1344 (YdiV) [EII]	
STM2503 [SGHDL/EAL]	
STM3615 (YhjK) [SGYDF/EAL]	
STM2410 (YfeA) [PGSEL/EAL]	

.

RESULTS AND DISCUSSION

Screen for diguanylate cyclases and phosphodiesterases that modulate intracellular levels of c-di-GMP in *Salmonella*

To see which of the several GGDEF/EAL domain proteins in *Salmonella* are involved in modulating the intracellular levels of c-di-GMP under laboratory conditions, the motility behavior of single mutants was compared to that of wild type in a soft agar plate assay. A single mutation of the well-known PDE YhjH impaired motility, while that of the other 18 GGDEF/EAL domain proteins had no impact on motility (Figure 3.1A). Since it was possible that the strong PDE YhjH masked the contribution of these 18 proteins to cellular c-di-GMP levels, mutants in these genes were constructed in a Δ*yhjH* background. In this background, mutations in two GGDEF domain proteins, YfiN and STM4551, and two EAL domain proteins, YjcC and YfeA, resulted in enhanced or impaired motility, respectively (Figure 3.1B), suggesting that these four proteins, as well as YhjH, are involved with motility regulation by increasing or decreasing c-di-GMP levels in *Salmonella*.

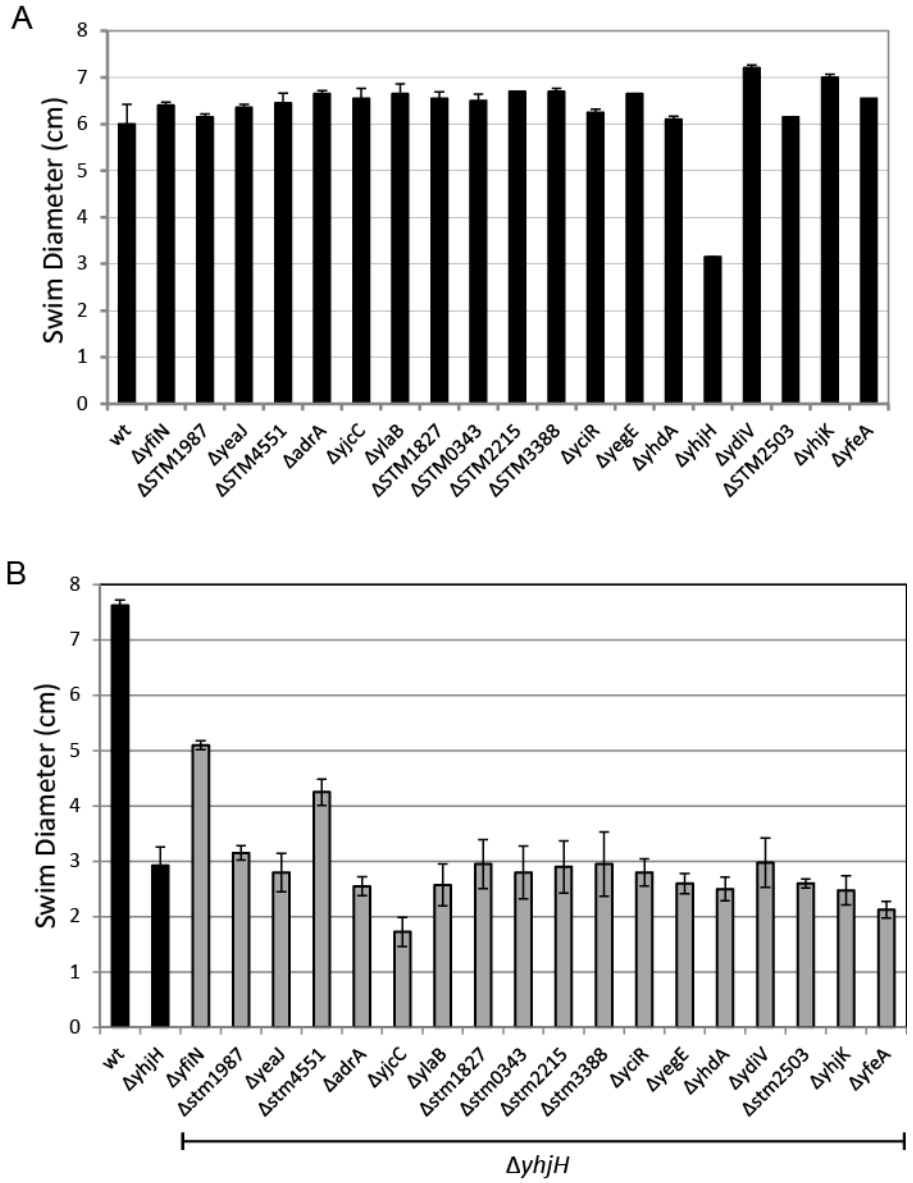

Figure 3.1 Identification of diguanylate cyclases (DGCs) and phosphodiesterases (PDEs) that contribute to motility. Swimming motility of *Salmonella* wild type (14028), and of single gene knockouts of GGDEF/EAL domain proteins in the wild type (A) and in Δ*yhjH* (B) strains. Besides the well-known PDE YhjH, YfiN, STM4551, YjcC and YfeA were also shown to modulate motility. Overnight cultures of each strain were inoculated at the center of 0.3% agar swim plates and incubated at 37°C for 8 hrs. Error bars indicate standard deviation observed in four experimental repeats.

Differential localization of diguanylate cyclases and phosphodiesterases

Several GGDEF/EAL proteins have been reported to have a discrete cellular location or to exist in a complex with their downstream targets (30, 36, 40, 49, 50), prompting us to examine localization of the five GGDEF/EAL proteins that we found to be active as DGC/PDEs under laboratory conditions, YhjH (PDE), YfiN (DGC), STM4551 (DGC), YjcC (PDE) and YfeA (PDE). Fusions of the green fluorescent protein (GFP) to the C termini of the five DGC/PDEs were constructed, and were shown to complement the motility phenotypes of the respective mutants and thus confirmed to be functional (Figure 3.2).

When expressed from an inducible promoter with a low concentration of inducer (0.005% arabinose), the GFP fusion of the cytoplasmic single domain PDE YhjH localized to the pole (Figure 3.3). The polar localization of YhjH was reminiscent of the dynamic polar localization of PdeA in *C. crescentus* (40). The asymmetric cell division of *C. crescentus* generates two daughter cells having opposite characteristics, a motile swarmer cell and a sessile stalked cell. While the newborn stalked cell immediately reinitiates chromosome replication, cell cycle progression is halted in the flagellated swarmer cell by entering into a non-replicative and motile phase. After the period of motility is completed, the swarmer cell transforms into a stalked cell, a transition that is promoted by an increase in the intracellular c-di-GMP levels (38). PdeA was identified as a gatekeeper PDE whose activity is required in swarmer cells in order to prevent premature activation of the swarmer-to-stalked cell transition (40). When the transition is permitted, PdeA dynamically localizes to the ClpXP-occupied old pole to be degraded, thereby allowing an increase in c-di-GMP levels (40). Similar to *C. crescentus*, *E. coli*

cells undergo the motile-to-sessile lifestyle transition while entering stationary phase, which is also known to be driven by c-di-GMP accumulation. In the exponential growth phase, the transition is prevented by the gatekeeper PDE YhjH that maintains the c-di-GMP levels low in motile cells. Although it is known that the expression level of YhjH is down-regulated at the onset of stationery phase by proteolysis of the flagellar master regulator FlhDC that positively controls the expression of *yhjH* (67), there might be an additional mechanism to suppress the action of YhjH at the post-translational level. The polar localization of YhjH-GFP raises the possibility that the activity of YhjH is regulated by sequestering the protein to the pole for proteolysis during the motile-to-sessile transition.

Another example of a PDE localizing to the pole can be found in *P. aeruginosa*. Since *P. aeruginosa* is a uniflagellated bacterium, only one of the two daughter cells inherits a flagellum after cell division. Microscopy analysis using a FRET-based biosensor for c-di-GMP revealed a bimodal distribution of c-di-GMP in the two daughter cells; the flagellated cell always has a lower c-di-GMP concentration than the nonflagellated cell (39). The c-di-GMP heterogeneity of *P. aeruginosa* was found to result from asymmetric partitioning of a specific PDE that forms a complex with chemotaxis machinery at the flagellated pole (47). Interestingly, *Salmonella* with peritrichous flagella also exhibited the bimodal distribution of c-di-GMP upon cell division (39), which could be caused by asymmetric partitioning of polar-localized YhjH. However, it is not obvious what factors recruit YhjH to the pole in *Salmonella*, since the polar localization of YhjH-GFP was retained in a *flhDC* mutant (Figure 3.4), which lacks flagellar and chemotaxis proteins. Also, to ensure biological relevance of the polar localization of YhjH expressed from a multicopy plasmid, further investigation using a

gfp fusion of *yhjH* under the control of its native promoter on the chromosome will be required.

The other four DGC/PDEs, in which at least two transmembrane helices were predicted, showed membrane-distributed localization (Figure 3.3). However, while the PDEs YjcC and YfeA were evenly distributed throughout the membrane, the DGC STM4551 showed a patchy pattern of localization. The most striking localization was found in the DGC YfiN. Cells expressing YfiN-GFP showed a fluorescent band at the cell midpoint and had longer lengths, suggesting that YfiN might block cell division by localizing to the division site. This observation was pursued further, and is described in the next chapter.

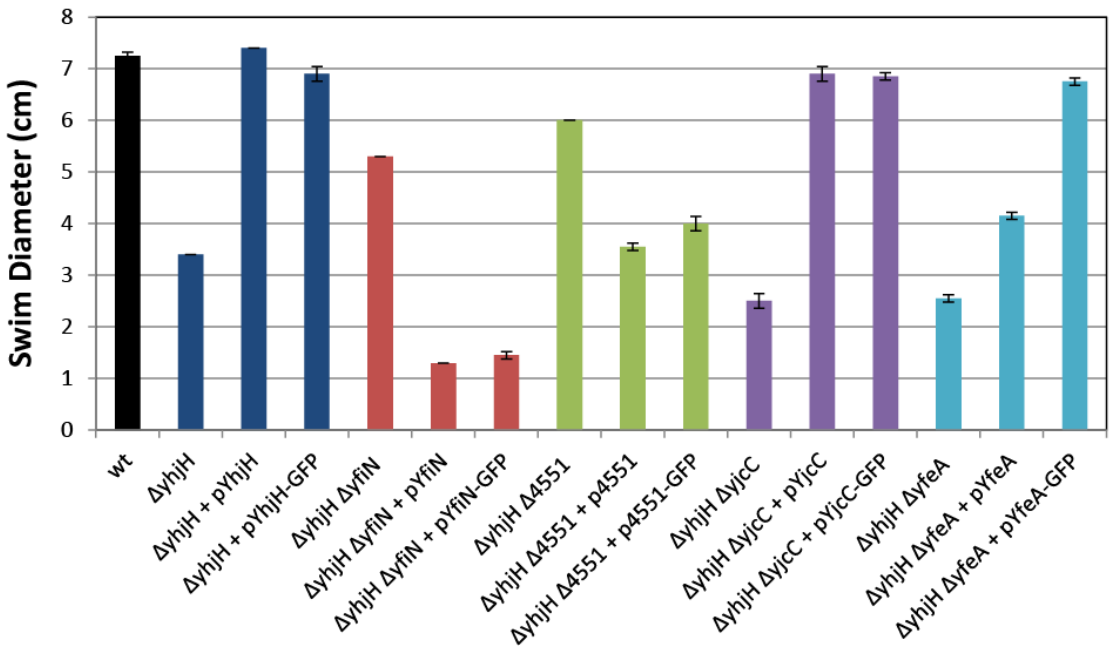

Figure 3.2 GFP fusions of YhjH, YfiN, STM4551, YjcC and YfeA are functional. Overnight cultures of each strain were inoculated at the center of 0.3% agar swim plates containing 0.2% arabinose (inducer) and incubated at 37°C for 8 hrs. The motility phenotypes of mutants were complemented by GFP fusions as well as intact proteins. Error bars indicate standard deviation observed in two experimental repeats.

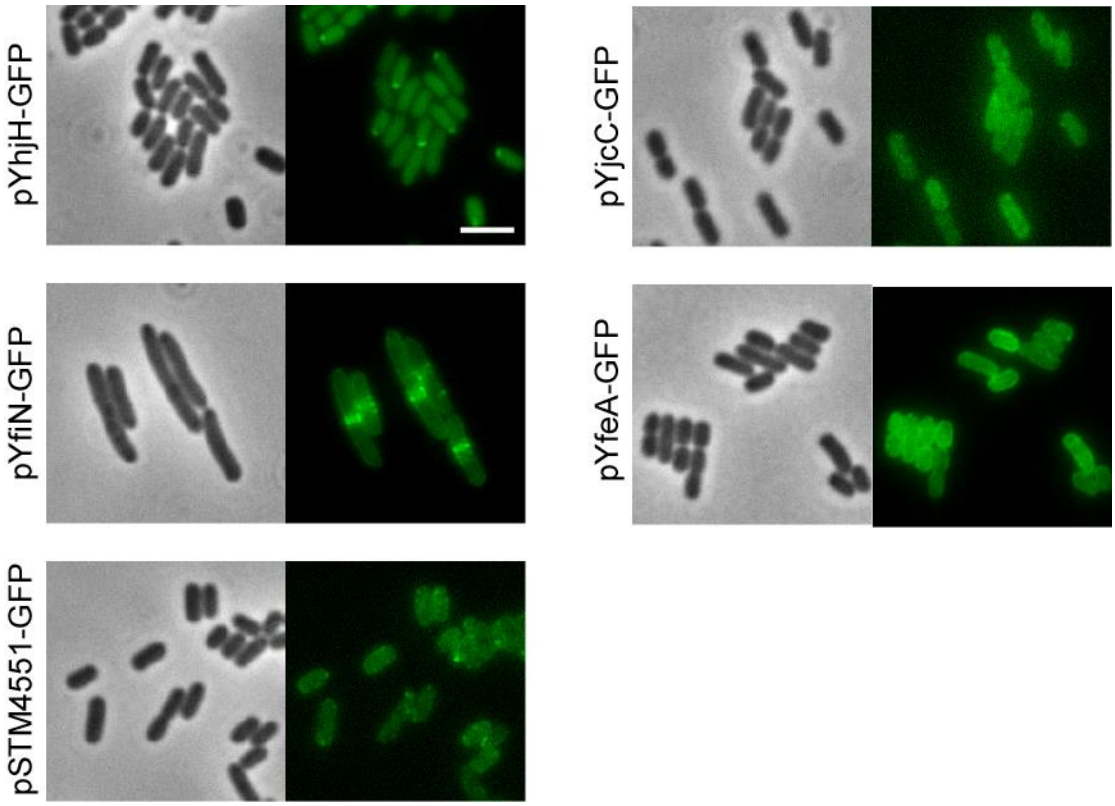

Figure 3.3 Differential localization of DGC/PDEs. Cells expressing the indicated GFP fusion construct were transferred onto 1% agar pad and observed by microscopy. While STM4551, YjcC and YfeA were membrane-distributed, YhjH localized to the pole, and YfiN displayed a ring-like structure at the mid-cell. Scale bar, 3 μm in all images in this study.

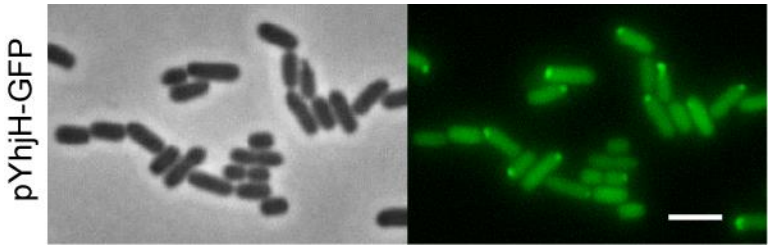

Figure 3.4 The polar localization of YhjH is independent of chemotaxis or flagella complex. Δ*flhDC* mutant cells expressing YhjH-GFP were imaged.

Chapter 4. The diguanylate cyclase YfiN acts as a cell division inhibitor by dynamically localizing to the division site

ABSTRACT

Cell division arrest is a universal checkpoint in response to environmental assaults that generate cellular stress. In bacteria, the cyclic-di-GMP signaling network is one of several signal transduction systems that regulate key processes in response to extra/intracellular stimuli. In this study, I find that the diguanylate cyclase YfiN acts as a bifunctional protein, which produces c-di-GMP in response to reducing stress, and then dynamically relocates to the division site to arrest cell division in response to envelope stress in *E. coli*. YfiN localizes to the Z ring by interacting with early division proteins and stalls cell division by preventing initiation of septal peptidoglycan synthesis. These findings reveal a new role for a diguanylate cyclase in responding to environmental change, as well as a novel mechanism for arresting cell division.

Chapter 4 was adapted from the reference below with permission.

- Kim HK and Harshey RM. A diguanylate cyclase acts as a cell division inhibitor in a two-step response to reductive and envelope stresses. MBio. 2016 Aug 9;7(4). pii: e00822-16. doi: 10.1128/mBio.00822-16.
- Kim HK designed and performed experiments, and wrote the manuscript.

INTRODUCTION

Bacteria sense and respond to environmental signals through a variety of signaling pathways (25, 68, 69). Signaling through the second messenger cyclic di-GMP (c-di-GMP) is ubiquitous in bacteria, where its major role is to control the transition between motile and sessile lifestyles (25, 70). However, recent studies have shown that c-di-GMP also regulates other processes including cell cycle progression, RNA metabolism, resistance to antimicrobial agents, virulence and pathogenesis (36, 71-74).

Cellular c-di-GMP levels are set by enzymes that synthesize and degrade this molecule in response to a variety of external and internal signals, both physical and metabolic. Diguanylate cyclases (DGCs), identifiable by a signature GGDEF active site motif, produce c-di-GMP from GTP, while phosphodiesterases (PDEs), identifiable by an EAL (or HD-GYP) active site motif, degrade c-di-GMP into pGpG (75). Most DGCs and PDEs harbor various N-terminal sensory input domains, which allow environmental and cellular signals to be integrated into the c-di-GMP signaling network. Although several environmental stimuli regulating DGCs and PDEs have been identified (26, 28, 30), the majority of input signals that orchestrate the c-di-GMP signaling network remain to be discovered, especially given the multiplicity of GGDEF/EAL domain proteins in single bacterial species (25).

The DGC YfiN, also called DgcN (24) or TpbB (76), is an inner membrane protein with a PAS (Per-Arnt-Sim)-like domain in the periplasm, and HAMP (Histidine kinases, Adenyl cyclases, Methyl-accepting proteins and Phosphatases) and GGDEF domains in the cytoplasm. YfiN has been identified as a key contributor to intracellular c-di-GMP levels in various bacteria, and all of the YfiN-mediated cellular processes described to date are in keeping with the major role of c-di-GMP in inhibiting motility

and promoting the biofilm state (76-79). In *P. aeruginosa*, where the function of YfiN has been best studied (77, 80), YfiN was found to be regulated by YfiR and YfiB, which are encoded within the same operon (Figure 4.1A). The periplasmic protein YfiR is proposed to inhibit YfiN, the inhibition relieved by reducing conditions that misfold YfiR (80) or by the lipoprotein YfiB that sequesters YfiR to the outer membrane (77) (Figure 4.1B). The *yfi* operon is widespread in Gram-negative bacteria, but does not always encode *yfiB* (80). For example, *yfiB* is absent in *Salmonella* but present in *E. coli* and *P. aeruginosa* (Figure 4.1A). Consistent with the proposal in *P. aeruginosa*, derepression of YfiN caused by disruption of the inhibitor YfiR enhances biofilm formation by activating cellulose production in *E. coli* (79, 81). In *Salmonella*, YfiN was reported to contribute to cellular c-di-GMP levels and inhibit motility through the c-di-GMP receptor YcgR (78). The Yfi system has been suggested to play an important role in host colonization and persistence of *P. aeruginosa* as well as a uropathogenic *E. coli* strain (77, 80, 81). Given the distinct localization of YfiN shown in Chapter 3, I have studied a novel second function for YfiN as an inhibitor of cell division in *E. coli* and *Salmonella* in this chapter, which is a function promoted by interaction of YfiN with components of the division machinery.

Bacterial cell division is orchestrated by the divisome, a dynamic multi-protein assembly that constricts cell envelope layers at the mid-cell, timed with completion of DNA replication (82-85). Cell division proteins assemble into the divisome broadly in two steps (84, 85). In an early step, well before the onset of cell constriction and while the cell is still elongating, the tubulin-like protein FtsZ forms a ring at the mid-cell, which is anchored to the membrane by two proteins, FtsA and ZipA (83, 84). Once assembled, this Z ring recruits downstream components to form a constriction-competent complex,

which coordinates septum synthesis and invagination (cytokinesis) (84, 85). While FtsA and ZipA play redundant roles in anchoring the Z ring to the membrane, they are both essential for cytokinesis (55, 83, 84). FtsZ assembly is the major target of cell division checkpoints sensing various stresses including DNA damage, defective cell wall synthesis and nutrient starvation (86-89). Here I show that in both *E. coli* and *Salmonella*, YfiN localizes to the mid-cell in a Z ring-dependent manner and halts cell division without disassembling the Z ring, but blocking its further progress toward cytokinesis. In *E. coli*, the mid-cell localization of YfiN, which requires FtsZ and ZipA, is stimulated by multiple conditions that cause cell envelope stress. The data suggest that while the primary role of the DGC YfiN is to promote biofilm formation under reducing conditions, it has a second role in inhibiting cell division in response to envelope stress.

Since the experiments described below study YfiN from three different bacteria – *E. coli, S. enterica* and *P. aeruginosa* – I will henceforth use the superscripts E, S and P, respectively, to indicate the bacterial source of YfiN or other proteins as necessary. I will also use the subscripts GFP, YFP and CFP for fluorescent fusions, placed before or after the protein to indicate N- or C-terminal locations, respectively.

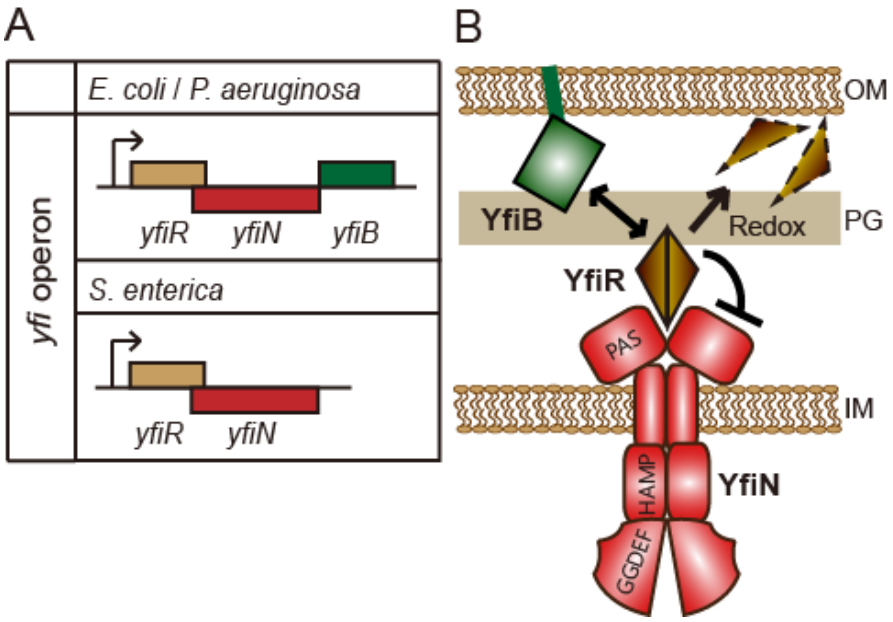

Figure 4.1 The components of the Yfi system. (A) *yfi* operon organization in various bacteria. (B) Function of the Yfi system and YfiN domain organization as deduced from studies in *P. aeruginosa* (77, 80).

RESULTS

YfiN accumulates at the mid-cell in a Z ring-dependent manner and negatively regulates cell division in *Salmonella*

A fusion of the green fluorescent protein (GFP) to *Salmonella* YfiN ($^{S}YfiN_{GFP}$) displayed a fluorescent band at the mid-cell in Δ*yfiN* (Figure 4.2), which implicated YfiN in cell division. Some of the cells displayed spiral-like structures (Figure 4.2, right panel), suggesting that YfiN may associate with the Z ring whose intermediate structures in various bacteria appear in a spiral/helical configuration at the mid-cell (90-92). The cytoskeleton protein MreB has also been proposed to polymerize into helical structures in the cell (93). However, $^{S}YfiN_{GFP}$ maintained its structures in the presence of A22, an inhibitor of MreB polymerization (Figure 4.3), indicating the mid-cell localization of YfiN is independent of MreB. Interestingly, when $^{S}YfiN_{GFP}$ was at the mid-cell, no visible cell constriction could be observed (Figure 4.2), whereas in cells with a constriction, $^{S}YfiN_{GFP}$ was at the quarter positions, which are future division sites (Figure 4.2, arrowheads). These observations indicate that YfiN is likely recruited to the mid-cell by early division proteins such as FtsZ, FtsA and ZipA, prior to constriction.

To detect co-localization of ^{S}YfiN with FtsZ, we used FtsA, the essential division protein that anchors FtsZ to the membrane (83), as proxy, because cells expressing FtsZ fluorescent fusions grew poorly. In cells co-expressing $^{S}YfiN_{YFP}$ and $^{S}FtsA_{CFP}$, the two proteins co-localized within rings at the mid-cell in a majority of the cells (Figure 4.4A), and also within spiral structures along the length of the cell (Figure 4.4A; bottom panels). When the Z ring was disassembled by expression of the SOS cell division inhibitor SulA (94), $^{S}YfiN_{GFP}$ failed to localize to the mid-cell (Figure 4.4B). These results suggest that the recruitment of YfiN to the division site is dependent on assembly of the Z ring.

The accumulation of ^{S}YfiN at the division site was accompanied by cell lengthening in an inducer (arabinose) concentration-dependent manner: at 0.2% inducer concentration, cells were approximately twice as long as without inducer (Figure 4.2 and 4.5A), indicating that cell division is blocked by YfiN. In addition, cells expressing either ^{S}YfiN or ^{S}YfiN$_{GFP}$ showed a growth defect concomitant with the mid-cell accumulation of ^{S}YfiN$_{GFP}$ (Figure 4.5B). No cell lengthening or growth defect was observed in cells overexpressing a constitutively active DGC, DgcA, from *Caulobacter crescentus* (58) (Figure 4.5B), indicating that the cell division defect caused by YfiN is not merely a consequence of elevated c-di-GMP levels.

Absence of a visible mid-cell invagination and a moderate cell lengthening in cells expressing ^{S}YfiN suggests that YfiN inhibits Z ring constriction as well as septal peptidoglycan (PG) synthesis. Constriction begins after the last essential division protein FtsN is recruited to the mid-cell, whose arrival has been suggested to activate septal PG synthesis (95, 96). To determine whether YfiN prevents recruitment of FtsN, we examined localization of $_{CFP}^{S}$FtsN in cells expressing ^{S}YfiN$_{YFP}$. The majority of cells (79.5%: n=239) expressing both proteins showed the presence of either one or the other protein, but not both, at the mid-cell (Figure 4.6A). While no cell showed colocalization of ^{S}YfiN$_{YFP}$ and $_{CFP}^{S}$FtsN at the mid-cell, some cells that showed a visible septal invagination (10.4%) exhibited distinct localization of the two fluorescent proteins, with ^{S}YfiN$_{YFP}$ at the quarter positions (Figure 4.6A, arrowheads) and $_{CFP}^{S}$FtsN at the constricting septum (arrows).

To examine the effects of YfiN on PG synthesis, we made a use of a fluorescent D-amino acid that labels sites of nascent PG synthesis through incorporation into the cell wall (62). In the majority of cells in which expression of ^{S}YfiN$_{YFP}$ was repressed by

glucose, the blue-fluorescent D-amino acid HADA was found incorporated as a band at the mid-cell, regardless of whether a cell constriction was visible (Figure 4.6B). In contrast, when expression of $^{S}YfiN_{YFP}$ was induced by arabinose, the number of cells showing HADA at the mid-cell decreased from 72.6% to 5.6% (Figure 4.6B, compare +glu to +ara), which indicates that YfiN inhibits septal PG synthesis. In the 5.6% of cells that showed HADA at the constriction site, $^{S}YfiN_{YFP}$ was exclusively at the quarter sites (Figure 4.6B, arrowheads). The stalled septal PG synthesis and the distinct localization patterns of YfiN and FtsN raise the possibility that YfiN accumulation prevents the Z ring from maturing into a constriction-competent division complex, possibly by inhibiting the recruitment of late division proteins.

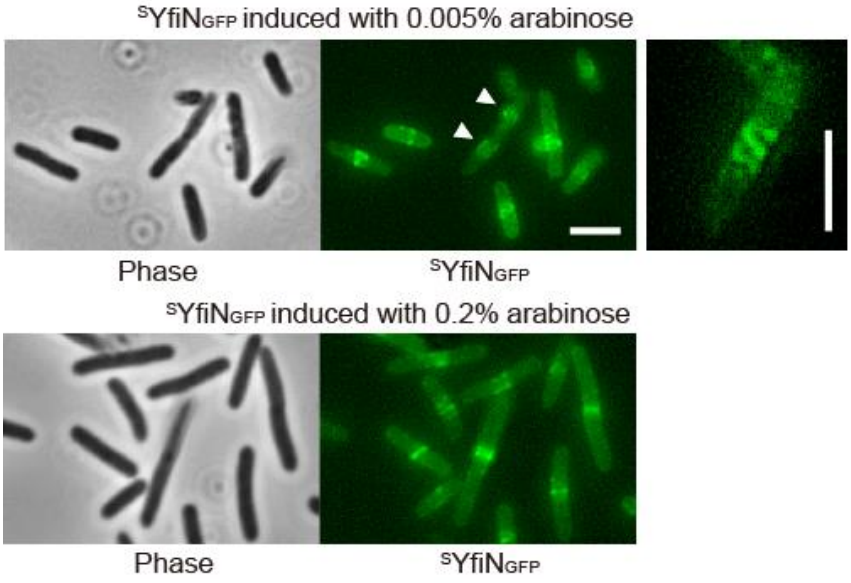

Figure 4.2 YfiN localizes at the mid-cell. Phase contrast and fluorescent images of $^{S}YfiN_{GFP}$ expressed from pBAD30 with different concentrations of inducer arabinose (0.005 and 0.2%) in a *Salmonella* Δ*yfiN* background are shown. Unless otherwise noted, all strains in this chapter were grown with 0.005% arabinose at 30°C for 4 hrs before imaging.

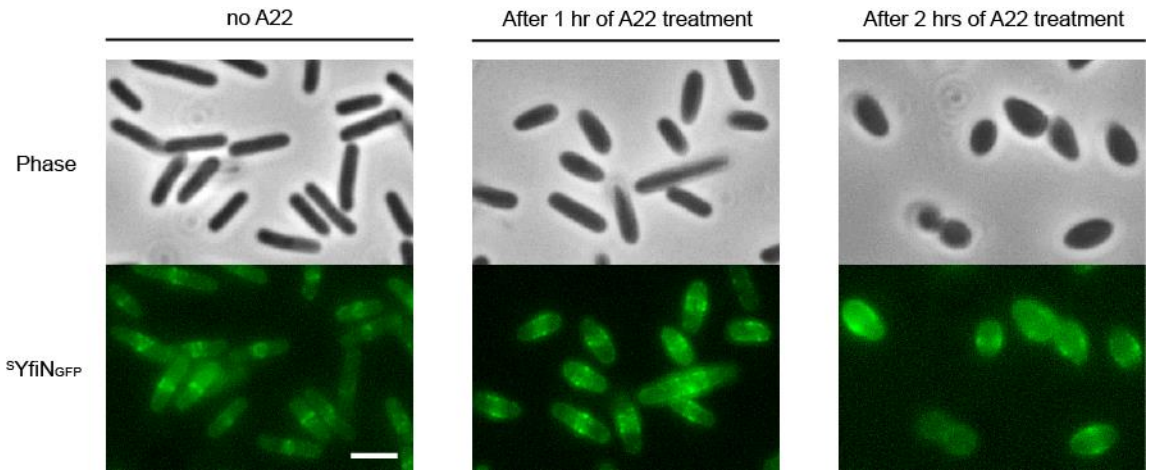

Figure 4.3 YfiN localization in the absence and presence of A22, an inhibitor of MreB. *Salmonella* Δ*yfiN* cells expressing $^{S}YfiN_{GFP}$ were treated with 5 μg/ml A22 for the indicated times. While cell morphology was affected by A22, it did not alter the mid-cell localization of YfiN.

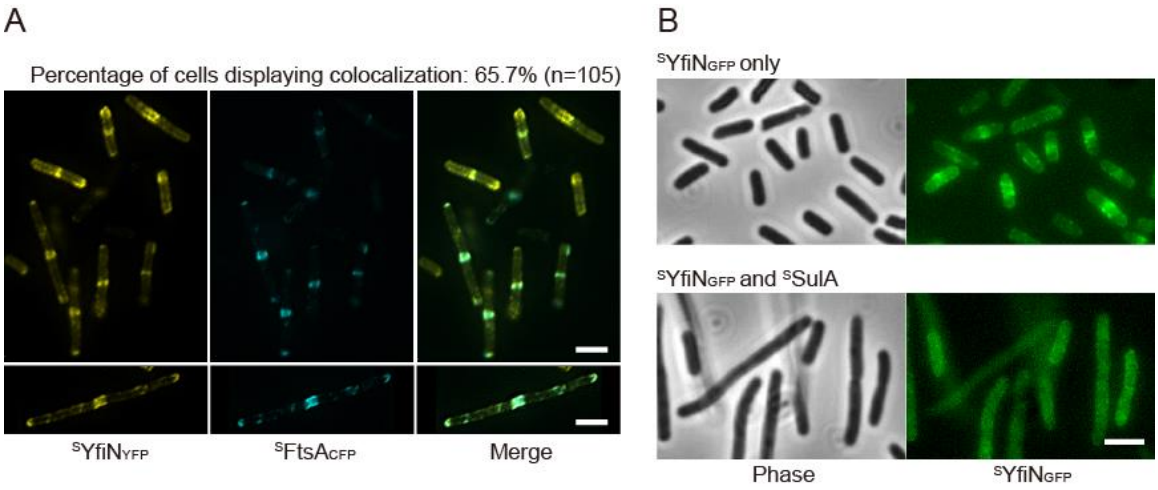

Figure 4.4 YfiN mid-cell localization requires the Z ring. (A) Co-localization of YfiN and FtsA. $^{S}YfiN_{YFP}$ and $^{S}FtsA_{CFP}$ were co-expressed from pBAD plasmids in Δ*yfiN* cells. (B) Localization of YfiN in the absence and presence of SulA. After 3 hrs of growth, expression of $^{S}YfiN_{GFP}$ and ^{S}SulA from pBAD plasmids was induced in a Δ*yfiN* strain, and cells were grown for one further hour before imaging.

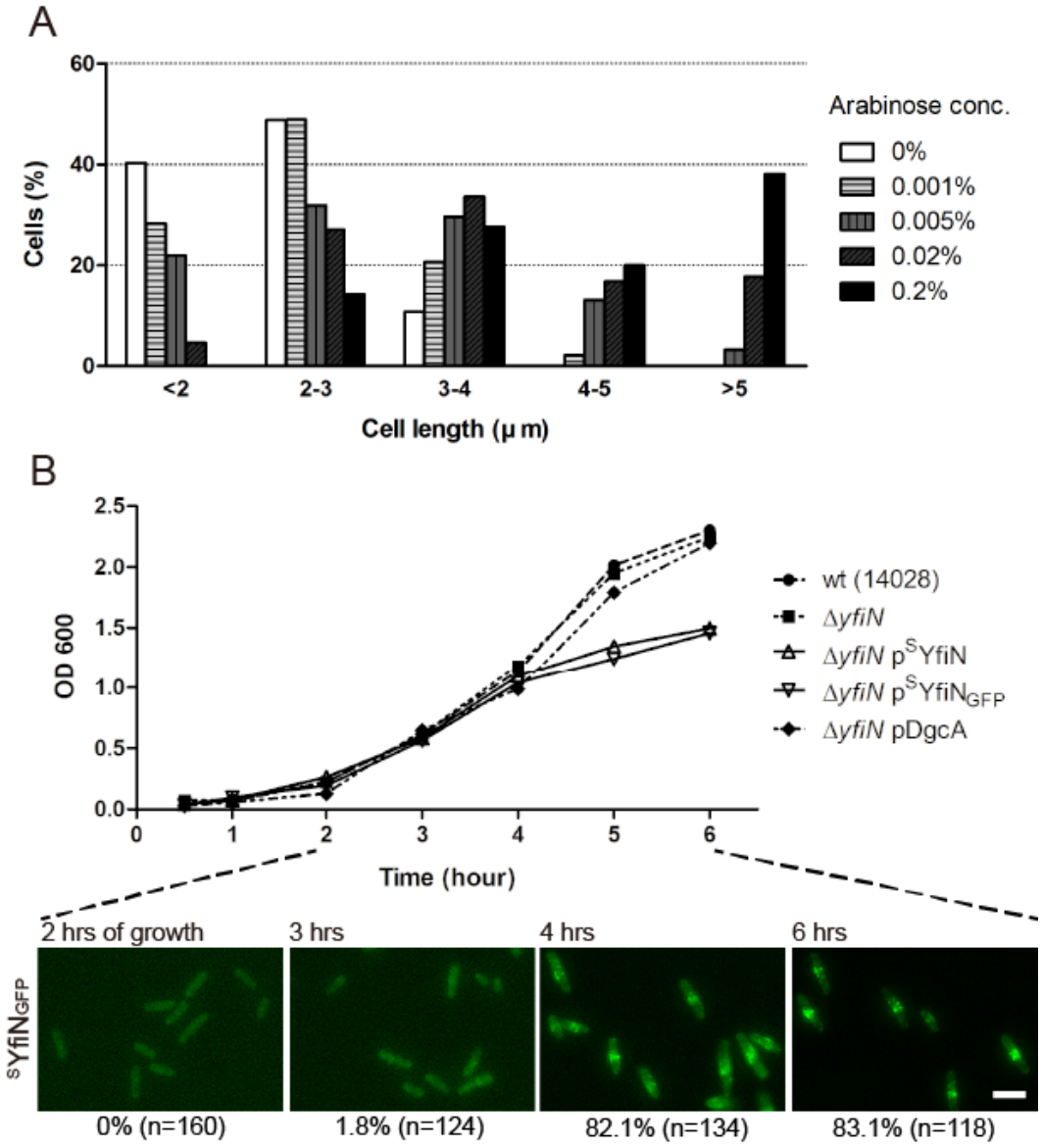

Figure 4.5 YfiN mid-cell localization leads to cell lengthening and growth defect. (A) Histogram of cell length distribution of Δ*yfiN* cells expressing ^{S}YfiN with different concentrations of inducer arabinose. Cell length was measured manually as the distance between two poles, and the distribution is shown as percentage of cells in the indicated range. Cell numbers (n) in arabinose 0%: n=154; 0.001%: n=192; 0.005%: n=191; 0.02%: n=197; 0.2%: n=210. (B) Growth curves of wild-type (14028), its derivative Δ*yfiN* and Δ*yfiN* expressing ^{S}YfiN, ^{S}YfiN$_{GFP}$ or DgcA from pBAD30. Inducer arabinose (0.005%) was added at time 0 in this experiment, and localization of ^{S}YfiN$_{GFP}$ at selected time points is shown below. The numbers at the bottom of the image panel indicate % of cells showing ^{S}YfiN$_{GFP}$ at the mid-cell (n=total number of cells counted).

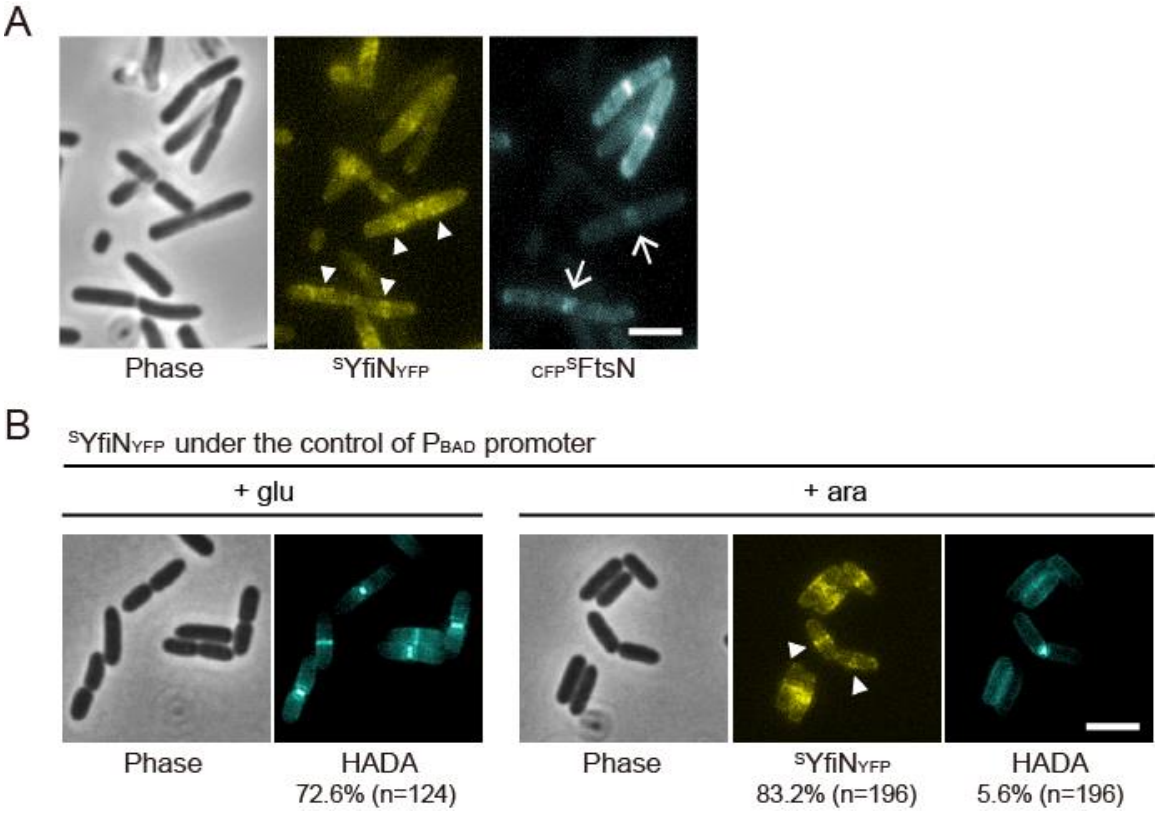

Figure 4.6 YfiN accumulation at the mid-cell inhibits septal PG synthesis. (A) Localization of YfiN and FtsN. $^{S}YfiN_{YFP}$ and $^{S}{}_{CFP}FtsN$ were co-expressed from pBAD plasmids in Δ*yfiN* cells. (B) Nascent peptidoglycan synthesis in cells expressing YfiN. Δ*yfiN* cells expressing $^{S}YfiN_{YFP}$ from pBAD33 were grown with either glucose or arabinose, and labeled with the blue fluorescent D-amino acid HADA for 1 min. The numbers at the bottom indicate % of cells displaying HADA or $^{S}YfiN_{YFP}$ at the mid-cell.

YfiN is recruited to the division site in response to cell envelope stress in *E. coli*

To determine if YfiN has the same cell division arrest function in the closely related bacterium *E. coli*, a GFP fusion of *E. coli* YfiN ($^{E}YfiN_{GFP}$) was constructed and confirmed to be functional (Figure 4.7). When measured by using liquid chromatography-tandem mass spectrometry, the intracellular c-di-GMP concentration of cells expressing $^{E}YfiN_{GFP}$ was 14.46 μM while that of wild type cells was 0.23 μM, confirming the c-di-GMP synthetic activity of $^{E}YfiN_{GFP}$. $^{E}YfiN_{GFP}$ expressed in an *E. coli* Δ*yfiN* background localized to the mid-cell concomitant with a growth defect (Figure 4.8), similar to the result in Figure 4.5B. A membrane-dispersed localization of $^{E}YfiN_{GFP}$ was clearly evident until the mid-log phase (after 4 hrs of growth), and one or more hours of further growth was required for $^{E}YfiN_{GFP}$ to relocate to the mid-cell (Figure 4.8).

The relocation of $^{E}YfiN_{GFP}$ to the mid-cell near the stationary phase of growth suggested that the mid-cell localization might be a response to depletion of nutrients, changes in pH or some other stressful condition. Previous studies in *P. aeruginosa* and *E. coli* have shown that misfolding of the periplasmic inhibitor YfiR caused by reducing environments leads to activation of YfiN, identifying reducing stress as one of the input signals of the Yfi system (79, 80). Additionally, in *P. aeruginosa*, the Yfi system was proposed to contribute to biofilm formation under cell envelope stress conditions such as osmotic upshift and exposure to the detergent sodium dodecyl sulfate (SDS) (80). To identify input stimuli that promote the observed $^{E}YfiN$ relocation to the mid-cell, I tested conditions suggested to activate the Yfi system in previous studies and a variety of other stressors as well, including nutrient starvation and acid stress. Cells producing $^{E}YfiN_{GFP}$ were exposed to a stress condition after 4 hrs of growth, when $^{E}YfiN_{GFP}$ was still dispersed throughout the membrane (Figure 4.8). Of the many stressors tested, only the

following conditions were observed to trigger $^{E}YfiN_{GFP}$ relocation within 30 min of exposure at room temperature: osmotic upshift with either NaCl (250 mM) or sucrose (10%), and treatment with the envelope-targeting antibiotic polymyxin B (PMB; 2.5 μg/ml) (Figure 4.9A). No new protein synthesis was required for this response (Figure 4.9B).

PMB, a polycationic molecule, is thought to increase cell permeability in Gram-negative bacteria by interacting with both the outer (OM) and inner membranes (IM) in a dual mechanism of action (97-99). PMB first binds to the negative charges on LPS and removes the divalent cations that stabilize the LPS structure (97, 98). This results in an increase in OM permeability, which allows PMB to penetrate into the IM, causing leakage of cell contents and cell death (97, 98). To determine whether alteration of the OM or the IM stimulates the $^{E}YfiN$ relocation, I tested two more agents, EDTA (ethylenediaminetetraacetate) and polymyxin B nonapeptide (PMBN). EDTA is a strong divalent cation chelator known to disrupt the OM in the same manner as PMB, but EDTA is not an IM stressor (97, 99). The polymyxin derivative PMBN is less lethal than PMB due to the absence of the fatty acid tail required for the IM disruption, but PMBN still retains the ability to permeabilize the OM (97). Both of the OM permeabilizing agents, EDTA (10 mM) and PMBN (200 μg/ml), induced mid-cell localization of $^{E}YfiN_{GFP}$ (Figure 4.10A), indicating that OM disruption is most likely the trigger for $^{E}YfiN$ relocation. In agreement with the known property of high divalent cation concentrations in blocking the effect of PMB on OM permeabilization (97), addition of external $MgCl_2$ (10 mM) prevented PMB treatment from triggering $^{E}YfiN_{GFP}$ relocation (Figure 4.10B). Other membrane-targeting agents, including a β-lactam antibiotic, SDS and lysozyme failed to relocate $^{E}YfiN_{GFP}$ (Figure 4.11). Taken together, these data suggest that envelope

stress caused by osmotic upshift or OM permeabilization by divalent ion extraction is the input signal for ^{E}YfiN to relocate to the division site.

While $^{E}YfiN_{GFP}$ relocated to the mid-cell in response to envelope stress, the same conditions had no impact on $^{S}YfiN_{GFP}$ localization in *Salmonella* (Figure 4.12). This observation led us to hypothesize that the lipoprotein YfiB, which is absent in *Salmonella,* might function as a sensor that couples envelope stress to ^{E}YfiN localization. It is worth noting that YfiB is a structural homolog of Pal, a component of the Tol-Pal complex that plays a crucial role in maintaining OM integrity in Gram-negative bacteria (100, 101). However, in a *yfiB* knockout mutant of *E. coli*, $^{E}YfiN_{GFP}$ still retained its ability to relocate upon envelope stress (Figure 4.13), indicating that YfiB is not involved in the ^{E}YfiN relocation.

Next, we fused GFP to the *yfiN* chromosomal locus in *E. coli* to observe localization of endogenously expressed ^{E}YfiN. However, $^{E}YfiN_{GFP}$ expressed under its native promoter failed to display enough fluorescence to be observed regardless of exposure to stress (not shown). When the native promoter was replaced with an inducible promoter (P_{BAD}), $^{E}YfiN_{GFP}$ expressed from the chromosomal locus was able to show relocation upon the envelope stress (Figure 4.14). These data suggest that a single copy on the chromosome is sufficient to produce ^{E}YfiN serving as a cell division inhibitor, but it requires activation at the transcriptional level by as yet unknown signals.

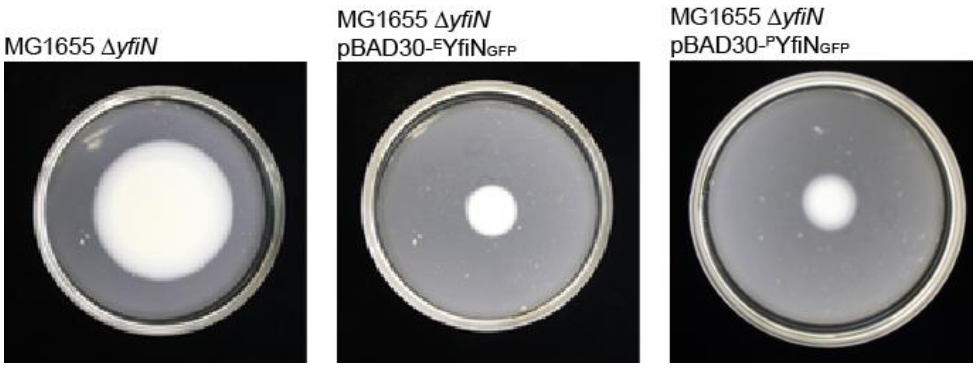

Figure 4.7 *E. coli* and *P. aeruginosa* YfiN-GFP fusions are functional as measured by a motility assay. $^{E}YfiN_{GFP}$ and $^{P}YfiN_{GFP}$ were induced by 0.2% arabinose in *E. coli* Δ*yfiN*.

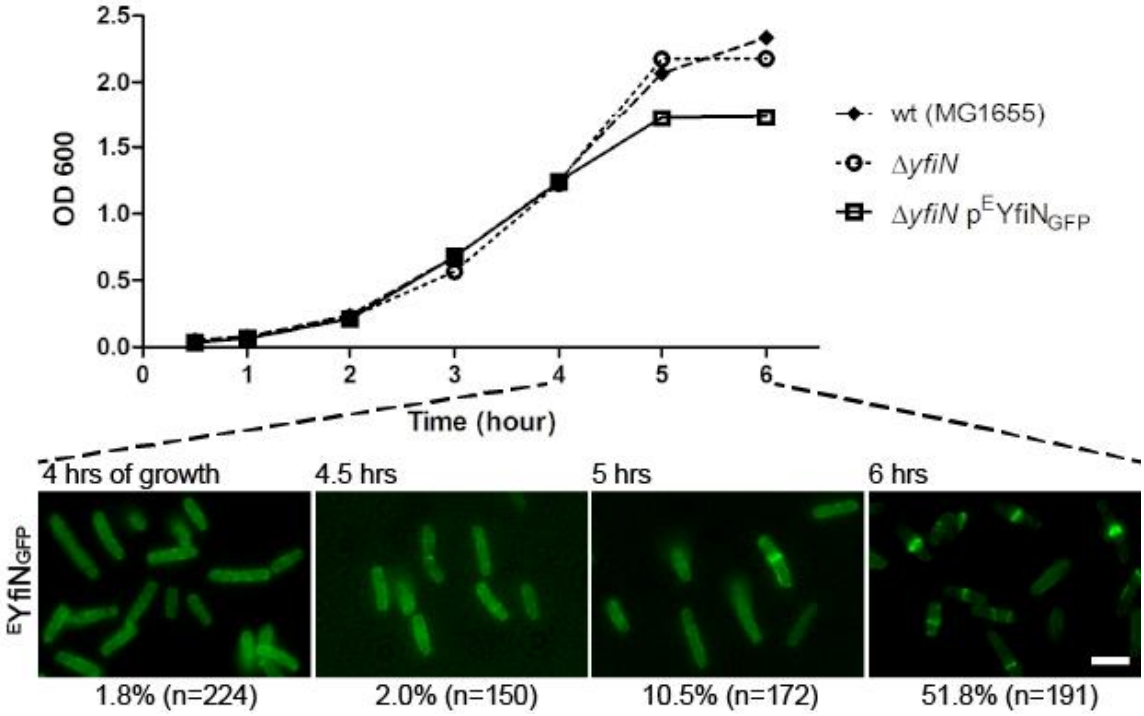

Figure 4.8 YfiN localization in *E. coli*. Growth curves of *E. coli* wild type (MG1655), Δ*yfiN* and Δ*yfiN* cells expressing $^{E}YfiN_{GFP}$ from pBAD30 with inducer arabinose added at time 0. Localization of $^{E}YfiN_{GFP}$ at selected time points is shown below. YfiN relocated to the mid-cell at the onset of stationary phase.

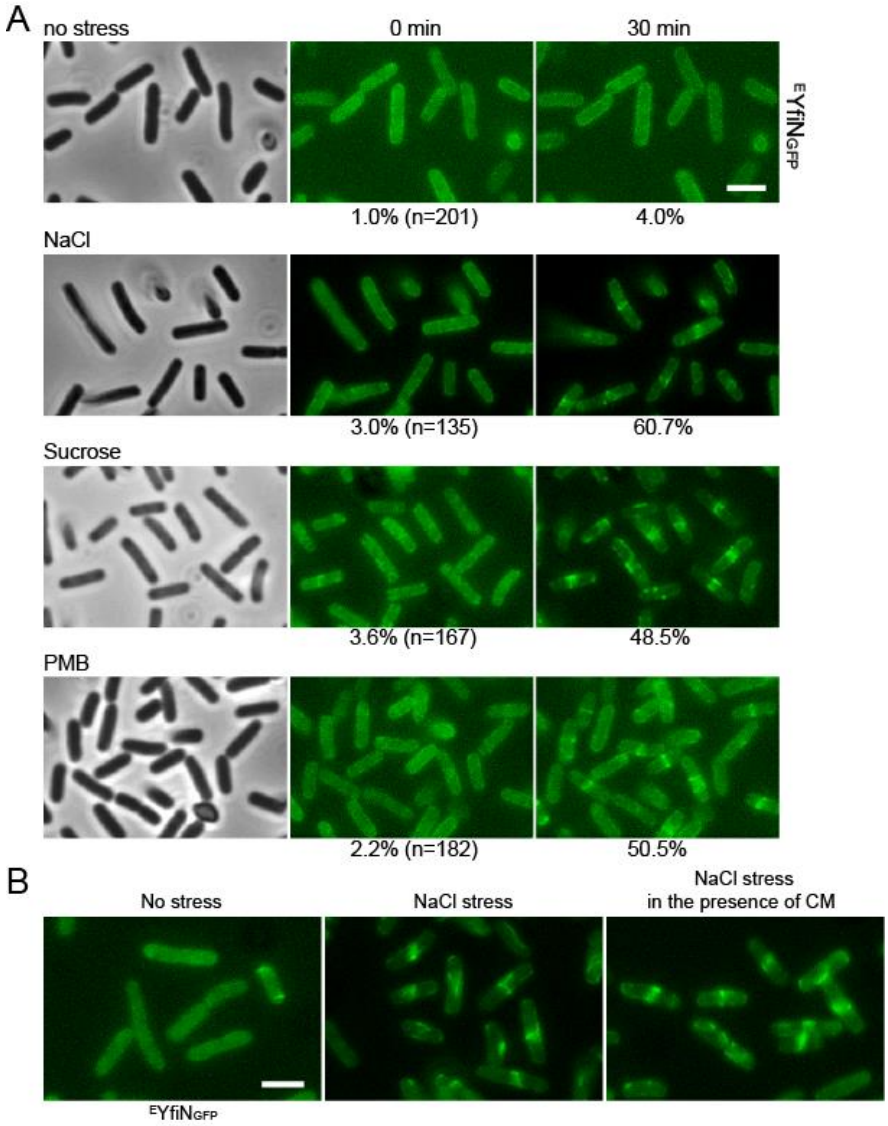

Figure 4.9 *E.coli* YfiN relocates to the mid-cell upon envelope stress. (A) *E. coli* Δ*yfiN* cells expressing $^{E}YfiN_{GFP}$ were exposed to the indicated stresses. The same microscope fields were photographed before and 30 min after exposure to no stress (LB medium only), osmotic upshift (LB with 250 mM additional NaCl or 10% sucrose) or envelope permeabilization (LB with 2.5 µg/ml PMB). For each stressor, the same field of cells were observed to count the fraction of cells showing mid-cell foci. (B) ^{E}YfiN relocation to the mid-cell in presence of the protein synthesis inhibitor chloramphenicol (CM). *E. coli* Δ*yfiN* cells expressing $^{E}YfiN_{GFP}$ were exposed to no stress, 250 mM NaCl and 250 mM NaCl in the presence of CM (300 µg/ml).

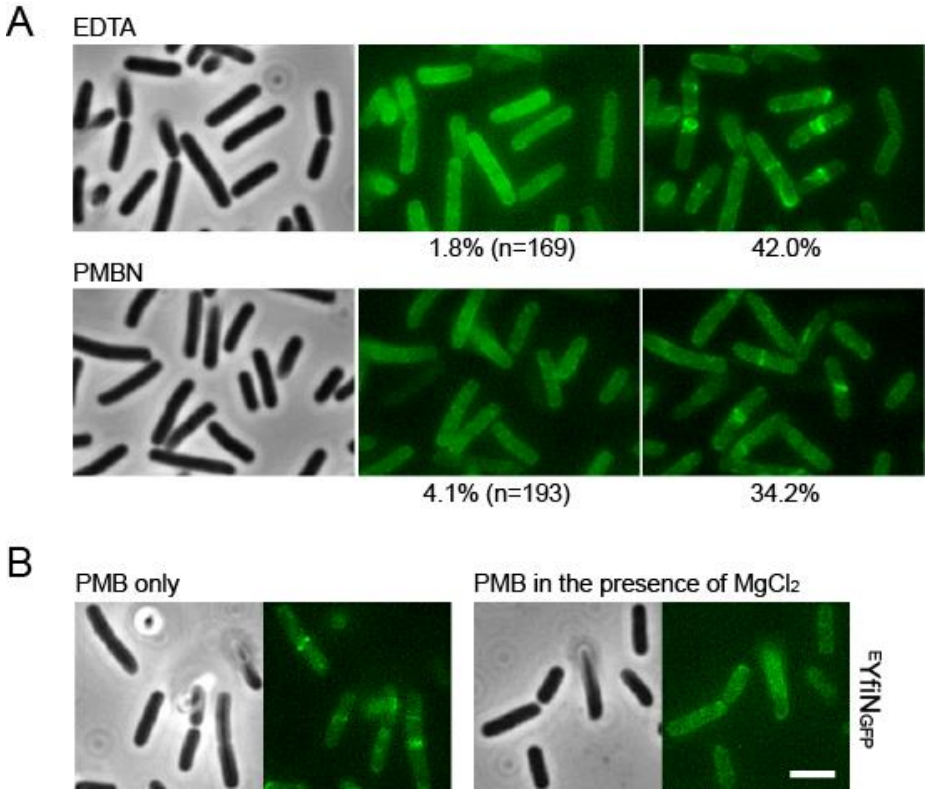

Figure 4.10 OM permeabilization triggers YfiN relocation to the mid-cell. (A) *E. coli* Δ*yfiN* cells expressing $^{E}YfiN_{GFP}$ were exposed to 10 mM EDTA or 200 µg/ml PMBN for 30 min. (B) Effect of additional Mg^{2+} on PMB-triggered ^{E}YfiN relocation. *E. coli* Δ*yfiN* cells expressing $^{E}YfiN_{GFP}$ were exposed to 2.5 µg/ml PMB for 30 min in the absence and presence of 10 mM $MgCl_2$.

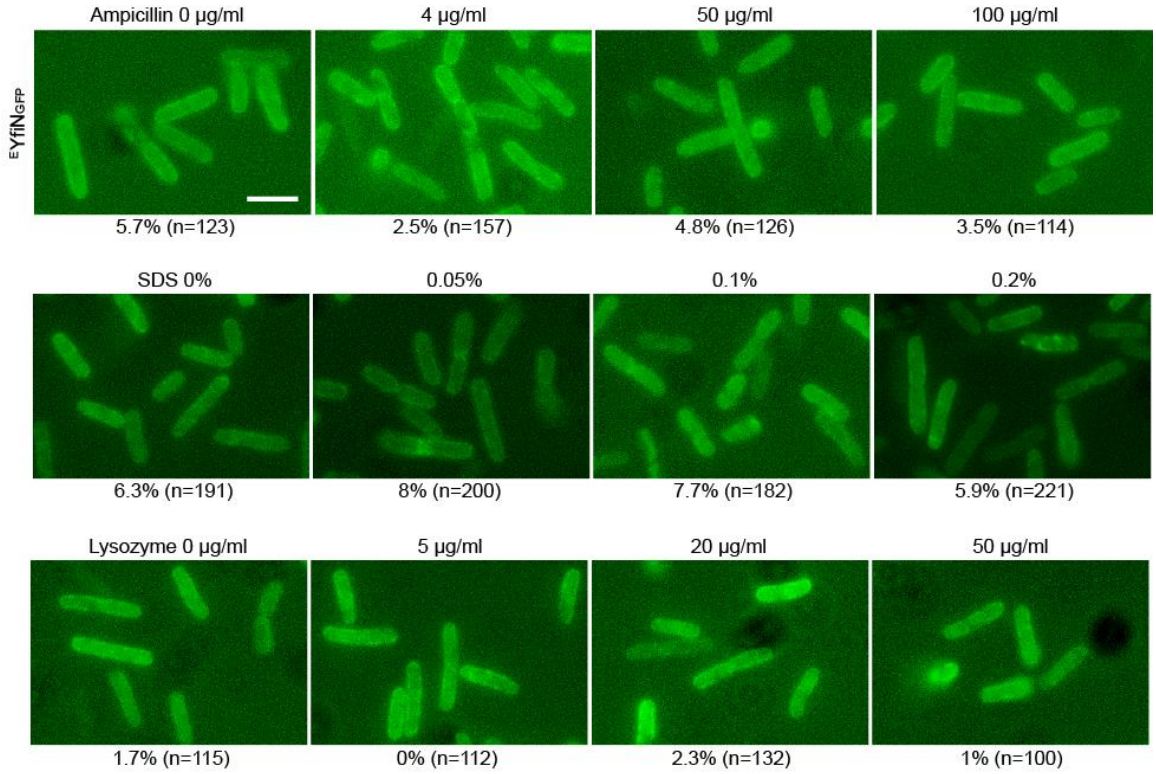

Figure 4.11 Effects of other envelope-targeting stress conditions on *E.coli* YfiN localization. Ampicillin, sodium dodecyl sulfate (SDS) and lysozyme failed to induce ^{E}YfiN relocation. *E. coli* Δ*yfiN* cells expressing $^{E}YfiN_{GFP}$ were grown in LB with inducer at 30°C for 4 hrs, and then exposed to the indicated stress condition in LB for 30 min.

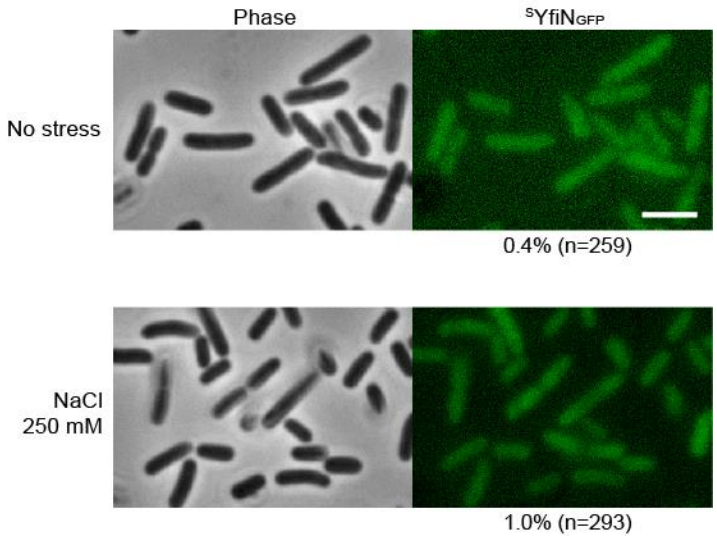

Figure 4.12 Effect of envelope stress on SYfiN localization. *Salmonella* Δ*yfiN* cells expressing SYfiNGFP were grown in LB with inducer at 30°C for 3 hrs, and then exposed to no stress or 250 mM NaCl for 30 min. SYfiN localization was not affected by envelope stress. The numbers at the bottom indicate % of cells showing SYfiNGFP at the mid-cell.

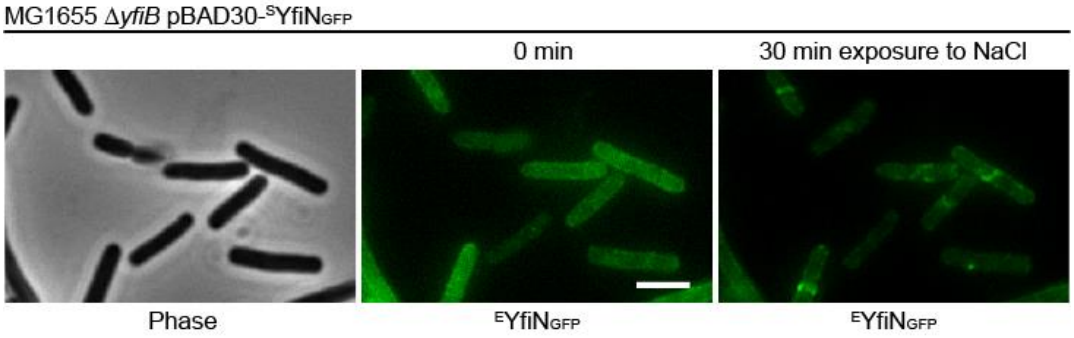

(Figure 4.13: continued next page)

Figure 4.13 ^{E}YfiN relocation is independent of YfiB. *E. coli* Δ*yfiB* cells expressing ^{E}YfiN$_{GFP}$ were exposed to osmotic upshift. The same microscope field was photographed before and 30 min after exposure to 250 mM NaCl.

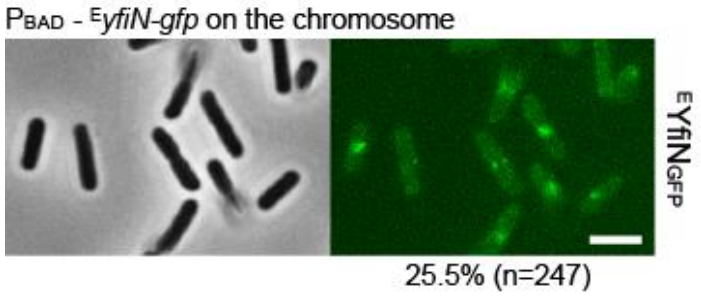

Figure 4.14 Localization of *E. coli* YfiN$_{GFP}$ expressed from the chromosomal inducible promoter. *E. coli yfiR::kan* mutant strain, in which ^{E}*yfiN-gfp* is encoded under the P$_{BAD}$ promoter on the chromosome, was grown with arabinose at 30°C for 4 hrs and exposed to 250 mM NaCl for 30 min.

Localization of YfiN to the division site is dependent on its interaction with FtsZ and ZipA in *E. coli*

Having observed that ^{S}YfiN is associated with the Z ring (Figure 4.4), we monitored ^{E}YfiN$_{GFP}$ localization in temperature-sensitive mutants of *E. coli* cell division proteins in order to validate specific binding targets of ^{E}YfiN. We used *ftsZ84* (WM1125), *ftsA12* (WM1115) and *zipA1* (PS223) mutant strains that are defective in assembly/recruitment of the respective protein to the division site at the non-permissive temperature (42°C). The essential division proteins FtsA and ZipA serve as redundant membrane anchors for the Z ring (55, 83). At the non-permissive temperature (42°C), lack of Z ring assembly in *ftsZ84* results in loss of localization of all divisome components (102). The absence of either FtsA or ZipA in *ftsA12 or zipA1* at 42°C is not expected to disrupt the Z ring because FtsZ remains at the mid-cell as long as either one of these proteins is present, but assembly of downstream components that mediate cytokinesis is inhibited in both of these mutants (55, 102).

The *E. coli* mutant cells expressing ^{E}YfiN$_{GFP}$ were first exposed to PMB for 30 min at room temperature to promote ^{E}YfiN relocation, and then shifted to 30° or 42°C for another 30 min. At 30°C, ^{E}YfiN$_{GFP}$ remained in spiral/ring structures at the mid-cell in a wild type background and in all the three mutants (Figure 4.15A). At 42°C, while wild type cells maintained ^{E}YfiN$_{GFP}$ at the mid-cell, both *ftsZ84* and *zipA1* mutants lost the localization and showed dispersed clusters of ^{E}YfiN$_{GFP}$ (Figure 4.15A), suggesting that ^{E}FtsZ and ^{E}ZipA are essential for ^{E}YfiN localization. In contrast, ^{E}YfiN$_{GFP}$ localization was unaffected in the *ftsA12* mutant at 42°C (Figure 4.15A), indicating that ^{E}YfiN$_{GFP}$ localization to the mid-cell does not require ^{E}FtsA, and therefore also does not require cell division components that act downstream of ^{E}FtsA. NaCl was not used as a stressor in these experiments because the *ftsZ84* mutation can be suppressed by high salt (103).

However, similar results were obtained when EDTA was used as a stressor (Figure 4.15B). In summary, these data show that ^{E}YfiN localization at the mid-cell depends on the ^{E}FtsZ ring and its ^{E}ZipA tether, but not on ^{E}FtsA or downstream events known to be dependent on ^{E}FtsA assembly.

To further investigate interactions between ^{E}YfiN and the cell division proteins, the bacterial adenylate cyclase two-hybrid (BACTH) assay was performed. The BACTH assay has been used successfully for analyzing interactions between membrane proteins, including cell division and cytoskeleton proteins (104, 105). For this assay, FtsZ, FtsA, ZipA and YfiN from *E. coli* were fused to two fragments of the *Bordetella pertusis* adenylate cyclase, T18 and T25, and their interaction was monitored by measuring the synthesis of β-galactosidase, which is dependent on the adenylate cyclase activity. The results showed self-interaction of ^{E}YfiN (Figure 4.15C), which is expected because dimerization is required for DGCs to exert their enzymatic activity (64). A positive result was obtained with ^{E}YfiN and either ^{E}FtsZ or ^{E}ZipA, supporting their interaction (Figure 4.14C). No interaction was detected between ^{E}YfiN and ^{E}FtsA (Figure 4.15C), in agreement with the persistence of ^{E}YfiN$_{GFP}$ at the mid-cell in the *ftsA12* mutant at 42°C (Figure 4.15A and B). The cytoskeletal protein ^{E}MreB, previously shown to co-localize with ^{E}FtsZ and directly interact with it using the BACTH assay (105), showed interaction with ^{E}FtsZ but not with ^{E}YfiN (Figure 4.15D). Taken together, the data in Figure 4.15 show that ^{E}YfiN relocation at the mid-cell is dependent on ^{E}FtsZ and ^{E}ZipA, but not on ^{E}FtsA or ^{E}MreB.

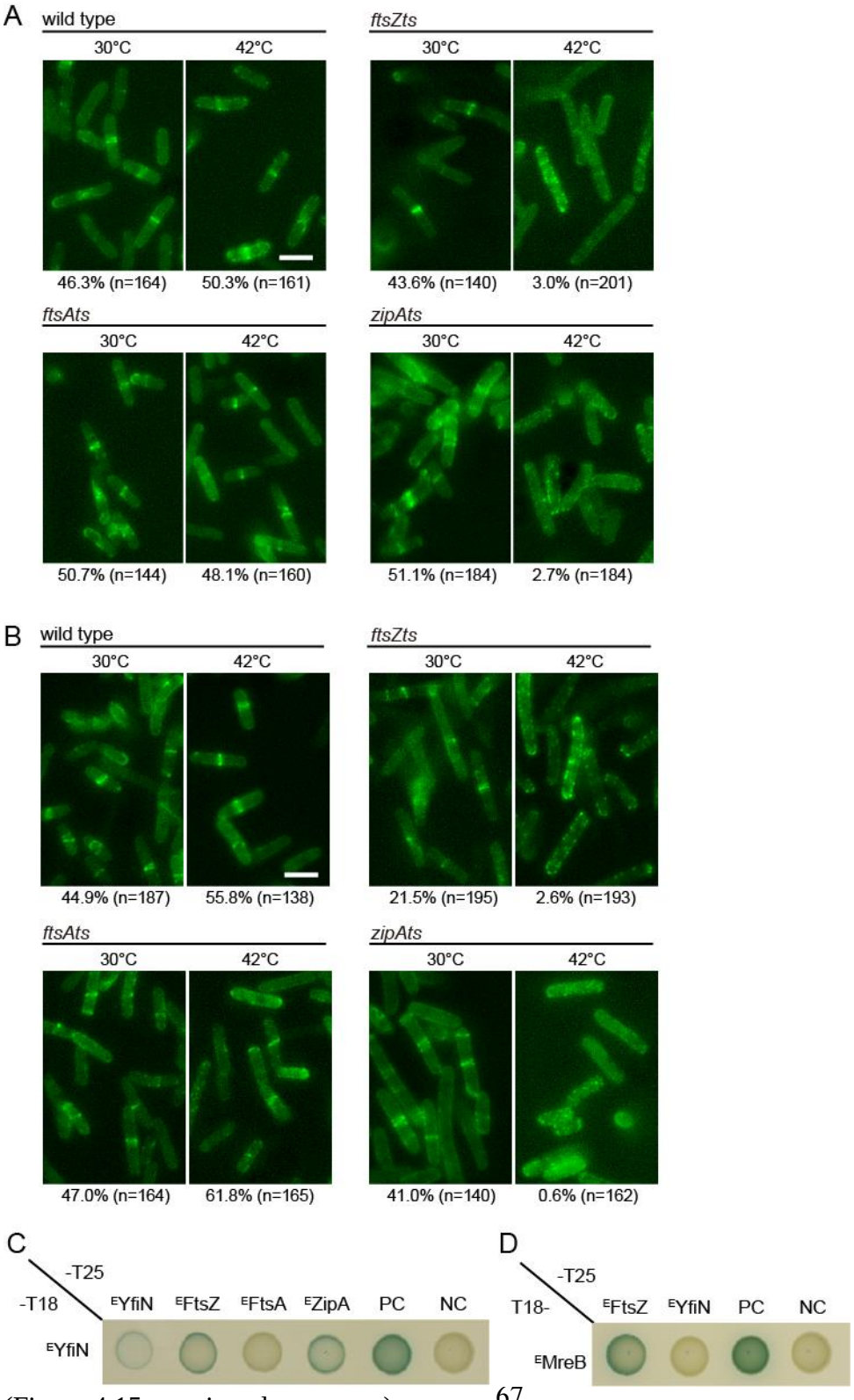

(Figure 4.15: continued next page)

Figure 4.15 YfiN interacts with FtsZ and ZipA in *E. coli*. (A and B) Localization of $^{E}YfiN_{GFP}$ in wild type (MG1655) and temperature sensitive mutants of cell division proteins in *E. coli*. For each strain, cells producing $^{E}YfiN_{GFP}$ were exposed to 2.5 μg/ml PMB (A) or 10 mM EDTA (B) for 30 min. Following the exposure, cells were incubated for another 30 min at two different temperatures, 30° and 42°C, before imaging. (C and D) Bacterial adenylate cyclase two-hybrid (BACTH) analysis of *E. coli* division proteins (C) and MreB (D) against ^{E}YfiN. PC, positive control (T18-leucine zipper/T25-leucine zipper); NC, negative control (T18/T25 empty vectors).

High intracellular c-di-GMP is required for mid-cell localization of YfiN in *E. coli*

Given the unexpected role of the c-di-GMP synthetic enzyme YfiN in cell division regulation, we wondered whether the DGC activity of YfiN was required for its cell division arrest function, or whether this was a separate function of YfiN. We therefore inactivated the DGC active site of $^{E}YfiN_{GFP}$ (GGDEF→GGAAF). Like the wild type protein, the mutant protein was evenly distributed throughout the membrane before exposure to stress, but failed to localize to the mid-cell when exposed to osmotic upshift (Figure 4.16A), suggesting that relocation to the division site is dependent on the DGC activity. To determine whether the requirement for the DGC activity can be bypassed by high levels of c-di-GMP, we artificially provided c-di-GMP by expressing the constitutively active heterologous DGC DgcA (58). Under this condition, the mutant ^{E}YfiN was able to relocate to the mid-cell in response to envelope stress (Figure 4.16B). This suggests that high intracellular c-di-GMP levels are required for ^{E}YfiN to interact with cell division proteins. To assess the c-di-GMP dependence of YfiN interaction with division proteins, BACTH analysis was performed again. The interaction of the mutant ^{E}YfiN with ^{E}FtsZ or ^{E}ZipA was observed to be strengthened in the presence of DgcA (Figure 4.16C), consistent with the localization data (Figure 4.16B). These results suggest two possible models: 1) c-di-GMP directly binds to ^{E}YfiN, which then causes its direct interaction with cell division proteins, and 2) c-di-GMP indirectly promotes ^{E}YfiN interaction with cell division proteins via some other factor that binds c-di-GMP.

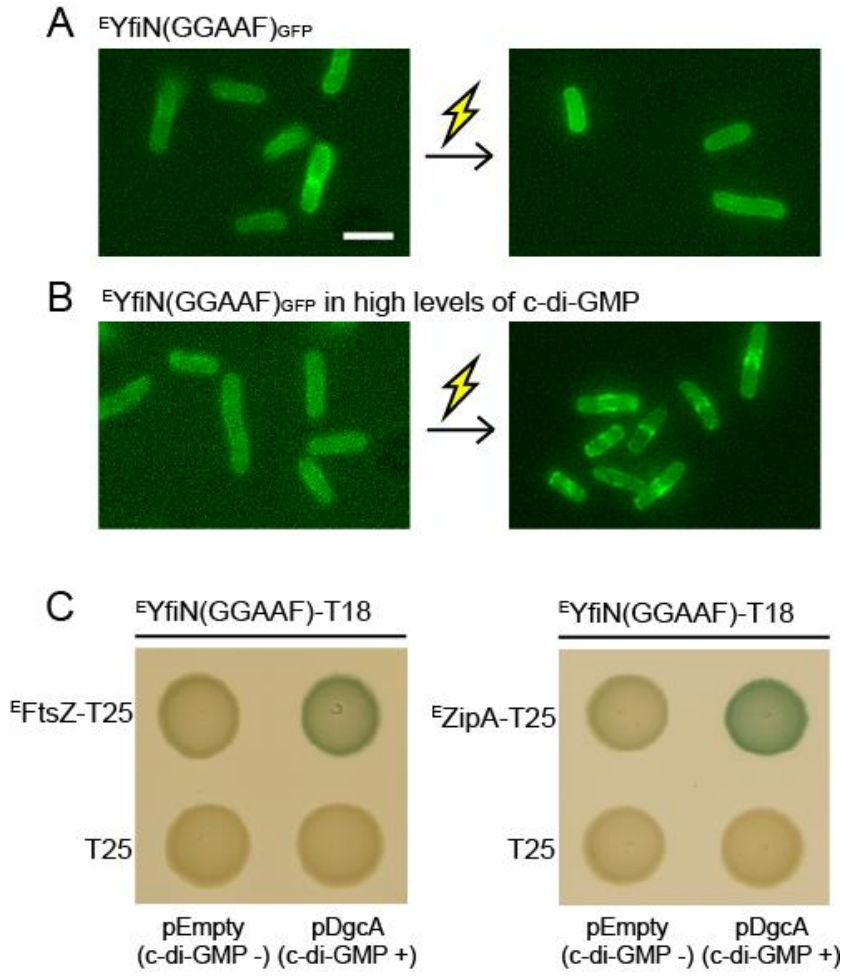

Figure 4.16 High levels of c-di-GMP provided by a heterologous DGC restore mid-cell relocation of an active site mutant of *E. coli* YfiN. (A and B) *E. coli* Δ*yfiN* cells expressing ^{E}YfiN(GGAAF)$_{GFP}$ alone (A) or with the *C. crescentus* DGC DgcA (B) were grown at 30°C for 4 hrs and exposed to 250 mM NaCl. Images were taken before and 30 min after the osmotic upshift. Thunderbolt represents envelope stress. (C) BACTH analysis of c-di-GMP-stimulated interaction between ^{E}YfiN(GGAAF) and cell division proteins ^{E}FtsZ and ^{E}ZipA. Along with the T18 and T25 constructs, each strain contains an empty pBAD33 or a plasmid carrying *dgcA*, whose expression was induced with 0.2% arabinose. Overexpression of DgcA alone did not affect the results of BACTH as shown with control strains in the bottom row.

Mid-cell relocation of YfiN in response to envelope stress requires release of its periplasmic inhibitor YfiR by reductive stress in *E. coli*

The periplasmic protein YfiR inhibits the c-di-GMP synthetic activity of YfiN by interacting with the PAS-like domain of YfiN in the periplasm (77, 79, 81). To assess if YfiR also counteracts the function of YfiN in cell division, ^{E}YfiR was co-expressed with ^{E}YfiN$_{GFP}$ in *E. coli*. In the presence of ^{E}YfiR, ^{E}YfiN$_{GFP}$ remained localized throughout the membrane and failed to relocate to the mid-cell when exposed to envelope stress (Figure 4.17A and B). These results indicate that ^{E}YfiR is a repressor of the cell division arrest function of ^{E}YfiN as well.

Previous studies in *P. aeruginosa* and *E. coli* suggested that YfiR is a periplasmic redox sensor that regulates YfiN activity in response to reducing conditions (79, 80). YfiR has two pairs of conserved cysteine residues whose intramolecular disulfide bonds play important roles in dimerization (106). Reducing environments are thought to disrupt the disulfide bonds in YfiR, thus derepressing YfiN (79, 80, 106). To test if the inhibitory effect of ^{E}YfiR on ^{E}YfiN relocation can be relieved by reducing conditions, *E. coli* cells co-expressing ^{E}YfiN$_{GFP}$ and ^{E}YfiR were treated with the reducing agent dithiothreitol (DTT). When DTT was added to a final concentration of 10 mM for 1 hr prior to envelope stress exposure, ^{E}YfiR lost its ability to repress ^{E}YfiN relocation (Figure 4.17C). Similar results were obtained in the absence of DsbA, a protein responsible for disulfide bond formation in periplasmic proteins (Figure 4.17D). The inactivation of disulfide bonding system (DSB) has been reported to relieve the repression of YfiN by YfiR (79, 80). Under both reducing conditions (Figure 4.17C and D), ^{E}YfiN remained dispersed in the membrane until exposed to envelope stress, which indicates that release of ^{E}YfiR is required but not sufficient for relocation of ^{E}YfiN. These results were also supported in an *yfiR* knockout mutant (Figure 4.17E).

Overall, these data identify ^{E}YfiN as a sensor that detects two different extracellular signals. A reducing stress signal is required to inactivate the inhibitor ^{E}YfiR and turn on the DGC activity of ^{E}YfiN, which is essential for responding to envelope stress and relocating to the mid-cell (Figure 4.16). Thus, ^{E}YfiN senses and responds to two sequential signals – reducing and envelope stress – before arresting cell division.

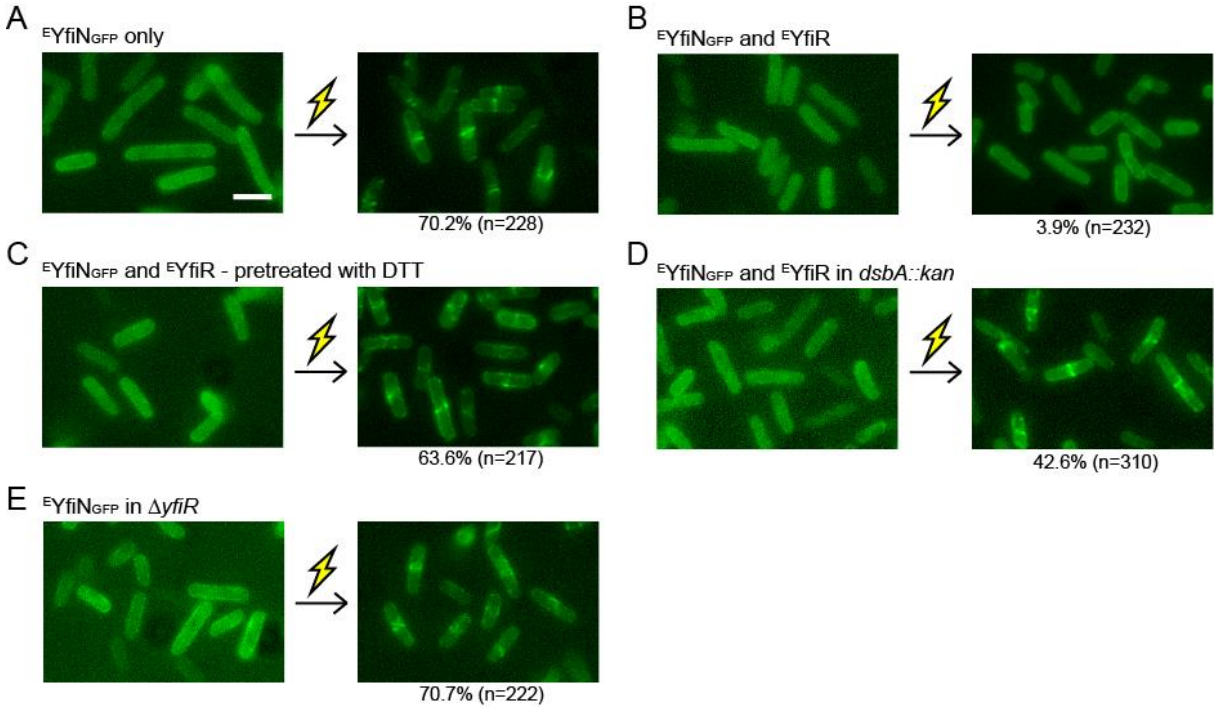

Figure 4.17 YfiR prevents YfiN relocation to the mid-cell in *E. coli*. Cells were grown with inducer at 30°C for 4 hrs and exposed to 250 mM NaCl. Images were taken before and 30 min after the osmotic upshift. Thunderbolt, envelope stress. (A) *E. coli* Δ*yfiN* cells expressing ^{E}YfiN$_{GFP}$ only. (B) *E. coli* Δ*yfiN* cells expressing ^{E}YfiN$_{GFP}$ and ^{E}YfiR. (C) *E. coli* Δ*yfiN* cells expressing ^{E}YfiN$_{GFP}$ and ^{E}YfiR. 10 mM DTT was added to the culture 1 hour prior to osmotic upshift. (D) *E. coli dsbA::kan* cells expressing ^{E}YfiN$_{GFP}$ and ^{E}YfiR. (E) *E. coli* Δ*yfiR* cells expressing ^{E}YfiN$_{GFP}$ only.

YfiN upregulation offers protection against polymyxin B in *E. coli*

The dynamic relocation of ^{E}YfiN to the division site in response to potentially lethal envelope stressors suggests that this response might provide protection and/or facilitate adaptation under such conditions. To test this, we examined the following several strains for their susceptibility to PMB: *E. coli* MG1655 wild type, Δ*yfiN* mutant, *yfiN-gfp* at its native chromosomal locus, Δ*yfiR* and Δ*yfiR* with ^{E}YfiN$_{GFP}$ expressed from the chromosomal inducible promoter (also used in Figure 4.14). Of these strains, only the one with ectopic expression of ^{E}YfiN from the chromosomal inducible promoter showed an approximately 10-fold increase in survival to 30 min of exposure to PMB (2.5 μg/ml) (Figure 4.18). While these data do not address whether the division arrest function of ^{E}YfiN is the cause of increased cell survival, it implicates ^{E}YfiN in participating in bacterial defense mechanisms against envelope stress. There was no difference in survival between wild type and Δ*yfiN* (Figure 4.18), indicating that the ^{E}*yfiN* gene under the control of its native promoter needs to be upregulated by unknown signals in order to offer protection. The data also show that the protection against PMB is not simply a consequence of elevated c-di-GMP levels, because overexpression of DgcA did not increase survival (Figure 4.18).

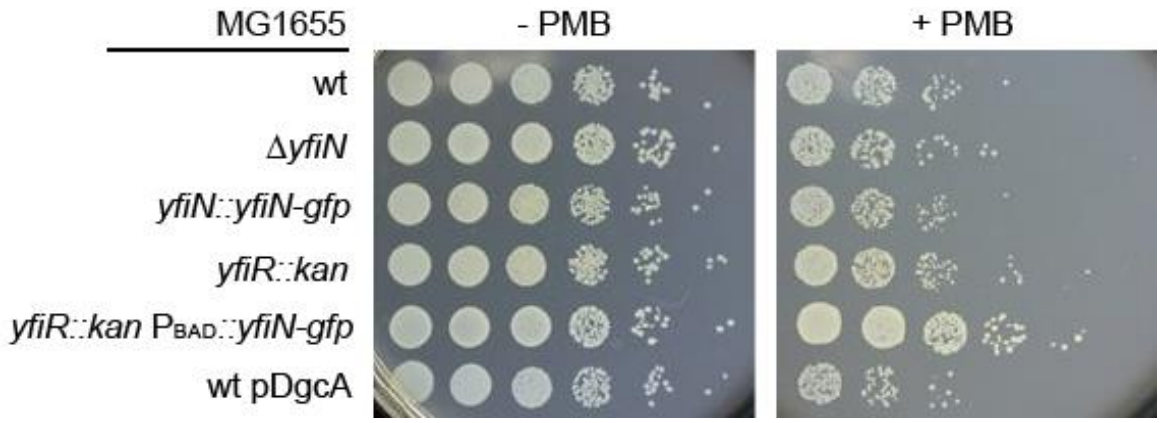

Figure 4.18 Ectopically expressed YfiN enhances cell viability after exposure to polymyxin B in *E. coli*. After growth to the mid-log phase (at 30°C for 4 hrs) with 0.005% arabinose, the indicated strains were incubated with or without 2.5 µg/ml PMB for 30 min at room temperature and plated in 10-fold dilutions (10^{-1}-10^{-6}) on LB agar plates. In the *yfiR::kan* mutants, the kan cassette is inserted in an orientation opposite to the direction of *yfi* operon transcription in order to avoid polar effects on the downstream *yfiN* gene.

Distinct localization patterns of YfiN from *Salmonella, E. coli* and *P. aeruginosa*

Although a sequence alignment of ^{S}YfiN and ^{E}YfiN shows high identity (74.38%, performed by ClustalW), the two proteins showed differences in their localization. In the mid-log phase (4 hrs), $^{S}YfiN_{GFP}$ appeared at the mid-cell in *Salmonella* without additional stress exposure (Figure 4.19A). In this same phase of growth, $^{E}YfiN_{GFP}$ was dispersed throughout the membrane in *E. coli* and required an additional envelope stress for mid-cell recruitment (Figure 4.19A). These distinct localization patterns of the two proteins were retained when expressed in a heterologous host. For example, $^{S}YfiN_{GFP}$ expressed in *E. coli* appeared at the mid-cell at 4 hrs even without envelope stress (Figure 4.19B), and $^{E}YfiN_{GFP}$ expressed in *Salmonella* relocated from the membrane to the mid-cell only when exposed to envelope stress at this time point (Figure 4.19B).

Next we examined the localization of *P. aeruginosa* YfiN, reported to be a strong DGC contributing biofilm formation (77). An active GFP fusion of *P. aeruginosa* YfiN ($^{P}YfiN_{GFP}$, Figure 4.7) was expressed in all three bacterial species, but failed to localize to the mid-cell in any host, whether exposed to envelope stress or not (Figure 4.20). These results suggest either that ^{P}YfiN does not have a role in cell division or that it needs as yet undiscovered signals to be recruited to the division site. The DGC activity of ^{P}YfiN was comparable with that of ^{S}YfiN or ^{E}YfiN in motility assays (Figure 4.21), which excludes the possibility that the difference in localization results from different enzymatic activities. Overall, these data imply that, even though the DGC activity of YfiN is conserved in *Salmonella*, *E. coli* and *P. aeruginosa* (Figure 4.21) (79, 80), its secondary function as a cell division regulator is distinct in these bacteria.

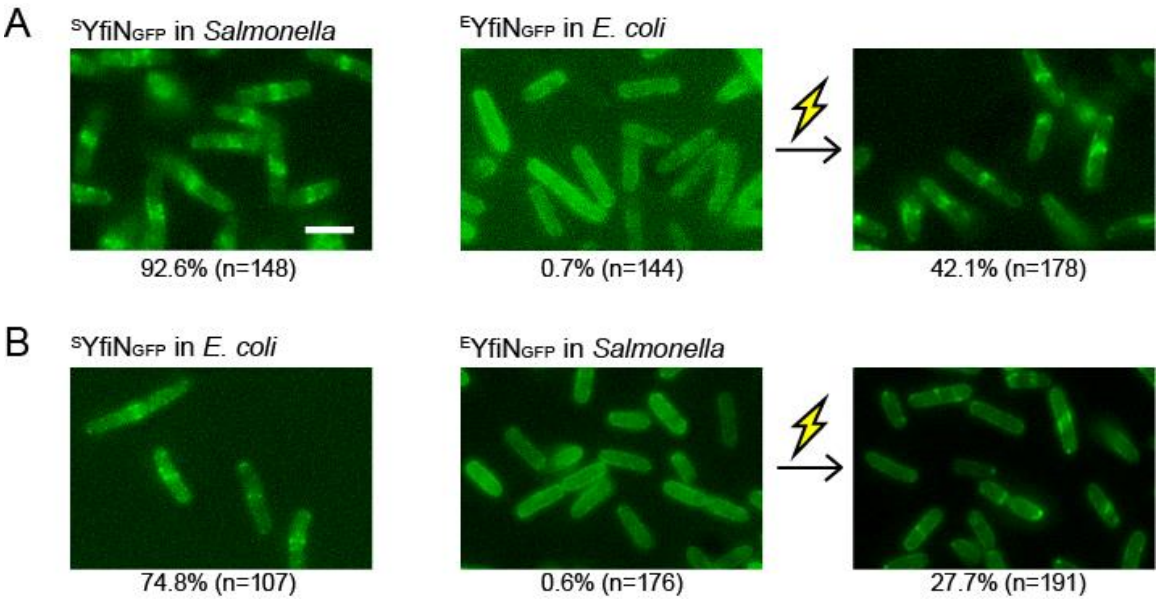

Figure 4.19 Distinct localization of YfiN from *E. coli* and *Salmonella*. $^{S}YfiN_{GFP}$ and $^{E}YfiN_{GFP}$ were expressed in Δ*yfiN* of homologous hosts (A) or heterologous hosts (B). While ^{S}YfiN localized to the mid-cell in the absence of additional stress, ^{E}YfiN only did so in response to envelope stress, regardless in which species they were expressed. For $^{E}YfiN_{GFP}$, images were taken before and 30 min after osmotic upshift (250 mM NaCl).

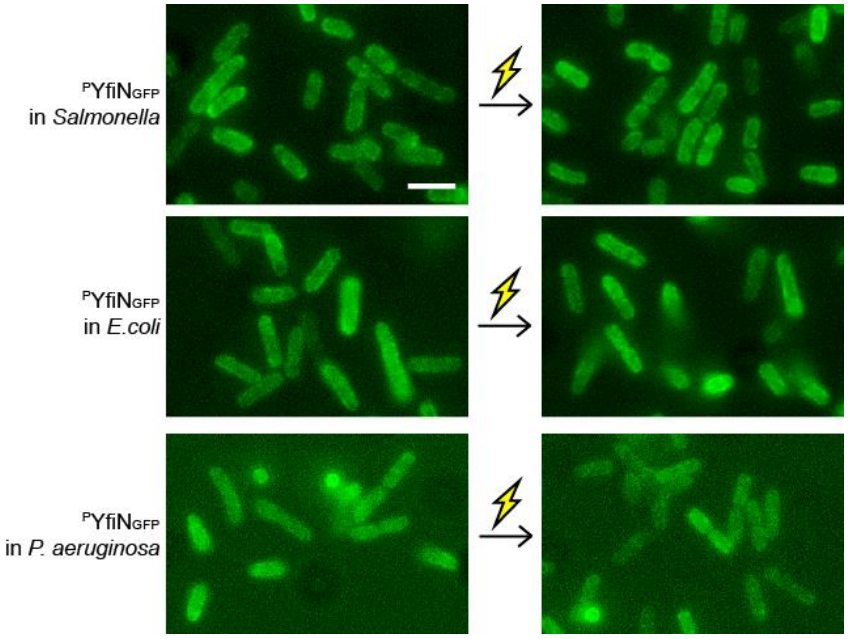

Figure 4.20 Localization of YfiN from *P. aeruginosa*. ^{P}YfiN failed to localize to the mid-cell in any of the host species. The indicated host cells expressing $^{P}YfiN_{GFP}$ were photographed before and 30 min after osmotic upshift (250 mM NaCl).

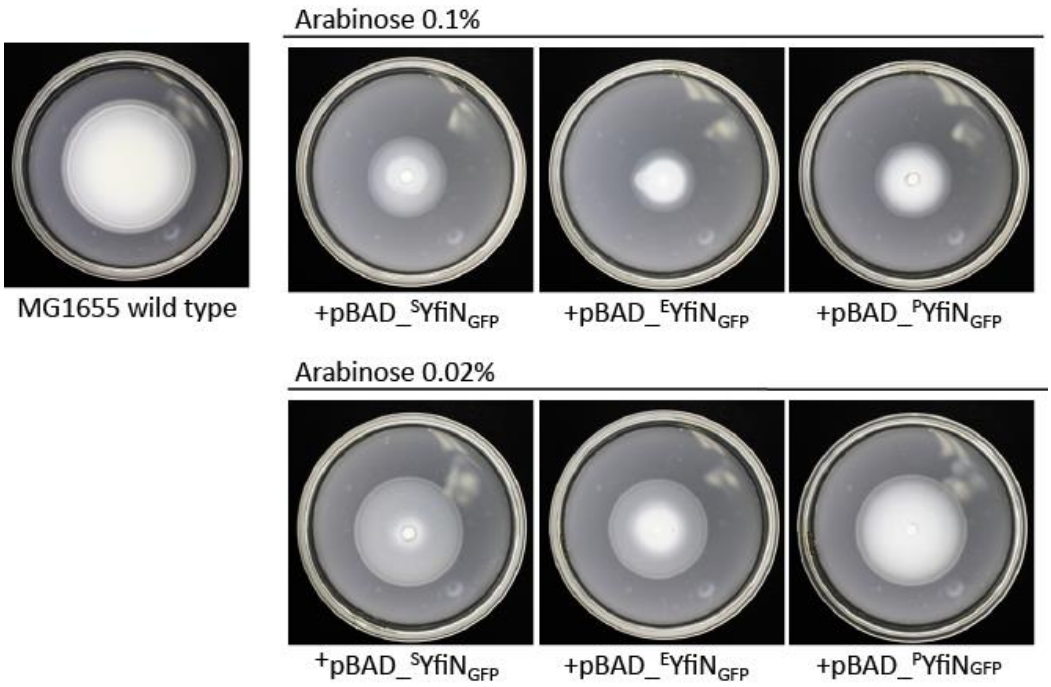

Figure 4.21 Swimming motility of cells expressing *Salmonella*, *E. coli* and *P. aeruginosa* YfiN. Each of the three different YfiN proteins were expressed in the same background (*E. coli* wild type) in order to monitor their c-di-GMP-synthetic activities as measured by motility. The enzymatic activities of YfiN from the three species are comparable as judged by the extent of motility inhibition.

E. coli YfiN senses envelope stress via the extracellular domains

Based on the observation that the localization properties of ^{E}YfiN and ^{S}YfiN are inherent to the protein and not the host (Figure 4.19), we set out to identify the domain of ^{E}YfiN responsible for sensing the envelope stress by swapping domains with ^{S}YfiN. The extracellular region of ^{E}YfiN, including the two transmembrane (TM) domains and the periplasmic PAS-like domain, was first replaced with the corresponding region of ^{S}YfiN and expressed in both *Salmonella* and *E. coli*. The chimeric ^{E}YfiN protein (^{E}YfiN[^{S}TM^{S}PAS]) failed to relocate to the mid-cell in response to envelope stress and appeared to be evenly distributed in the membrane in both hosts (Figure 4.22A), indicating that the extracellular domains of ^{E}YfiN are required for sensing the stress. To determine whether the TM or PAS-like domain is responsible, chimeras with either of these domain swaps were constructed. While ^{E}YfiN[^{S}PAS] retained the sensing ability (Figure 4.22B), ^{E}YfiN[^{S}TM] was inactive (Figure 4.22C), suggesting that the TM domains of ^{E}YfiN are essential for sensing. However, one cannot rule out the possibility that the PAS-like domain also plays a role in sensing stress because although this domain of ^{E}YfiN could be swapped with the corresponding domain of ^{S}YfiN without loss of the relocation ability (Figure 4.22B), it was not replaceable with that of ^{P}YfiN (Figure 4.22D). Finally, we swapped the TM domains of ^{S}YfiN with those of ^{E}YfiN and tested if they would confer stress-sensing ability to ^{S}YfiN, but the chimera ^{S}YfiN[^{E}TM] localized to the mid-cell even without envelope stress exposure (Figure 4.22E). We interpret these data as suggesting perhaps that the cytoplasmic portion of ^{S}YfiN interacts more readily with cell division proteins compared to ^{E}YfiN, masking the effect of the TM domain swap. Indeed, the BACTH analysis of ^{S}YfiN showed stronger interaction with cell division proteins than that of ^{E}YfiN (compare Figure 4.15 and 4.23). In summary, the

transmembrane and PAS-like domains of *E. coli* YfiN are important for sensing envelope stress.

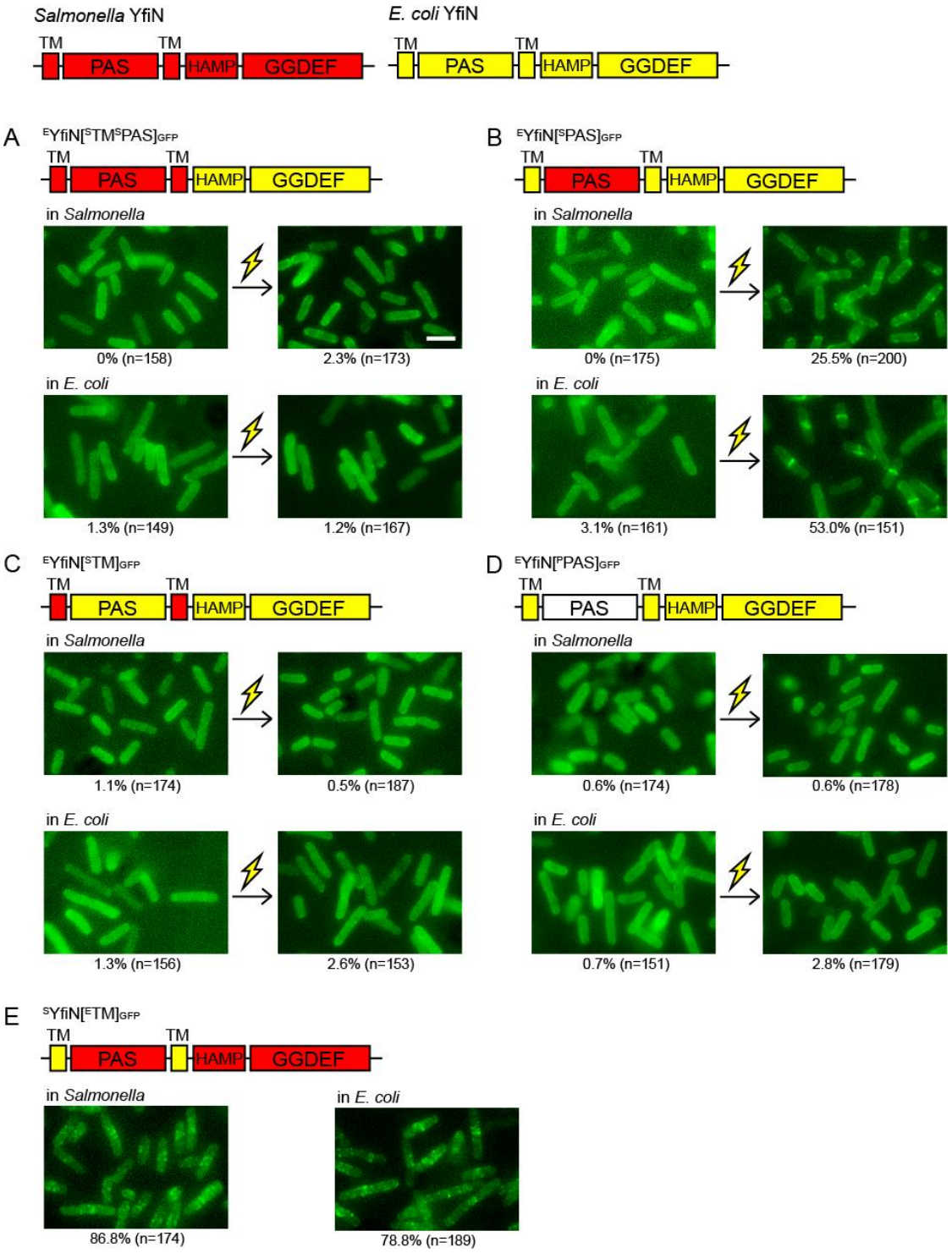

(Figure 4.22: continued next page)

Figure 4.22 Localization of chimeric proteins between *E. coli* and *Salmonella* YfiN. ^{E}YfiN[^{S}TM^{S}PAS]$_{GFP}$ (A), ^{E}YfiN[^{S}PAS]$_{GFP}$ (B), ^{E}YfiN[^{S}TM]$_{GFP}$ (C), ^{E}YfiN[^{P}PAS]$_{GFP}$ (D) and ^{S}YfiN[^{E}TM]$_{GFP}$ (E) were expressed and observed before and 30 min after osmotic upshift (250 mM NaCl) in *Salmonella* and *E. coli*. The extracellular PAS and TM domains are essential for ^{E}YfiN to sense envelope stress.

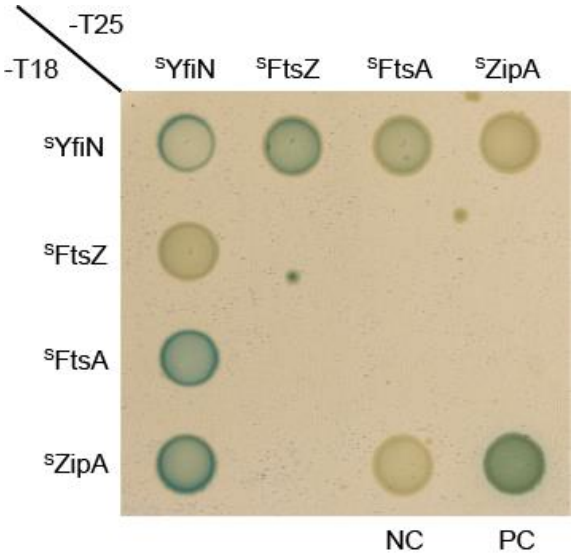

Figure 4.23 BACTH analysis with *Salmonella* YfiN and cell division proteins. Either the T18 or T25 fragment was fused to the C-terminal ends of ^{S}YfiN and cell division proteins. ^{S}YfiN showed positive interaction with the cell division proteins. PC, positive control (T18-leucine zipper/T25-leucine zipper); NC, negative control (T18/T25 empty vectors).

The GGDEF domain of YfiN mediates the mid-cell localization

Using the domain swapping approach, we sought to identify the domain in YfiN that mediates the interaction with cell division proteins. Since the early cell division proteins FtsZ and ZipA, which are responsible for YfiN recruitment to the division site as described above, predominantly reside in the cytoplasm, we hypothesized that the interface might locate at the two cytoplasmic domains of YfiN, HAMP and GGDEF domains. To test this, HAMP and GGDEF domains were swapped between ^{S}YfiN and ^{P}YfiN. Although the two proteins show 36.95% of sequence identity (performed by ClustalW), ^{P}YfiN does not localize to the division site in any host (Figure 4.20). First, each of HAMP and GGDEF domains of ^{S}YfiN was replaced with the corresponding domain of ^{P}YfiN. The chimeric proteins ^{S}YfiN[^{P}HAMP] and ^{S}YfiN[^{P}GGDEF] failed to localize to the mid-cell (Figure 4.24A and B), indicating that both domains contribute to the interaction of ^{S}YfiN with division proteins. Next, we constructed chimeric ^{P}YfiN proteins in which the HAMP or GGDEF domain was replaced with that of ^{S}YfiN. While the replacement of HAMP domain had no effect (Figure 4.24C), the GGDEF domain of ^{S}YfiN alone was able to confer the mid-cell localization to ^{P}YfiN (Figure 4.24D), assigning the division protein-binding region of ^{S}YfiN to the GGDEF domain. However, the HAMP domain also seemed to be involved with interaction to some extent, because the probability of mid-cell localization increased when ^{P}YfiN had both HAMP and GGDEF domains from ^{S}YfiN (Figure 4.24E).

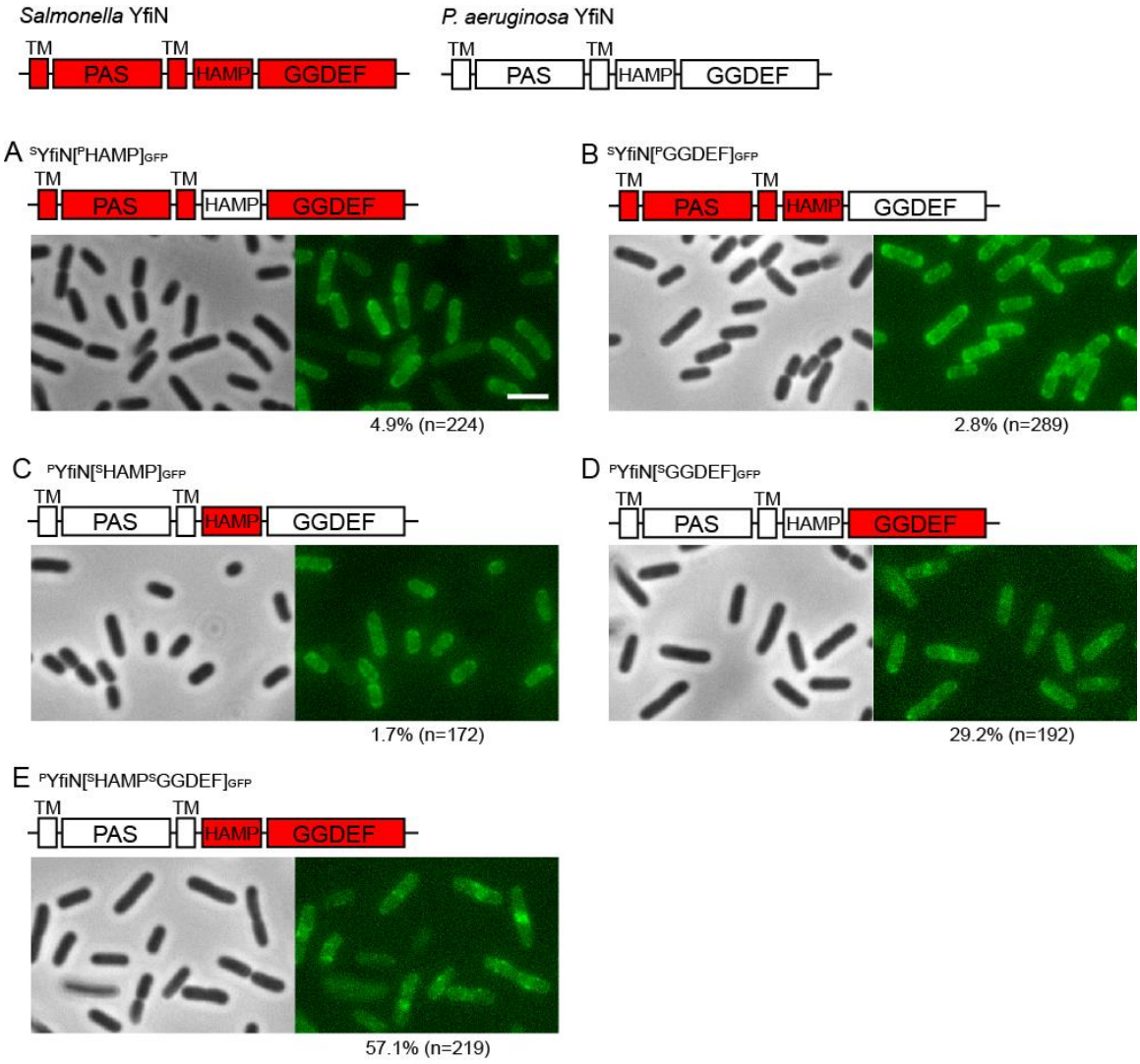

Figure 4.24 Localization of chimeric proteins between *Salmonella* and *P. aeruginosa* YfiN. ^{S}YfiN[^{P}HAMP]$_{GFP}$ (A), ^{S}YfiN[^{P}GGDEF]$_{GFP}$ (B), ^{P}YfiN[^{S}HAMP]$_{GFP}$ (C), ^{P}YfiN[^{S}GGDEF]$_{GFP}$ (D) and ^{P}YfiN[^{S}HAMP^{S}GGDEF]$_{GFP}$ (E) were expressed and observed in *Salmonella*. The GGDEF domain of ^{S}YfiN confers mid-cell localization specificity.

DISCUSSION

Since the original discovery of c-di-GMP as an allosteric effector of a bacterial cellulose synthase (23), and the later revelation of its major role as a second messenger that controls the decision between motile and sedentary bacterial lifestyles, the function of c-di-GMP has steadily expanded to include a remarkably diverse set of cellular processes. In this work I establish a new and unique role for the diguanylate cyclase YfiN as both an enzyme and an effector, which stalls cell division by interacting with early cell division proteins in *E. coli* and *Salmonella*.

YfiN as a sensor for multiple environmental stresses

In both *Salmonella* and *E. coli*, YfiN localizes to the division site and arrests cell division, which is exerted through direct interaction with cell division proteins. In *E. coli*, the trigger for recruitment of YfiN to the mid-cell is osmotic upshift and membrane permeabilization. The OM permeabilizers that stimulate ^{E}YfiN relocation – PMB, EDTA and a high concentration of PMBN (Figure 4.9 and 4.10) – have all been reported to induce release of LPS and leakage of periplasmic proteins by altering LPS-LPS interactions in the OM (97, 107). Hyperosmotic stress also causes periplasmic contents to leak out (97, 108). This common attribute of the agents suggests that periplasmic leakage might be the specific input signal for the ^{E}YfiN-mediated cell division inhibition. One might then imagine that loss of the periplasmic protein YfiR by periplasmic leakage might be the trigger of ^{E}YfiN relocation, given the function of YfiR as an inhibitor of YfiN (77, 79). However, this is not the case because inactivation of ^{E}YfiR by either reducing stress or genetic mutation was not enough to relocate ^{E}YfiN to the mid-cell

without envelope stress (Figure 4.17). Thus, ^{E}YfiN is a membrane-associated sensor that responds to two independent environmental cues, reducing and envelope stresses.

While mid-cell localization of YfiN in *E. coli* is stimulated by osmotic upshift and OM permeabilization, the same conditions did not lead to a change in YfiN localization in *Salmonella* (Figure 4.12), suggesting that signals that cause division arrest by YfiN differ between *E. coli* and *Salmonella*. In both bacteria, YfiN mid-cell localization was dependent on growth phase (Figure 4.5 and 4.8), but the exact stress sensed in the stationary phase is not known. Surprisingly, *P. aeruginosa* YfiN does not localize to the division site either during the stationary phase or with envelope stress exposure in any of the bacterial species tested (Figure 4.20). Thus, despite the overall conservation as a c-di-GMP synthetic enzyme, YfiN appears to have evolved to acquire an additional cell division arrest function in *E. coli* and *Salmonella*, which is activated in response to different environmental signals.

Thus far, DGCs are known to produce c-di-GMP in response to environmental cues, which then serves as a second messenger that binds to a protein or an RNA effector and elicits a downstream response. A DGC-inactive ^{E}YfiN regained the ability to interact with cell division proteins when intracellular c-di-GMP levels were elevated (Figure 4.16). This suggests that ^{E}YfiN in a c-di-GMP-bound state itself might be the effector that interacts with the division proteins. Alternatively, c-di-GMP could bind to some other division protein that binds c-di-GMP, which in turn promotes the recruitment of ^{E}YfiN to the division site. However, the former possibility is more likely because many GGDEF domain proteins have been reported to have a c-di-GMP-binding site (109). Although ^{E}YfiN does not have a conserved I-site (RXXD motif at five amino acids upstream of the GGDEF active site), which is the best characterized c-di-GMP-binding

site in GGDEF domain proteins, a recent study reported an example of a DGC that exists in a complex with c-di-GMP even when it has no I-site (110). We therefore favor the idea that high levels of c-di-GMP might enhance the interaction of ^{E}YfiN with division proteins by binding to ^{E}YfiN and stabilizing the conformational change induced by envelope stress.

Based on these results, we propose a model in which ^{E}YfiN acts as a bifunctional protein exhibiting both enzymatic and effector activities (Figure 4.25). The enzymatic function of ^{E}YfiN is activated by release of ^{E}YfiR under reducing conditions, and the c-di-GMP thus generated impairs motility and enhances biofilm formation (79, 81). The effector function exerted by c-di-GMP-bound ^{E}YfiN requires an additional envelope stress cue, which likely results in an additional conformation change that exposes binding sites on ^{E}YfiN to the division proteins FtsZ and ZipA, leading to cell division arrest.

The idea of bifunctional GGDEF/EAL domain proteins acting as an enzyme and an effector was previously proposed for a couple of PDEs, YciR (also called PdeR) (50) and PdeL (111). Such bi-functionality of a DGC/PDE, now seen with YfiN, would achieve local specificity of c-di-GMP signaling, since the second function is restricted to distinct downstream targets by their specific spatial organization. All of these examples share a requirement for enzymatic activity for their dual action, but YfiN requires an additional input signal – envelope stress - to serve its second function of cell division control. While we accidentally unearthed the distinct responses of YfiN to different stimuli, such multi-tasking may be common in c-di-GMP signaling, enabling bacteria to differentially respond to multiple environmental challenges.

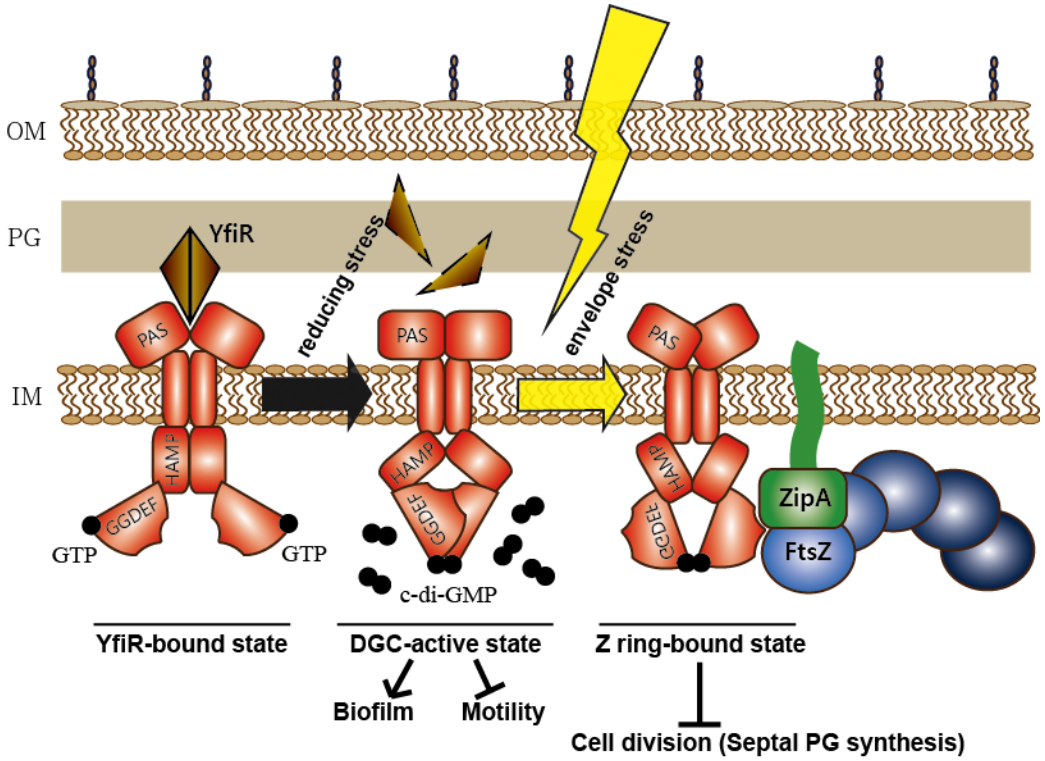

Figure 4.25 Model for YfiN as a cell division inhibitor. ^{E}YfiN is a bifunctional protein that responds to two different environmental stresses – reductive and envelope stress. The DGC function is known to be activated when reducing stress inactivates the periplasmic repressor ^{E}YfiR. The c-di-GMP thus produced inhibits motility and activates biofilm formation. The second function of ^{E}YfiN as a cell division inhibitor as revealed in this study, requires an additional envelope stress after the DGC function is activated. The envelope stress-induced conformation of ^{E}YfiN, which is likely in a c-di-GMP-bound state, exposes binding sites for division proteins FtsZ and ZipA, directing ^{E}YfiN to the future division site, where it halts division by preventing the initiation of septal peptidoglycan synthesis.

YfiN as a cell division checkpoint for adaptation to envelope stress

From bacteria to eukaryotes, cell division regulation is used as a checkpoint to ensure survival upon exposure to stress. In bacteria, DNA damage (88) or envelope stress caused by inactivation of the peptidoglycan synthase PBP3 (89) triggers the SOS response, in which expression of the cell division inhibitor SulA is activated. While SulA directly inhibits FtsZ polymerization and leads to disassembly of the Z ring (94), YfiN retains the Z ring at the mid-cell (Figure 4.5 and 4.8). This feature of YfiN as a cell division inhibitor can also be observed with two DNA damage-induced proteins SidA and DidA in *C. crescentus*, a bacterium that does not have a SulA homolog. SidA and DidA arrest cell division by inhibiting late cell division events, while retaining the Z ring (112, 113). Unlike SidA and DidA, however, cells with YfiN at the mid-cell have no visible constriction site (Figure 4.2), suggesting that YfiN inhibits the initiation of constriction. Although precisely which step in cell division is blocked by YfiN is not yet clear, exclusion of the late division protein FtsN and stalled septal PG synthesis at the future division sites occupied by YfiN raise the possibility that YfiN inhibits the initiation of constriction by using early division proteins as docking sites and preventing the recruitment of late division proteins (Figure 4.6). It has been reported that the interplay between FtsN and two early division proteins FtsA and ZipA is essential for activation of constriction (95, 96), which might be affected by YfiN. We also note that some cells expressing $YfiN_{GFP}$ show wide rings at the mid-cell, which are often slanted or off-center, reminiscent of FtsZ structures seen under several conditions including: mutations in FtsZ (114, 115), overexpression of FtsZ (116, 117), overexpression of the FtsZ polymerization regulator ZapA (118) and the absence of low-molecular-weight penicillin-binding

proteins (LMW PBPs) (117). It is possible that the observed aberrant localization of $YfiN_{GFP}$ is due to altered polymerization of FtsZ.

Another unusual (and thus far unique) feature of YfiN as a cell division inhibitor is that, unlike the known division inhibitors SulA (119), SidA (112) and DidA (113), cell division arrest by YfiN only leads to a modest level of cell lengthening, but does not lead to filamentation (Figure 4.26). This suggests that YfiN may inhibit the synthesis of nascent PG, not only at the division site, but also along the lateral wall. Rod-shaped bacteria are thought to have two modes of cell wall synthesis catalyzed by different PG synthases: one responsible for cell elongation along the lateral wall and the other for formation of the division septum (120). Our results suggest that YfiN might target a common step that these two modes share. Unlike general inhibition of PG synthesis by β-lactam antibiotics (121, 122), the action of YfiN does not trigger cell lysis, as judged by the observation that cell density did not decrease when cell division was arrested by YfiN (Figure 4.5 and 4.8).

Given the positive effect of YfiN on survival to lethal PMB exposure (Figure 4.18), it is tempting to speculate that the effector function of YfiN reported in this study is an adaptation mechanism that delays cell division and new peptidoglycan synthesis when *E. coli* experiences envelope-disrupting environments, ensuring that the cell wall is not mislaid while the cell is recovering from the stress. Further investigation of YfiN will provide new insights into the mechanism how bacterial cell division and cell wall synthesis are coordinated in response to environmental stress.

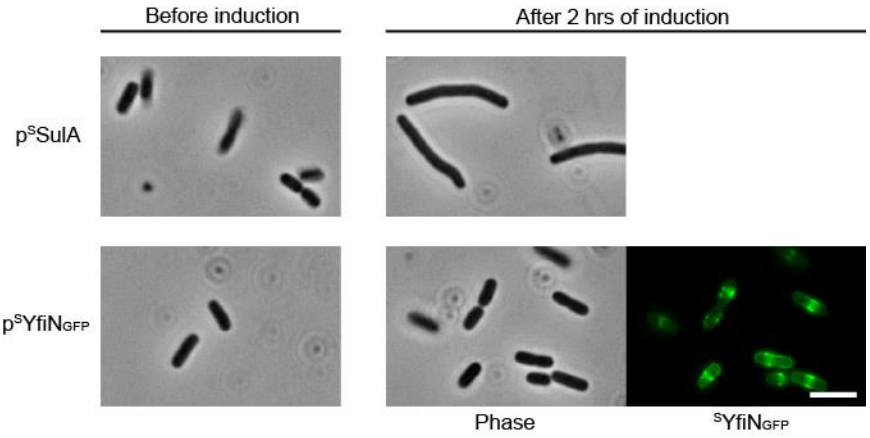

.

Figure 4.26 Cell division arrest by YfiN does not lead to cell flamentation. Cell morphology of *Salmonella* 14028 wild type expressing ^{S}SulA and ^{S}YfiN$_{GFP}$. Unlike that seen with SulA, cells did not filament with YfiN. Images were taken before and 2 hrs after adding inducer.

References

1. Galperin MY (2005) A census of membrane-bound and intracellular signal transduction proteins in bacteria: bacterial IQ, extroverts and introverts. *BMC microbiology* 5:35.
2. Alm E, Huang K, & Arkin A (2006) The evolution of two-component systems in bacteria reveals different strategies for niche adaptation. *PLoS computational biology* 2(11):e143.
3. Ulrich LE & Zhulin IB (2010) The MiST2 database: a comprehensive genomics resource on microbial signal transduction. *Nucleic acids research* 38(Database issue):D401-407.
4. Capra EJ & Laub MT (2012) Evolution of two-component signal transduction systems. *Annual review of microbiology* 66:325-347.
5. Skerker JM*, et al.* (2008) Rewiring the specificity of two-component signal transduction systems. *Cell* 133(6):1043-1054.
6. Weigt M, White RA, Szurmant H, Hoch JA, & Hwa T (2009) Identification of direct residue contacts in protein-protein interaction by message passing. *Proceedings of the National Academy of Sciences of the United States of America* 106(1):67-72.
7. Waters CM & Bassler BL (2005) Quorum sensing: cell-to-cell communication in bacteria. *Annual review of cell and developmental biology* 21:319-346.
8. Fuqua C, Parsek MR, & Greenberg EP (2001) Regulation of gene expression by cell-to-cell communication: acyl-homoserine lactone quorum sensing. *Annual review of genetics* 35:439-468.
9. Lyon GJ & Novick RP (2004) Peptide signaling in Staphylococcus aureus and other Gram-positive bacteria. *Peptides* 25(9):1389-1403.
10. Pesci EC*, et al.* (1999) Quinolone signaling in the cell-to-cell communication system of Pseudomonas aeruginosa. *Proceedings of the National Academy of Sciences of the United States of America* 96(20):11229-11234.
11. Mashburn LM & Whiteley M (2005) Membrane vesicles traffic signals and facilitate group activities in a prokaryote. *Nature* 437(7057):422-425.
12. Pesavento C & Hengge R (2009) Bacterial nucleotide-based second messengers. *Current opinion in microbiology* 12(2):170-176.
13. Harman JG (2001) Allosteric regulation of the cAMP receptor protein. *Biochimica et biophysica acta* 1547(1):1-17.

14. Magnusson LU, Farewell A, & Nystrom T (2005) ppGpp: a global regulator in Escherichia coli. *Trends in microbiology* 13(5):236-242.

15. An G, Justesen J, Watson RJ, & Friesen JD (1979) Cloning the spoT gene of Escherichia coli: identification of the spoT gene product. *Journal of bacteriology* 137(3):1100-1110.

16. Burdette DL*, et al.* (2011) STING is a direct innate immune sensor of cyclic di-GMP. *Nature* 478(7370):515-518.

17. Parvatiyar K*, et al.* (2012) The helicase DDX41 recognizes the bacterial secondary messengers cyclic di-GMP and cyclic di-AMP to activate a type I interferon immune response. *Nature immunology* 13(12):1155-1161.

18. Witte G, Hartung S, Buttner K, & Hopfner KP (2008) Structural biochemistry of a bacterial checkpoint protein reveals diadenylate cyclase activity regulated by DNA recombination intermediates. *Molecular cell* 30(2):167-178.

19. Oppenheimer-Shaanan Y, Wexselblatt E, Katzhendler J, Yavin E, & Ben-Yehuda S (2011) c-di-AMP reports DNA integrity during sporulation in Bacillus subtilis. *EMBO reports* 12(6):594-601.

20. Corrigan RM, Abbott JC, Burhenne H, Kaever V, & Grundling A (2011) c-di-AMP is a new second messenger in Staphylococcus aureus with a role in controlling cell size and envelope stress. *PLoS Pathog* 7(9):e1002217.

21. Sureka K*, et al.* (2014) The cyclic dinucleotide c-di-AMP is an allosteric regulator of metabolic enzyme function. *Cell* 158(6):1389-1401.

22. Davies BW, Bogard RW, Young TS, & Mekalanos JJ (2012) Coordinated regulation of accessory genetic elements produces cyclic di-nucleotides for V. cholerae virulence. *Cell* 149(2):358-370.

23. Ross P*, et al.* (1987) Regulation of cellulose synthesis in Acetobacter xylinum by cyclic diguanylic acid. *Nature* 325(6101):279-281.

24. Hengge R*, et al.* (2015) Systematic nomenclature for GGDEF and EAL domain-containing c-di-GMP turnover proteins of Escherichia coli. *Journal of bacteriology*.

25. Hengge R (2009) Principles of c-di-GMP signalling in bacteria. *Nature reviews. Microbiology* 7(4):263-273.

26. Tuckerman JR*, et al.* (2009) An oxygen-sensing diguanylate cyclase and phosphodiesterase couple for c-di-GMP control. *Biochemistry* 48(41):9764-9774.

27. Sasakura Y, Yoshimura-Suzuki T, Kurokawa H, & Shimizu T (2006) Structure-function relationships of EcDOS, a heme-regulated phosphodiesterase from Escherichia coli. *Accounts of chemical research* 39(1):37-43.

28. Hasegawa K, Masuda S, & Ono TA (2006) Light induced structural changes of a full-length protein and its BLUF domain in YcgF(Blrp), a blue-light sensing protein that uses FAD (BLUF). *Biochemistry* 45(11):3785-3793.

29. Nakasone Y, Ono TA, Ishii A, Masuda S, & Terazima M (2010) Temperature-sensitive reaction of a photosensor protein YcgF: possibility of a role of temperature sensor. *Biochemistry* 49(10):2288-2296.

30. Guvener ZT & Harwood CS (2007) Subcellular location characteristics of the Pseudomonas aeruginosa GGDEF protein, WspR, indicate that it produces cyclic-di-GMP in response to growth on surfaces. *Molecular microbiology* 66(6):1459-1473.

31. Paul R*, et al.* (2004) Cell cycle-dependent dynamic localization of a bacterial response regulator with a novel di-guanylate cyclase output domain. *Genes & development* 18(6):715-727.

32. Boehm A*, et al.* (2010) Second messenger-mediated adjustment of bacterial swimming velocity. *Cell* 141(1):107-116.

33. Paul K, Nieto V, Carlquist WC, Blair DF, & Harshey RM (2010) The c-di-GMP binding protein YcgR controls flagellar motor direction and speed to affect chemotaxis by a "backstop brake" mechanism. *Molecular cell* 38(1):128-139.

34. Fang X & Gomelsky M (2010) A post-translational, c-di-GMP-dependent mechanism regulating flagellar motility. *Molecular microbiology* 76(5):1295-1305.

35. Li B*, et al.* (2012) Structural insight of a concentration-dependent mechanism by which YdiV inhibits Escherichia coli flagellum biogenesis and motility. *Nucleic acids research* 40(21):11073-11085.

36. Tuckerman JR, Gonzalez G, & Gilles-Gonzalez MA (2011) Cyclic di-GMP activation of polynucleotide phosphorylase signal-dependent RNA processing. *Journal of molecular biology* 407(5):633-639.

37. Pultz IS*, et al.* (2012) The response threshold of Salmonella PilZ domain proteins is determined by their binding affinities for c-di-GMP. *Molecular microbiology* 86(6):1424-1440.

38. Abel S*, et al.* (2013) Bi-modal distribution of the second messenger c-di-GMP controls cell fate and asymmetry during the caulobacter cell cycle. *PLoS genetics* 9(9):e1003744.

39. Christen M*, et al.* (2010) Asymmetrical distribution of the second messenger c-di-GMP upon bacterial cell division. *Science* 328(5983):1295-1297.

40. Abel S, *et al.* (2011) Regulatory cohesion of cell cycle and cell differentiation through interlinked phosphorylation and second messenger networks. *Molecular cell* 43(4):550-560.

41. McCormick K & Baillie GS (2014) Compartmentalisation of second messenger signalling pathways. *Current opinion in genetics & development* 27:20-25.

42. Zaccolo M, *et al.* (2006) Restricted diffusion of a freely diffusible second messenger: mechanisms underlying compartmentalized cAMP signalling. *Biochemical Society transactions* 34(Pt 4):495-497.

43. Bacskai BJ, *et al.* (1993) Spatially resolved dynamics of cAMP and protein kinase A subunits in Aplysia sensory neurons. *Science* 260(5105):222-226.

44. Chen C, Nakamura T, & Koutalos Y (1999) Cyclic AMP diffusion coefficient in frog olfactory cilia. *Biophysical journal* 76(5):2861-2867.

45. Zaccolo M & Pozzan T (2002) Discrete microdomains with high concentration of cAMP in stimulated rat neonatal cardiac myocytes. *Science* 295(5560):1711-1715.

46. Lugnier C (2006) Cyclic nucleotide phosphodiesterase (PDE) superfamily: a new target for the development of specific therapeutic agents. *Pharmacology & therapeutics* 109(3):366-398.

47. Kulasekara BR, *et al.* (2013) c-di-GMP heterogeneity is generated by the chemotaxis machinery to regulate flagellar motility. *eLife* 2:e01402.

48. Mills E, Petersen E, Kulasekara BR, & Miller SI (2015) A direct screen for c-di-GMP modulators reveals a Salmonella Typhimurium periplasmic L-arginine-sensing pathway. *Science signaling* 8(380):ra57.

49. Dahlstrom KM, Giglio KM, Collins AJ, Sondermann H, & O'Toole GA (2015) Contribution of Physical Interactions to Signaling Specificity between a Diguanylate Cyclase and Its Effector. *mBio* 6(6):e01978-01915.

50. Lindenberg S, Klauck G, Pesavento C, Klauck E, & Hengge R (2013) The EAL domain protein YciR acts as a trigger enzyme in a c-di-GMP signalling cascade in E. coli biofilm control. *The EMBO journal* 32(14):2001-2014.

51. Datsenko KA & Wanner BL (2000) One-step inactivation of chromosomal genes in Escherichia coli K-12 using PCR products. *Proceedings of the National Academy of Sciences of the United States of America* 97(12):6640-6645.

52. Wang Q, Mariconda S, Suzuki A, McClelland M, & Harshey RM (2006) Uncovering a large set of genes that affect surface motility in Salmonella enterica serovar Typhimurium. *Journal of bacteriology* 188(22):7981-7984.

53. Yu XC & Margolin W (2000) Deletion of the min operon results in increased thermosensitivity of an ftsZ84 mutant and abnormal FtsZ ring assembly, placement, and disassembly. *Journal of bacteriology* 182(21):6203-6213.

54. Geissler B, Elraheb D, & Margolin W (2003) A gain-of-function mutation in ftsA bypasses the requirement for the essential cell division gene zipA in Escherichia coli. *Proceedings of the National Academy of Sciences of the United States of America* 100(7):4197-4202.

55. Pichoff S & Lutkenhaus J (2002) Unique and overlapping roles for ZipA and FtsA in septal ring assembly in Escherichia coli. *The EMBO journal* 21(4):685-693.

56. Baba T*, et al.* (2006) Construction of Escherichia coli K-12 in-frame, single-gene knockout mutants: the Keio collection. *Molecular systems biology* 2:2006 0008.

57. Karimova G, Pidoux J, Ullmann A, & Ladant D (1998) A bacterial two-hybrid system based on a reconstituted signal transduction pathway. *Proceedings of the National Academy of Sciences of the United States of America* 95(10):5752-5756.

58. Steiner S, Lori C, Boehm A, & Jenal U (2013) Allosteric activation of exopolysaccharide synthesis through cyclic di-GMP-stimulated protein-protein interaction. *The EMBO journal* 32(3):354-368.

59. Guzman LM, Belin D, Carson MJ, & Beckwith J (1995) Tight regulation, modulation, and high-level expression by vectors containing the arabinose PBAD promoter. *Journal of bacteriology* 177(14):4121-4130.

60. Amann E, Brosius J, & Ptashne M (1983) Vectors bearing a hybrid trp-lac promoter useful for regulated expression of cloned genes in Escherichia coli. *Gene* 25(2-3):167-178.

61. Newman JR & Fuqua C (1999) Broad-host-range expression vectors that carry the L-arabinose-inducible Escherichia coli araBAD promoter and the araC regulator. *Gene* 227(2):197-203.

62. Kuru E, Tekkam S, Hall E, Brun YV, & Van Nieuwenhze MS (2015) Synthesis of fluorescent D-amino acids and their use for probing peptidoglycan synthesis and bacterial growth in situ. *Nature protocols* 10(1):33-52.

63. Spangler C, Bohm A, Jenal U, Seifert R, & Kaever V (2010) A liquid chromatography-coupled tandem mass spectrometry method for quantitation of cyclic di-guanosine monophosphate. *Journal of microbiological methods* 81(3):226-231.

64. Schirmer T & Jenal U (2009) Structural and mechanistic determinants of c-di-GMP signalling. *Nature reviews. Microbiology* 7(10):724-735.

65. Ferreira RB, Antunes LC, Greenberg EP, & McCarter LL (2008) Vibrio parahaemolyticus ScrC modulates cyclic dimeric GMP regulation of gene expression relevant to growth on surfaces. *Journal of bacteriology* 190(3):851-860.

66. Duerig A*, et al.* (2009) Second messenger-mediated spatiotemporal control of protein degradation regulates bacterial cell cycle progression. *Genes & development* 23(1):93-104.

67. Pesavento C*, et al.* (2008) Inverse regulatory coordination of motility and curli-mediated adhesion in Escherichia coli. *Genes & development* 22(17):2434-2446.

68. Krell T*, et al.* (2010) Bacterial sensor kinases: diversity in the recognition of environmental signals. *Annual review of microbiology* 64:539-559.

69. Wadhams GH & Armitage JP (2004) Making sense of it all: bacterial chemotaxis. *Nature reviews. Molecular cell biology* 5(12):1024-1037.

70. Romling U, Galperin MY, & Gomelsky M (2013) Cyclic di-GMP: the first 25 years of a universal bacterial second messenger. *Microbiology and molecular biology reviews : MMBR* 77(1):1-52.

71. Lori C*, et al.* (2015) Cyclic di-GMP acts as a cell cycle oscillator to drive chromosome replication. *Nature*.

72. Tamayo R, Pratt JT, & Camilli A (2007) Roles of cyclic diguanylate in the regulation of bacterial pathogenesis. *Annual review of microbiology* 61:131-148.

73. Hoffman LR*, et al.* (2005) Aminoglycoside antibiotics induce bacterial biofilm formation. *Nature* 436(7054):1171-1175.

74. Tschowri N*, et al.* (2014) Tetrameric c-di-GMP mediates effective transcription factor dimerization to control Streptomyces development. *Cell* 158(5):1136-1147.

75. Jenal U & Malone J (2006) Mechanisms of cyclic-di-GMP signaling in bacteria. *Annu. Rev. Genet.* 40:385-407.

76. Ueda A & Wood TK (2009) Connecting quorum sensing, c-di-GMP, pel polysaccharide, and biofilm formation in Pseudomonas aeruginosa through tyrosine phosphatase TpbA (PA3885). *PLoS Pathog* 5(6):e1000483.

77. Malone JG*, et al.* (2010) YfiBNR mediates cyclic di-GMP dependent small colony variant formation and persistence in Pseudomonas aeruginosa. *PLoS pathogens* 6(3):e1000804.

78. Le Guyon S, Simm R, Rhen M, & Romling U (2014) Dissecting the c-di-GMP signaling network regulating motility in Salmonella enterica serovar Typhimurium. *Environmental microbiology*.

79. Hufnagel DA, DePas WH, & Chapman MR (2014) The disulfide bonding system suppresses CsgD-independent cellulose production in Escherichia coli. *Journal of bacteriology* 196(21):3690-3699.

80. Malone JG*, et al.* (2012) The YfiBNR signal transduction mechanism reveals novel targets for the evolution of persistent Pseudomonas aeruginosa in cystic fibrosis airways. *PLoS Pathog* 8(6):e1002760.

81. Raterman EL, Shapiro DD, Stevens DJ, Schwartz KJ, & Welch RA (2013) Genetic analysis of the role of yfiR in the ability of Escherichia coli CFT073 to control cellular cyclic dimeric GMP levels and to persist in the urinary tract. *Infection and immunity* 81(9):3089-3098.

82. Adams DW & Errington J (2009) Bacterial cell division: assembly, maintenance and disassembly of the Z ring. *Nature reviews. Microbiology* 7(9):642-653.

83. Margolin W (2005) FtsZ and the division of prokaryotic cells and organelles. *Nature reviews. Molecular cell biology* 6(11):862-871.

84. Egan AJ & Vollmer W (2013) The physiology of bacterial cell division. *Annals of the New York Academy of Sciences* 1277:8-28.

85. Aarsman ME*, et al.* (2005) Maturation of the Escherichia coli divisome occurs in two steps. *Molecular microbiology* 55(6):1631-1645.

86. Jonas K (2014) To divide or not to divide: control of the bacterial cell cycle by environmental cues. *Current opinion in microbiology* 18:54-60.

87. Weart RB*, et al.* (2007) A metabolic sensor governing cell size in bacteria. *Cell* 130(2):335-347.

88. Huisman O & D'Ari R (1981) An inducible DNA replication-cell division coupling mechanism in E. coli. *Nature* 290(5809):797-799.

89. Miller C*, et al.* (2004) SOS response induction by beta-lactams and bacterial defense against antibiotic lethality. *Science* 305(5690):1629-1631.

90. Ben-Yehuda S & Losick R (2002) Asymmetric cell division in B. subtilis involves a spiral-like intermediate of the cytokinetic protein FtsZ. *Cell* 109(2):257-266.

91. Thanedar S & Margolin W (2004) FtsZ exhibits rapid movement and oscillation waves in helix-like patterns in Escherichia coli. *Current biology : CB* 14(13):1167-1173.

92. Specht M, Dempwolff F, Schatzle S, Thomann R, & Waidner B (2013) Localization of FtsZ in Helicobacter pylori and consequences for cell division. *Journal of bacteriology* 195(7):1411-1420.

93. Shih YL, Kawagishi I, & Rothfield L (2005) The MreB and Min cytoskeletal-like systems play independent roles in prokaryotic polar differentiation. *Molecular microbiology* 58(4):917-928.

94. Mukherjee A, Cao C, & Lutkenhaus J (1998) Inhibition of FtsZ polymerization by SulA, an inhibitor of septation in Escherichia coli. *Proceedings of the National Academy of Sciences of the United States of America* 95(6):2885-2890.

95. Busiek KK & Margolin W (2014) A role for FtsA in SPOR-independent localization of the essential Escherichia coli cell division protein FtsN. *Molecular microbiology* 92(6):1212-1226.

96. Pichoff S, Du S, & Lutkenhaus J (2015) The bypass of ZipA by overexpression of FtsN requires a previously unknown conserved FtsN motif essential for FtsA-FtsN interaction supporting a model in which FtsA monomers recruit late cell division proteins to the Z ring. *Molecular microbiology* 95(6):971-987.

97. Vaara M (1992) Agents that increase the permeability of the outer membrane. *Microbiological reviews* 56(3):395-411.

98. Daugelavicius R, Bakiene E, & Bamford DH (2000) Stages of polymyxin B interaction with the Escherichia coli cell envelope. *Antimicrobial agents and chemotherapy* 44(11):2969-2978.

99. Hancock RE (1984) Alterations in outer membrane permeability. *Annual review of microbiology* 38:237-264.

100. Cascales E, Bernadac A, Gavioli M, Lazzaroni JC, & Lloubes R (2002) Pal lipoprotein of Escherichia coli plays a major role in outer membrane integrity. *Journal of bacteriology* 184(3):754-759.

101. Gerding MA, Ogata Y, Pecora ND, Niki H, & de Boer PA (2007) The trans-envelope Tol-Pal complex is part of the cell division machinery and required for proper outer-membrane invagination during cell constriction in E. coli. *Molecular microbiology* 63(4):1008-1025.

102. Addinall SG, Bi E, & Lutkenhaus J (1996) FtsZ ring formation in fts mutants. *Journal of bacteriology* 178(13):3877-3884.

103. Varma A & Young KD (2004) FtsZ collaborates with penicillin binding proteins to generate bacterial cell shape in Escherichia coli. *Journal of bacteriology* 186(20):6768-6774.

104. Karimova G, Dautin N, & Ladant D (2005) Interaction network among Escherichia coli membrane proteins involved in cell division as revealed by bacterial two-hybrid analysis. *Journal of bacteriology* 187(7):2233-2243.

105. Fenton AK & Gerdes K (2013) Direct interaction of FtsZ and MreB is required for septum synthesis and cell division in Escherichia coli. *The EMBO journal* 32(13):1953-1965.

106. Yang X*, et al.* (2015) Crystal structures of YfiR from Pseudomonas aeruginosa in two redox states. *Biochemical and biophysical research communications*.

107. Dixon RA & Chopra I (1986) Leakage of periplasmic proteins from Escherichia coli mediated by polymyxin B nonapeptide. *Antimicrobial agents and chemotherapy* 29(5):781-788.

108. Anraku Y & Heppel LA (1967) On the nature of the changes induced in Escherichia coli by osmotic shock. *The Journal of biological chemistry* 242(10):2561-2569.

109. Chou SH & Galperin MY (2016) Diversity of Cyclic Di-GMP-Binding Proteins and Mechanisms. *Journal of bacteriology* 198(1):32-46.

110. Yang CY*, et al.* (2011) The structure and inhibition of a GGDEF diguanylate cyclase complexed with (c-di-GMP)(2) at the active site. *Acta crystallographica. Section D, Biological crystallography* 67(Pt 12):997-1008.

111. Reinders A*, et al.* (2015) Expression and Genetic Activation of Cyclic Di-GMP-Specific Phosphodiesterases in Escherichia coli. *Journal of bacteriology* 198(3):448-462.

112. Modell JW, Hopkins AC, & Laub MT (2011) A DNA damage checkpoint in Caulobacter crescentus inhibits cell division through a direct interaction with FtsW. *Genes & development* 25(12):1328-1343.

113. Modell JW, Kambara TK, Perchuk BS, & Laub MT (2014) A DNA damage-induced, SOS-independent checkpoint regulates cell division in Caulobacter crescentus. *PLoS biology* 12(10):e1001977.

114. Addinall SG & Lutkenhaus J (1996) FtsZ-spirals and -arcs determine the shape of the invaginating septa in some mutants of Escherichia coli. *Molecular microbiology* 22(2):231-237.

115. Stricker J & Erickson HP (2003) In vivo characterization of Escherichia coli ftsZ mutants: effects on Z-ring structure and function. *Journal of bacteriology* 185(16):4796-4805.

116. Ma X, Ehrhardt DW, & Margolin W (1996) Colocalization of cell division proteins FtsZ and FtsA to cytoskeletal structures in living Escherichia coli cells by using green fluorescent protein. *Proceedings of the National Academy of Sciences of the United States of America* 93(23):12998-13003.

117. Potluri LP, de Pedro MA, & Young KD (2012) Escherichia coli low-molecular-weight penicillin-binding proteins help orient septal FtsZ, and their absence leads

to asymmetric cell division and branching. *Molecular microbiology* 84(2):203-224.

118. Galli E & Gerdes K (2012) FtsZ-ZapA-ZapB interactome of Escherichia coli. *Journal of bacteriology* 194(2):292-302.

119. Huisman O, D'Ari R, & Gottesman S (1984) Cell-division control in Escherichia coli: specific induction of the SOS function SfiA protein is sufficient to block septation. *Proceedings of the National Academy of Sciences of the United States of America* 81(14):4490-4494.

120. Scheffers DJ & Pinho MG (2005) Bacterial cell wall synthesis: new insights from localization studies. *Microbiology and molecular biology reviews : MMBR* 69(4):585-607.

121. Chung HS, *et al.* (2009) Rapid beta-lactam-induced lysis requires successful assembly of the cell division machinery. *Proceedings of the National Academy of Sciences of the United States of America* 106(51):21872-21877.

122. Tomasz A (1979) The mechanism of the irreversible antimicrobial effects of penicillins: how the beta-lactam antibiotics kill and lyse bacteria. *Annual review of microbiology* 33:113-137.